

Space Lab PPT Test Stand



Design Document

AA 420 Capstone
Spring 2024

Version 1.0

Executive Summary

The purpose of this project was to design, build, and test an inverted pendulum test stand for SPACE Lab at University of Washington. This test stand will be used to characterize low thrust and low impulse thrusters, so it has to be sensitive enough to be able to respond to impulses on the order of ten micronewton and steady state forces on the order of one hundred of micronewtons. The test stand also had to be designed specifically to fit into the two new vacuum chambers acquired by SPACE Lab that thruster testing will take place in. There were many different components that were needed to make this test stand functional, a brief description of each component will follow.

There is a chamber interface subsystem that is where the test stand physically sits on the inside wall of the vacuum chamber. This subsystem has rubber isolators to isolate the stand from vibrations external to the vacuum chamber as well as protect the walls of the vacuum chamber from physical damage. This system also has a mount for the leveling motor used in the leveling system, as well as the support bushings for the leveling system that not only support the structure of the leveling system, but also allow it to pivot when leveling the stand.

Next is the leveling system subsystem. The test stand will need to be re-leveled after each thruster test from outside the vacuum chamber, or anytime the test stand is disturbed in a way that moves it away from equilibrium. A leveling motor attached to the chamber interface structure will be used to pivot the structure of the leveling system on nylon to bring the test stand back to equilibrium. The structure of the leveling system subsystem will also be the support structure for the thrust measurement subsystem.

The thrust measurement subsystem is the structure of the inverted pendulum and pendulum frame, as well as the laser displacement sensor and EMI noise reduction. Space was given for the calibration system SPACE Lab will be using, but it was never integrated into the stand. The test stand pendulum structure is what responds to the impulse or thrust produced by the thruster of interest. The whole structure is made of a fiberglass composite called Garolite except for spring steel flexures of the pendulum. These flexures act as leaf springs that oppose the forces being imparted on the pendulum. Different flexures are used depending on the strength of the thruster in question, stronger thrusters use thicker flexures. The pendulum frame acts as a stop for the pendulum in case a disturbance or thruster force is too much for the pendulum to remain stable. The frame also provides structure for mounting the laser displacement sensor and magnetic damper. The laser displacement sensor measures the displacement of the pendulum due to forces imparted by the thruster being tested, this displacement is then used to determine the thrust or impulse produced based on the thickness of the flexures being used. The laser displacement sensor is also used to give the position of the pendulum when leveling the test stand. Electric thrusters produce EMI that can cause noise in the electrical system, which would make accurate thrust measurements impossible. The EMI noise reduction component shields all electronic equipment, including wiring, from the EMI so that electrical signals are as clear as possible. The calibration system will be developed and installed by SPACE Lab in order to provide a known force to the test stand so that the stand can be calibrated for accurate characterization of thrusters.

The PPT mount subsystem provides the structure that the thruster sits on during testing, as well as motion damping and waterfall. The structure of the PPT mount subsystem is the thruster shelf, which is attached to the top of the pendulum such that the thruster is positioned in between the legs of the pendulum. There are two different shelf configurations used in order to center the thruster as much as possible inside the vacuum chamber. The magnetic damper will have a magnet inside of a magnet housing on the top of the pendulum and a piece of aluminum adhered to the stationary pendulum frame. This system will produce eddy currents that will oppose the direction of motion of the pendulum and provide damping that will bring the

pendulum to equilibrium in a short period of time. This is needed because there will be no air resistance inside the vacuum chamber where testing is taking place. The magnet housing also provides a target for the laser displacement sensor to measure the displacement of the pendulum. The waterfall is the method used for minimizing the impact of the wires needed to power the thrusters being tested on the displacement of the pendulum. The wires will have a clamp of the pendulum frame that guides the wires onto the shelf the thruster being tested sits on. These wires will have enough slack in them to minimize their resistance to motion, but not so much slack that they are hanging off the thruster shelf, which would add excessive resistance to motion.

The final subsystem is data acquisition. Data communication was optimized using NI-DAQmx Driver and PySerial. The PPT is triggered to fire and deflection data is measured with an IL-30 laser displacement sensor. A low pass filter minimizes noise to ensure the data signal is as clean as possible. Data is recorded to the DAQ for processing using MATLAB.

Table of Contents

Executive Summary	3
Table of Contents	5
List of Figures	10
List of Tables	13
Acronyms	16
1 Introduction	17
1.1 Motivation	17
1.2 Mission Objectives	17
1.3 CONOPS	18
1.4 System Requirements	19
2 Project Overview	21
2.1 System Architecture	22
2.1.1 Chamber Interface	22
2.1.2 Levelling System	23
2.1.3 Thrust Measurement	24
2.1.4 PPT Mount	26
2.1.5 Data Analysis	26
2.2 Work Breakdown Schedule (WBS)	26
2.3 Schedule & Budgets	27
3 Chamber Interface Subsystem Design	31
3.1 Functional Requirements	32
3.2 Design Overview	33
3.3 Budgets	34
3.4 Chamber Interface Subsystem - Structures	34
3.4.1 Structures Requirements	35
3.4.2 Interfaces	35
3.4.3 Trade Analysis	36
3.4.4 Detailed Design	36
3.4.5 Materials & Manufacturing	37
3.4.6 Verification	38
3.4.7 Risk Analysis	38
3.5 Chamber Interface Subsystem - Electrical Feedthrough	39
3.5.1 Electrical Feedthrough Requirements	39
3.5.2 Interfaces	39
3.5.3 Trade Analysis	39
3.5.4 Materials & Manufacturing	40
3.5.5 Detailed Design	40
3.5.6 Verification	40

3.5.7 Risk Analysis	41
3.6 Integration Plan/Process	41
4 Leveling System Subsystem Design	41
4.1 Functional Requirements	42
4.2 Design Overview	43
4.3 Budgets	43
4.4 Leveling System Subsystem - Structures	44
4.4.1 Structures Requirements	45
4.4.2 Interfaces	45
4.4.3 Trade Analysis	46
4.4.4 Materials & Manufacturing	46
4.4.5 Detailed Design	46
4.4.6 Verification	47
4.4.7 Risk Analysis	48
4.5 Leveling System Subsystem - Avionics	49
4.5.1 Avionics Requirements	49
4.5.2 Interfaces	50
4.5.3 Trade Analysis	50
4.5.4 Detailed Design	51
4.5.5 Materials & Manufacturing	51
4.5.6 Verification	52
4.5.7 Risk Analysis	52
4.6 Integration Plan/Process	53
5 Thrust Measurement Subsystem Design	53
5.1 Functional Requirements	53
5.2 Design Overview	54
5.3 Budgets	56
5.4 Thrust Measurement System - Structures	57
5.4.1 Structures Requirements	57
5.4.2 Interfaces	57
5.4.3 Trade Analysis	58
5.4.4 Detailed Design	59
5.4.5 Materials and Manufacturing	61
5.4.6 Verification	62
5.4.7 Risk Analysis	63
5.5 Thrust Measurement Subsystem - EMI Noise Reduction	65
5.5.1 EMI Noise Reduction Requirements	65
5.5.2 Interfaces	65
5.5.3 Trade Analysis	65
5.5.4 Detailed Design	66
5.5.5 Materials & Manufacturing	66

5.5.6 Verification	66
5.5.7 Risk Analysis	66
5.6 Thrust Measurement Subsystem - Avionics	67
5.6.1 Avionics Requirements	67
5.6.2 Interfaces	67
5.6.3 Trade Analysis	68
5.6.4 Detailed Design	68
5.6.5 Materials & Manufacturing	69
5.6.6 Verification	70
5.6.7 Risk Analysis	70
5.7 Thrust Measurement Subsystem - Calibration	71
5.7.1 Calibration Requirements	71
5.7.2 Interfaces	72
5.7.3 Trade Analysis	72
5.7.4 Detailed Design	73
5.7.5 Verification	73
5.7.6 Risk Analysis	73
5.8 Integration Plan/Process	73
6 PPT Mount Subsystem Design	74
6.1 Functional Requirements	74
6.2 Design Overview	75
6.3 Budgets	77
6.4 PPT Mount Subsystem - Structures	77
6.4.1 Structures Requirements	78
6.4.2 Interfaces	78
6.4.3 Trade Analysis	78
6.4.4 Detailed Design	80
6.4.5 Materials & Manufacturing	80
6.4.6 Verification	81
6.4.7 Risk Analysis	84
6.5 PPT Mount Subsystem - Motion Damping	84
6.5.1 Motion Damping Requirements	85
6.5.2 Interfaces	85
6.5.3 Trade Analysis	85
6.5.4 Detailed Design	87
6.5.5 Materials & Manufacturing	88
6.5.6 Verification	88
6.5.7 Risk Analysis	89
6.6 PPT Mount Subsystem - Waterfall	90
6.6.2 Interfaces	90
6.6.3 Trade Analysis	91

6.6.4 Detailed Design	91
6.6.5 Materials & Manufacturing	92
6.6.6 Verification	92
6.6.7 Risk Analysis	92
6.7 Integration Plan/Process	93
7 Data Analysis Subsystem Design	93
7.1 Functional Requirements	93
7.2 Design Overview	93
7.3 Budgets	93
7.4 Data Analysis Subsystem - DAQ	94
7.4.1 DAQ Requirements	94
7.4.2 Interfaces	94
7.4.3 Trade Analysis	95
7.4.4 Detailed Design	95
7.4.5 Verification	95
7.4.6 Risk Analysis	96
7.5 Data Analysis Subsystem - GUI	96
7.5.1 GUI Requirements	96
7.5.2 Interfaces	97
7.5.3 Trade Analysis	97
7.5.4 Detailed Design	97
7.5.5 Verification	97
7.5.6 Risk Analysis	98
7.6 Integration Plan/Process	98
8 System Conclusions	99
8.1 Integration Plan/Process	99
8.2 System Risk Analysis	99
8.3 Validation Analysis	100
8.4 Lessons Learned & Future Work	109
Team Contributors, Assignments	111
List of References	113
Version Log	114
Appendix A - Design and Analysis Code	115
Appendix B - Manufacturing Plan	129

List of Figures

Figure Title	Caption	Page #
1.3.1	Visual CONOPS	17
2.1.0.1	PPT Test Stand System Architecture	21
2.1.1.1	Chamber Interface	22
2.1.2.1	Stepper Motor and Actuation Rod	23
2.1.3.1	Flexure Locations	24
2.1.3.2	Maximum Pendulum Displacement	24
2.2.1a	Team Organizational Chart	26
2.2.1b	System Architecture Work Breakdown	26
2.3.4a	Capstone Schedule in Winter 2024	29
2.3.4b	Capstone Schedule in Spring 2024	30
3.2.1	Chamber Interface (all units in inches unless otherwise noted).	32
3.2.2	Chamber Interface Fit in VC1 (Left) and VC2 (Right) (all units in inches unless otherwise noted).	33
3.5.5.1	Soldered DB-25 electrical connection	39
3.5.7.1	Risk Analysis for Chamber Interface - Electrical Feedthrough. Likelihood is scored on a scale from 1-5. Consequence is scored on a scale from 1-5.	40
4.0.1	Leveling System Overview	41
4.4.6.1	CAD indicating the maximum deflection of the leveling system. Beyond this point, plastic deformation of the rubber isolator was predicted according to manufacturer specifications.	46
4.4.6.2	FEA results showing deflection and stresses meeting subsystem requirements. Max deflections and stresses were 0.0032 and 3.029 ksi, respectively.	47
4.5.2.1	Wiring harness location for leveling system avionics.	49
4.5.4.1	Leveling system avionics wiring diagram.	50
5.2.1	Pendulum frame(right) and pendulum(left)	53

5.2.2	Electrostatic comb location on frame(left) and on thruster shelf(right)	54
5.4.4.1	Equations used to model pendulum dynamics.	59
5.4.6.1	Cut-outs for access to flexure fasteners	62
5.4.6.2	Pin locations for supporting pendulum top during flexure change	62
5.6.2.1	Wiring harness location for laser output signal.	66
5.6.4.1	Thrust measurement avionics wiring diagram.	68
5.6.6.1	Rangefinder signal compared to CNC mill location averaged over three trials.	69
5.7.0.1	Electrostatic Comb Integration into Stand	70
5.7.2.1	Wiring harness location for calibration power	71
6.2.1	Thruster shelf designs for metal vacuum chamber(left) and crystal chamber(right)	75
6.4.6.1	Buckling data for 0.025" flexures	80
6.4.6.2	Thruster shelf centers thruster plume within 10% of the metal chamber radius	81
6.4.6.3	Thruster shelf centers thruster plume within 10% of the crystal chamber radius	82
6.5.2.1	Magnet Housing Screws	84
6.5.4.1a	Magnet housing installation on pendulum top.	86
6.5.4.1b	Conducting aluminum plate installation on removable pendulum frame	86
6.5.4.2	Annotated magnet housing (MH1) and conducting plate (MA1).	86
6.5.4.3	Damping ratio derivation	87
6.5.6.1	Pendulum Oscillation a) Without Damper, b) With Damper	88
6.6.2.1	Close up of waterfall clamp locations	89
6.6.2.2	Waterfall wiring diagram	90
7.4.2.1	Data analysis - DAQ Graphical User Interface	93

7.5.2.1	Data analysis - Leveling System Interfaces	96
8.3.1	Spring constant effect for eight 0.025" flexures.	100
8.3.2	Modeled vs. measured response of the pendulum due to a steady state force.	103
8.3.3	Settling time compared to effective spring constant for a damping coefficient of 0.3.	104
8.3.4	Measurement uncertainty for a given impulse.	105
8.3.5	Measurement uncertainty for a given steady state force.	106
8.3.6	Buckling data for 0.025" flexures	107
8.3.7	Validation of mission objective	108

Table 0.1. List of Figures

List of Tables

Table Title	Caption	Page #
0.1	List of figures	9
0.2	List of Tables	12
1.4.1	System requirements	19
2.3.1	Project Cost Budget. Yellow cells represent going into margin, green cells represent staying above margin.	27
2.3.2	Multi-subsystem Budget Summary	28
3.1.1	Chamber Interface Requirements	32
3.3.1	Chamber Interface Subsystem Budget Summary	33
3.4.1.1	Chamber interface - structures requirements	34
3.4.3.1	Structures Material Selection Matrix	35
3.4.5.1	Chamber Interface Structures Manufacturing Matrix	37
3.4.7.1	Risk Analysis for Chamber Interface - Structure. Likelihood is scored on a scale from 1-5. Consequence is scored on a scale from 1-5.	37
3.5.1.1	Chamber Interface - Electrical Feedthrough Requirements	38

4.1.1	Leveling system requirements	42
4.3.1	Leveling System Subsystem Budget Summary	43
4.4.1.1	Leveling system - structures requirements	44
4.4.4.1	Leveling system structures manufacturing matrix	45
4.4.7.1	Risk Analysis for Leveling System - Structure. Likelihood is scored on a scale from 1-5. Consequence is scored on a scale from 1-5.	48
4.5.1.1	Leveling system - avionics requirements	48
4.5.5.1	Leveling system avionics manufacturing matrix	51
4.5.7.1	Risk Analysis for Leveling System - Avionics. Likelihood is scored on a scale from 1-5. Consequences are scored on a scale from 1-5.	51
5.1.1	Thrust measurement requirements	53
5.3.1	Thrust Measurement Subsystem Budget Summary	55
5.4.1.1	Thrust measurement - structures requirements	56
5.4.3.1	Weighted decision matrix for pendulum and frame materials	58
5.4.5.1	Thrust measurement structures manufacturing matrix	61
5.4.7.1	Risk Analysis for Thrust Measurement - Structure. Likelihood is scored on a scale from 1-5. Consequences are scored on a scale from 1-5.	63
5.5.1.1	Thrust measurement - EMI noise reduction requirements	64
5.5.7.1	Risk Analysis for Thrust Measurement - EMI Noise Reduction. Likelihood is scored on a scale from 1-5. Consequences are scored on a scale from 1-5.	66
5.6.1.1	Thrust measurement - avionics requirements	66
5.6.5.1	Thrust measurement avionics manufacturing matrix	69
5.6.7.1	Risk Analysis for Thrust Measurement - Avionics. Likelihood is scored on a scale from 1-5. Consequences are scored on a scale from 1-5.	70
5.7.6.1	Risk Analysis for Thrust Measurement - Calibration. Likelihood is scored on a scale from 1-5. Consequences are scored on a scale from 1-5.	72
6.1.1	PPT mount requirements	74

6.3.1	PPT Mount Subsystem Budget Summary	76
6.4.1.1	PPT mount - structures requirements	77
6.4.3.1	Weighted decision matrix PPT mount materials	78
6.4.5.1	PPT mount structures manufacturing matrix	79
6.4.7.1	Risk Analysis for PPT Mount - Structure. Likelihood is scored on a scale from 1-5. Consequences are scored on a scale from 1-5.	82
6.5.3.1	Weight decision matrix for damping system selection	85
6.5.5.1	PPT mount motion damping manufacturing matrix	87
6.5.7.1	Risk Analysis for PPT Mount - Motion Damping. Likelihood is scored on a scale from 1-5. Consequences are scored on a scale from 1-5.	88
6.6.1.1	PPT Mount - Waterfall driving requirements.	89
6.6.5.1	PPT Mount Waterfall Manufacturing Matrix	91
6.6.7.1	Risk Analysis for PPT Mount - Waterfall. Likelihood is scored on a scale from 1-5. Consequences are scored on a scale from 1-5.	91
7.3.1	Data Analysis Subsystem Budget Summary	93
7.4.1.1	Data Analysis - DAQ Requirements	93
7.4.6.1	Risk Analysis for Data Analysis - DAQ. Likelihood is scored on a scale from 1-5. Consequences are scored on a scale from 1-5.	95
7.5.5.1	Data Analysis - GUI Requirements	95
7.5.6.1	Risk Analysis for Data Analysis - GUI. Likelihood is scored on a scale from 1-5. Consequences are scored on a scale from 1-5.	97
8.3.1	System Requirements Status	100
8.3.2	Conductive Material Quantities & Locations	101

Table 0.2 List of Tables

Acronyms

3D	3 Dimensional
AA	Aeronautics and Astronautics
CAD	Computer Aided Design
CONOPS	Concept of Operations
CVCM	Collected Volatile Compressible Material
DAQ	Data Acquisition
EMI	Electromagnetic Interference
FEA	Finite Element Analysis
GUI	Graphical User Interface
LVDT	Linear Variable Differential Transformer
NASA	National Aeronautics and Space Administration
PPT	Pulsed Plasma Thruster
SOP	Standard Operating Procedure
SPACE	Space Propulsion and Advanced Concepts Engineering
TML	Total Mass Loss

1 Introduction

This project outlines the design, construction, and testing of an inverted pendulum test stand. Its design is such that it is capable of operating in vacuum chambers with radii between 15-18", and is composed of materials such that no excessive EMI or outgassing will be generated. This stand is intended to resolve impulses from pulsed plasma thrusters ranging from 10 $\mu\text{N}^*\text{s}$ to 100 $\text{mN}^*\text{s} \pm 5 \mu\text{N}^*\text{s}$ and steady state thrusts ranging from 0.1 mN to 0.1 N \pm 0.05 mN.

This document contains descriptions of the system architecture, subsystem design and analysis, test results, system integration, and assessment of results. In addition, relevant documentation including budgets, bills of materials, part drawings, manufacturing and assembly plans, and code are included. The system architecture describes the relationships between each subsystem and how they fulfill the system requirements. Each subsystem's section details the reasoning and documentation behind its design, its manufacturing, test data analysis, and an assessment of whether the subsystem satisfied its requirements. The system integration section details the integration of each subsystem, description of system testing, and assessment of test results, concluding with an assessment of whether system requirements were met. Budgets were broken into subsections to detail the expenses associated with each subsystem, followed by a systems-level budget. The bills of materials are broken down by whether the parts referenced are manufactured, purchased, or borrowed, and highlight the quantities, materials, and manufacturing technique and/or sourcing of each part. The part drawings include dimensioned drawings and CAD files. The manufacturing and assembly plans detail the parts to be manufactured, standard operating procedures for their respective manufacturing techniques, and assembly instructions for the full system. The code includes both scripts for flexure sizing and test data analysis.

1.1 Motivation

The SPACE Lab recently acquired a new vacuum chamber from the Earth and Space Sciences department. Lab staff have designated it to be used for the purposes of characterizing pulsed plasma thruster (PPT) performance. A new test stand must be designed that can be integrated into this new chamber both the new chamber and a pre-existing composite chamber.

1.2 Mission Objectives

To design and build an operational, minimally conductive, inverted pendulum test stand for the University of Washington's SPACE Lab with the ability to accurately resolve impulses from pulsed plasma thrusters from 10 $\mu\text{N}^*\text{s}$ to 100 mN^*s and with the capacity to accommodate a variety of thruster dimensions and masses.

1.3 CONOPS

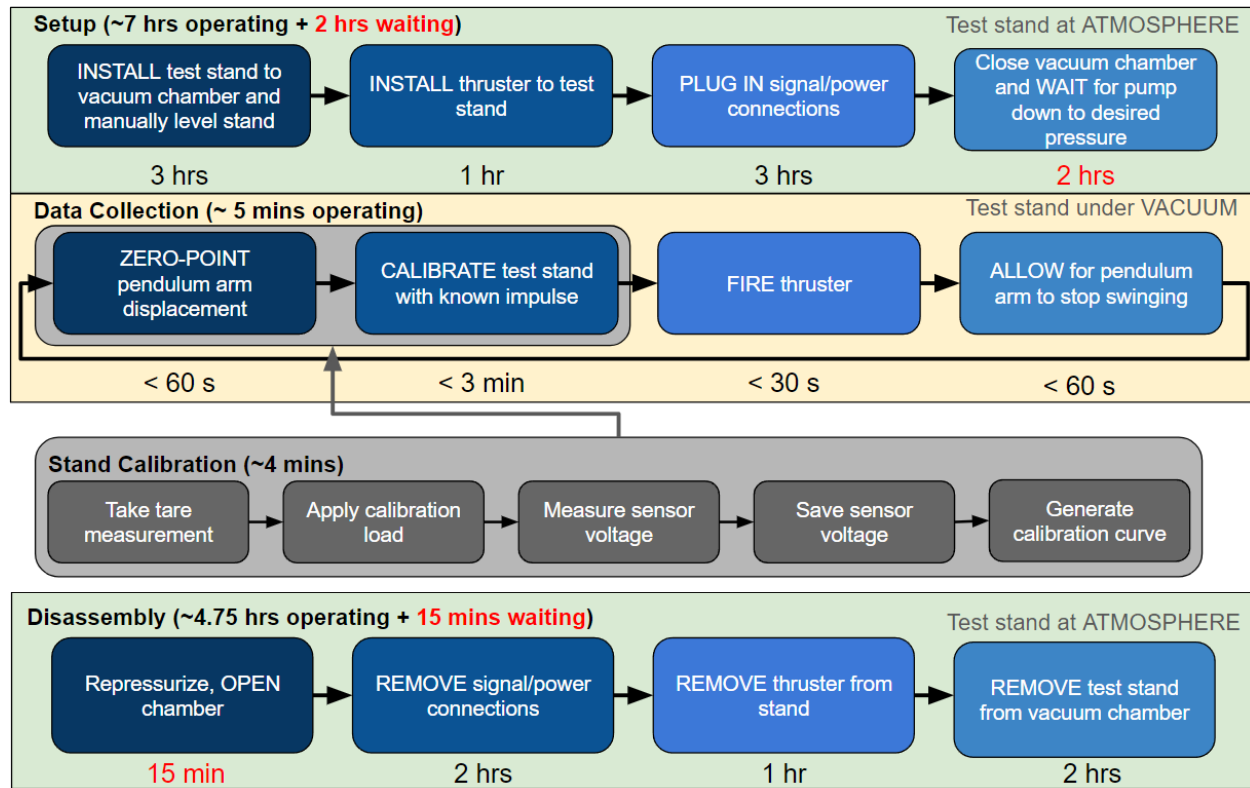


Fig. 1.3.1. Visual CONOPS

Setup:

The initial step in the setup is to physically install the test stand into the vacuum chamber. Confirm the vacuum chamber is at atmospheric pressure and open it. With 2 persons, lift the assembly (without the thruster installed) and place it inside, aligning it longitudinally with the chamber rails. Then, place the bubble level onto a rigid strut either on or above the leveling system. Next, manually level the stand, using the bubble level as a guide. Adjust until the bearing axis is level to ± 1.5 degrees. This procedure should be able to be completed within 3 hours.

The next step in setup is to install the thruster onto the test stand. First, while bringing the thruster closer to the PPT shelf, bundle the connections to the thruster such that they are easily guided toward the waterfall clamps. Then, place the thruster on the shelf. Next, secure the connections through the waterfall clamps. This procedure should be able to be completed within 1 hour.

The next step is to connect all necessary power and signal connections for both the test stand and the thruster. Wiring that connects to the pendulum must flow through the waterfall clamps. The laser rangefinder must be turned on and connected. Confirm data outflow on the oscilloscope and successful powering up of the calibration fins and thruster capacitors. This process should be able to be completed within 3 hours.

After the test stand is installed, the thruster is installed on the test stand, and all necessary power, signal, and gas connections have been made, then close the vacuum chamber and bring it down to test pressure. Pump down procedure will follow SPACE Lab protocol, using a sequence of roughing pumps and turbopumps, with final desired pressure on the magnitude of E-7 torr. This process will be completed within 2 hours.

Data Collection:

Upon completion of the setup procedure, record the nominal readout voltage transmitted to the oscilloscope. Tare the laser rangefinder at the current equilibrium point. Next, instruct the calibration fins to fire with a given voltage. Record the programmed voltage. To calibrate, set the oscilloscope to trigger, then discharge the fins. Save the rangefinder output's trace recorded on the oscilloscope. This will be completed in 15 minutes.

To test, confirm the system has damped to 2% of equilibrium. Set the oscilloscope to trigger, then fire the thruster. Save the rangefinder output's trace recorded on the oscilloscope. The timescale between tests should be within 5 minutes.

Disassembly:

Once testing is complete the disassembly process can begin. Bring the chamber back up to atmospheric pressure. Repressurization procedure will follow SPACE Lab protocol. This process should be able to be completed within 15 minutes. Once repressurization is complete, open the chamber.

Remove all connections to the PPT and test stand. This process should be able to be completed within 3 hours.

Remove the PPT from the test stand. This process should be able to be completed within 1 hour.

The final step in the disassembly procedure is to remove the test stand from the vacuum chamber. This process should be able to be completed within 3 hours.

1.4 System Requirements

ID	Requirement	Verification Method
Sys. 1	Test stand must be an inverted pendulum style	<i>Inspection</i>
Sys. 2	Test stand shall minimize the use of conductive materials	<i>Inspection</i>
Sys. 3	Test stand must be able to resolve a minimum stand	<i>Test</i>

	deflection of half the lowest predicted deflection such that impulse bits ranging from $2.25 \mu\text{lbf}^{\text{s}}$ to $22.5 \text{ mlbf}^{\text{s}} \pm 1.12 \mu\text{lbf}^{\text{s}}$ ($10 \mu\text{N}^{\text{s}}$ to $100 \text{ mN}^{\text{s}} \pm 5 \mu\text{N}^{\text{s}}$) can be measured	
Sys.4	Test stand must be able to resolve a minimum stand deflection of half the lowest predicted deflection such that steady-state thrusts ranging from $22.5 \mu\text{lbf}$ to $22.5 \text{ mlbf} \pm 11.3 \mu\text{lbf}$ (0.1 mN to $0.1 \text{ N} \pm 0.05 \text{ mN}$) can be measured	<i>Test</i>
Sys.5	Test stand must be able to support thrusters up to 17.6 lbf without buckling	<i>Analysis</i>
Sys.6	Test stand must accommodate thruster diameters up to 10.0 in , and thruster lengths up to 9.1 in	<i>Demonstration</i>
Sys.7	Test stand shall be able to be horizontally leveled to within $\pm 0.05 \text{ degrees}$	<i>Demonstration</i>
Sys.8	Test stand must return thruster to $0.002 \pm 0.001 \text{ degrees}$ of zero-point between tests	<i>Test</i>
Sys.9	The stand must be installed, securely operated, and safely removed from the vacuum chamber without causing any structural or cosmetic damage to the	<i>Inspection</i>

	chamber wall	
--	--------------	--

Table 1.4.1: System requirements

2 Project Overview

The purpose of this project is to design, build, and verify an inverted pendulum test stand to characterize the performance of PPTs, which have distinctly low impulses (on magnitudes of 10 $\mu\text{N}\cdot\text{s}$ to 100 $\text{mN}\cdot\text{s}$). Over the next sections the organization, design, and verification processes will be given in detail.

The order of content in this section will start with a detailed system architecture, which lays out the subsystems of the project. The next subsection will be the work breakdown structure, which will expand on the system architecture, detailing what roles each member of the team filled with regards to the subsystems. The system schedule and budget will then be detailed, which will include monetary budget for each subsystem, as well as size, weight, and power budgets.

Sections 3 through 7 will focus on the design of the test stand through its subsystem blocks, which will be detailed in subsection 2.1. Information on each subsystem will be broken down as follows: Functional requirements, design overview, budgets, and each subsystem's sub-block (e.g, chamber interface - structures). Going into detail, the functional requirements section will describe how this functional block supports the design of the total system through requirements or the mission objective. A design overview will then be given, which will go over how each subsystem will function, as well as all relevant specifications. A budget breakdown of each given subsystem will then be shared in more detail than the previous section. The details of each subsystem sub-block will then be given in the accompanying subsubsections, which will discuss: All subsystem requirements, interfaces between subsystems where failure is most likely to occur, all relevant trade studies conducted to advance design ideas, and all detailed design of each subsystem sub-block. The verification section will discuss the likelihood that each subsystem requirement will be met. This will be followed by a detailed risk analysis, which will discuss potential risks associated with each subsystem, and how they may or may not impact the test stand as a whole. Next, a detailed breakdown of each subsystem budget will be given, including how each budget was spent. And the design section will close with how each subsystem will be integrated, and how each subsystem was tested and verified.

2.1 System Architecture

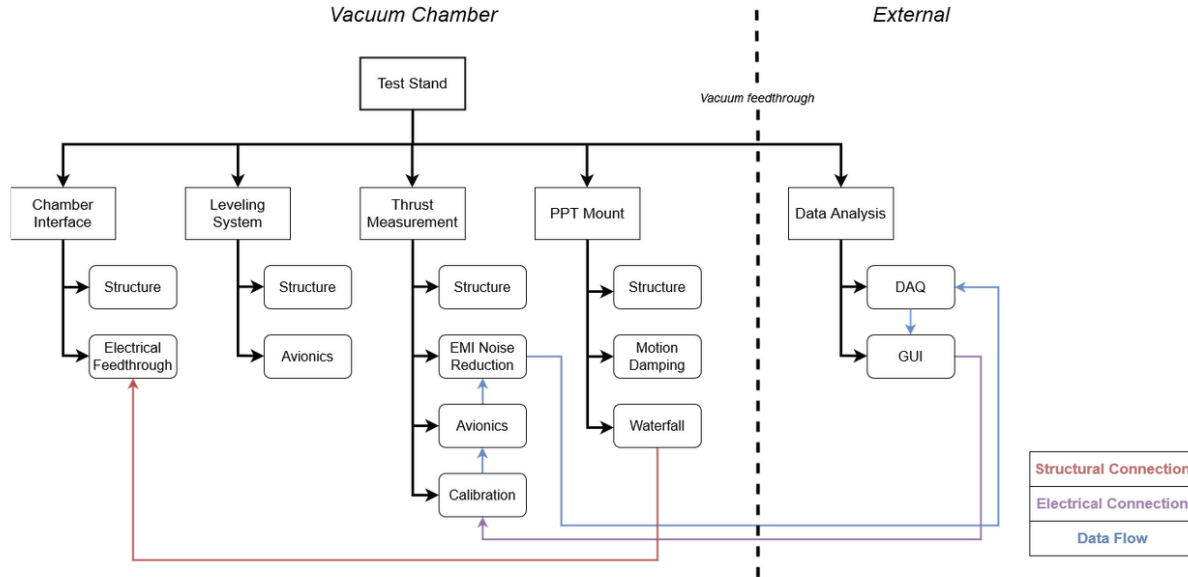


Fig. 2.1.0.1. PPT Test Stand System Architecture

The test stand system architecture exists in two different locations: Inside and outside of the vacuum chamber, with a vacuum feedthrough connecting the two sides of the architecture. Within the vacuum chamber there are four main systems: Chamber interface, leveling system, thrust measurement, and PPT mount. The system external to the vacuum chamber is data analysis. The test stand system was divided into these 5 respective subsystem blocks to correspond to the 5 primary functions of the fully integrated system; the stand sits stably in the chamber environment, be able to pitch such that it is level, collect thrust data, mount the PPT, and process thrust data. All components that exist inside the vacuum chamber will be inspected such that the system minimizes the use of conductive materials (Sys.2).

2.1.1 Chamber Interface

The chamber interface subsystem, which is any component of the test stand that is in direct contact with the vacuum chamber body, is broken down into two subsystem sub-blocks: structures and electrical feedthrough. Through demonstration, the chamber interface structure is verified to: not cause structural or cosmetic damage to the chamber wall (Sys.9), and pitch the stand level to ± 0.05 degrees (Sys.7). Of the total budget, the chamber interface utilized \$194.43 (4%) of the total budget. Going into the subsystem sub-blocks, the structure subsystem sub-block of the chamber interface system exists as the lower portion of the test stand structure. The structure interfaces with the chamber through the four feet on the bottom of the test stand structure.

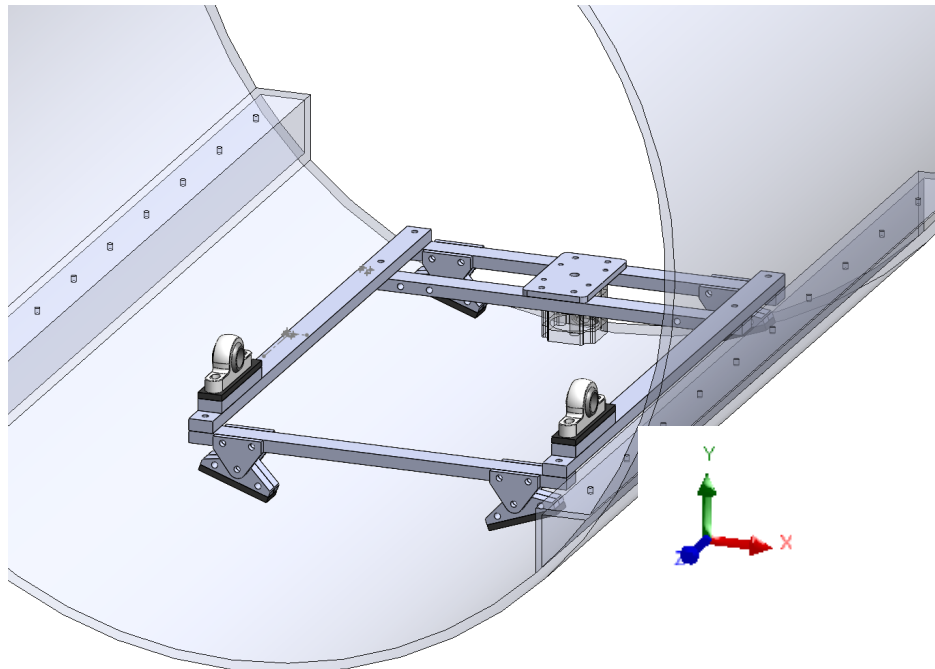


Figure 2.1.1.1. Chamber Interface

The electrical feedthrough subsystem sub-block encompasses the connectors and feedthroughs for all power and electrical signals going through the vacuum chamber.

2.1.2 Levelling System

The leveling system subsystem, which is any component of the test stand that acts to or is acted upon to bring the test stand back to a horizontally level state, is broken into two subsystem sub-blocks: Structure and avionics. These components were demonstrated to assist the stand in pitching it level to ± 0.05 degrees (Sys.7), and tested to be able to return the stand to a zero point between 0.002 ± 0.001 degrees (Sys.8). By the end of the project, the leveling system used \$356.96 (7%) of the total budget. Going into the subsystem sub-blocks, the structure subsystem sub-block of the leveling system is the middle portion of the test stand frame. It supports both the pendulum and pendulum frame, and pivots on nylon bushings resting on the chamber interface subsystem. There is a stepper motor pushrod that pitches the structure subsystem sub-block up and down to level the system with the use of a bubble level.

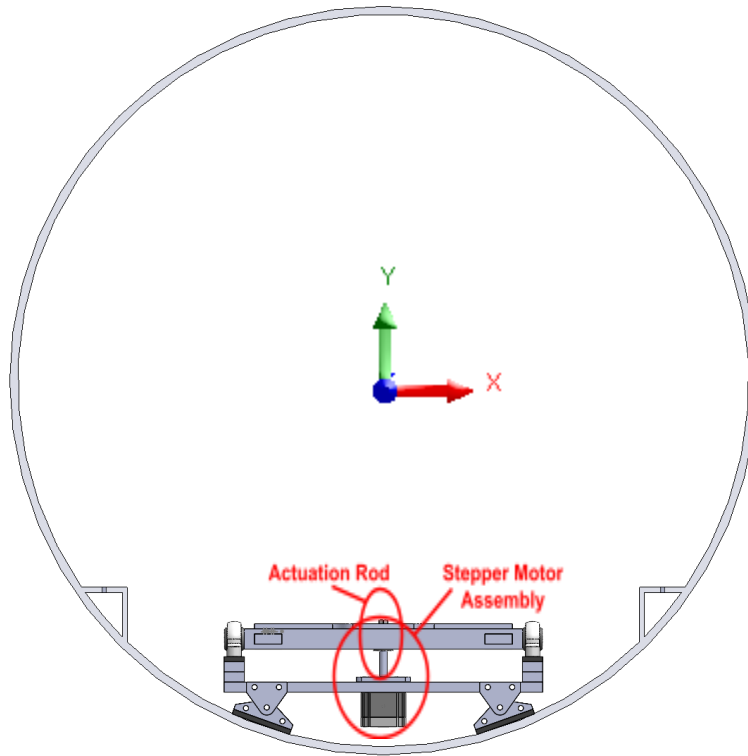


Figure 2.1.2.1. Stepper Motor and Actuation Rod

The avionics of this subsystem serve to power and control the stepper motor pushrod, such that it is able to level the stand. The motor rests on the undercarriage of the chamber interface system, on the side of the frame opposite to the direction of thrust. This motor is powered via an electrical connection through the chamber interface subsystem and waterfall subsystem sub-block.

2.1.3 Thrust Measurement

The thrust measurement subsystem is any component of the test stand directly responsible for physically measuring any parameter used to determine thrust produced by the PPT. It was inspected to be an inverted pendulum style (Sys.1), tested to be able to capture impulse bits (Sys.3), and data from the subsystem was analyzed to capture steady-state measurements (Sys.4). By the end of the project, the thrust measurement subsystem utilized \$1147.05 (24%) of the total budget. The subsystem is broken into four subsystem sub-blocks: Structure, EMI noise reduction, avionics, and calibration. The structure subsystem sub-block of the thrust measurement system consists of both the pendulum and the pendulum frame, both of which mount to the structure subsystem sub-block of the leveling system. There are 4 pendulum legs, each containing 2 spring steel flexures.

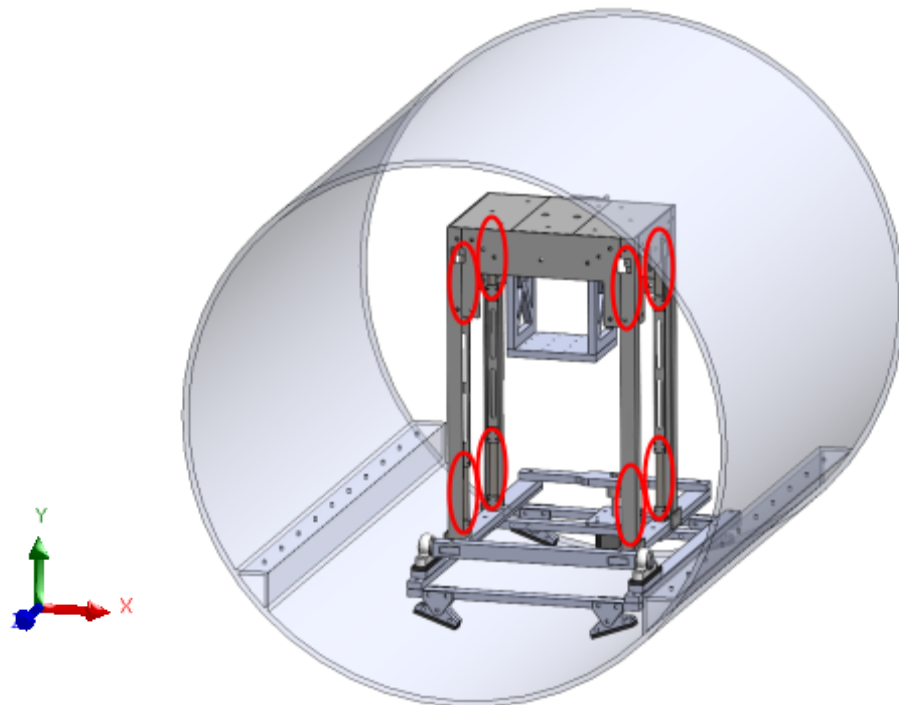


Figure 2.1.3.1. Flexure Locations

The spring steel flexures of the pendulum allow it to deflect in response to thruster impulses, while the pendulum frame acts as a physical stopper for the pendulum, resting as a rigid shell around the system and allowing it to displace a maximum of 0.197 inches.

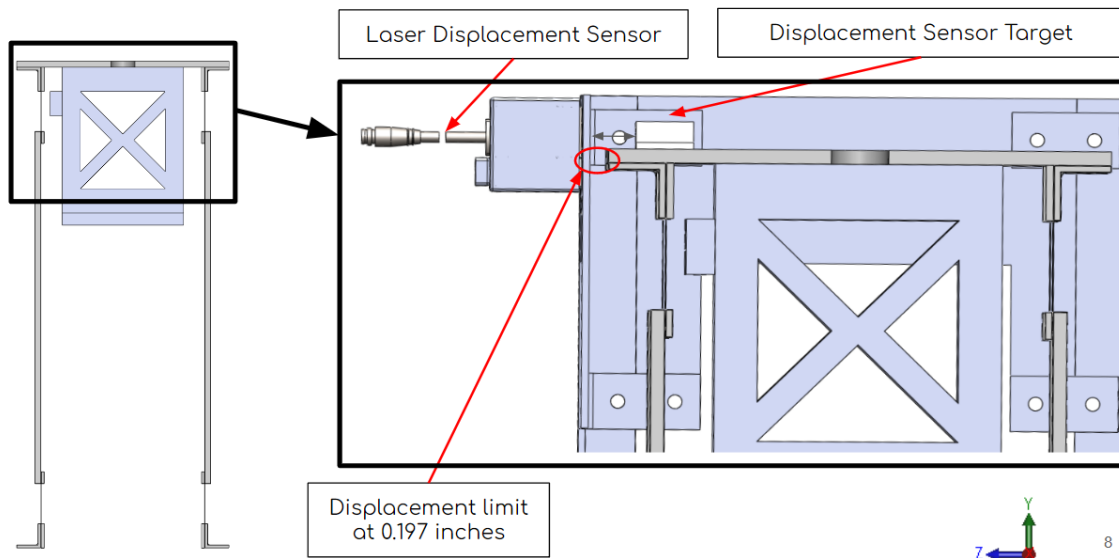


Fig. 2.1.3.2. Maximum Pendulum Displacement

To meet the impulse and steady-state requirements of Sys.3 and Sys.4, a total of 4 sets of flexures were manufactured. Next, all connections to the thrust measurement system must be shielded from EMI generated during the firing of the PPT. This shielding is composed of copper wire sheaths in the EMI subsystem sub-block. Additionally, data is captured during the operation of the test stand in the avionics subsystem sub-block. The deflection of the stand is captured by an IL-030 laser rangefinder, which is located in a housing attachment fastened away from the firing area on the pendulum frame. The laser points into the stand to an area of the moving pendulum, such that its deflection is captured while being as isolated from the PPT pulse as possible. The information is passed through an amplifier, then to an oscilloscope. The calibration subsystem sub-block will use electrostatic fins provided by the SPACE Lab, which will generate a fixed thrust when supplied with a voltage. There is a volume designated for the installation of this device on the pendulum such that it pulses in the same direction as a test thruster.

2.1.4 PPT Mount

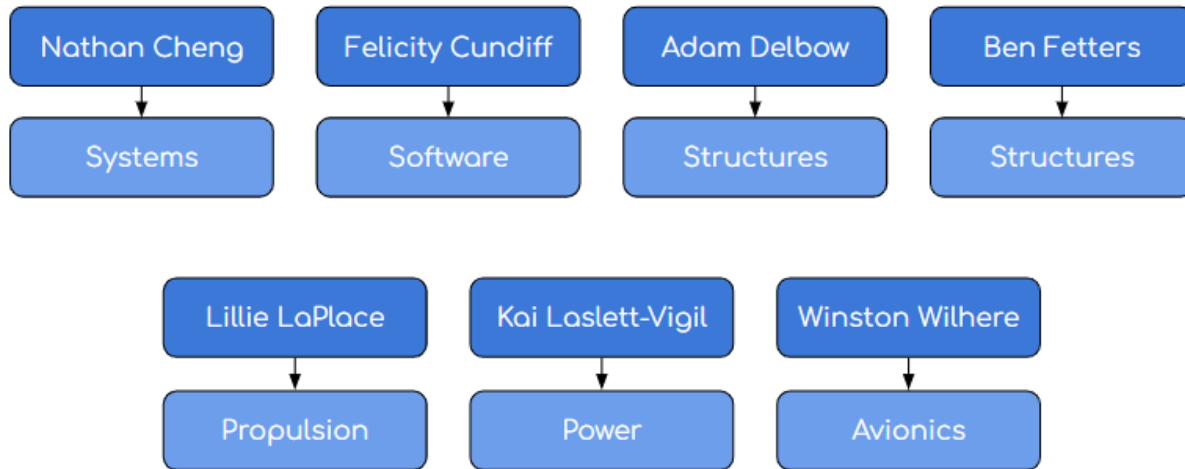
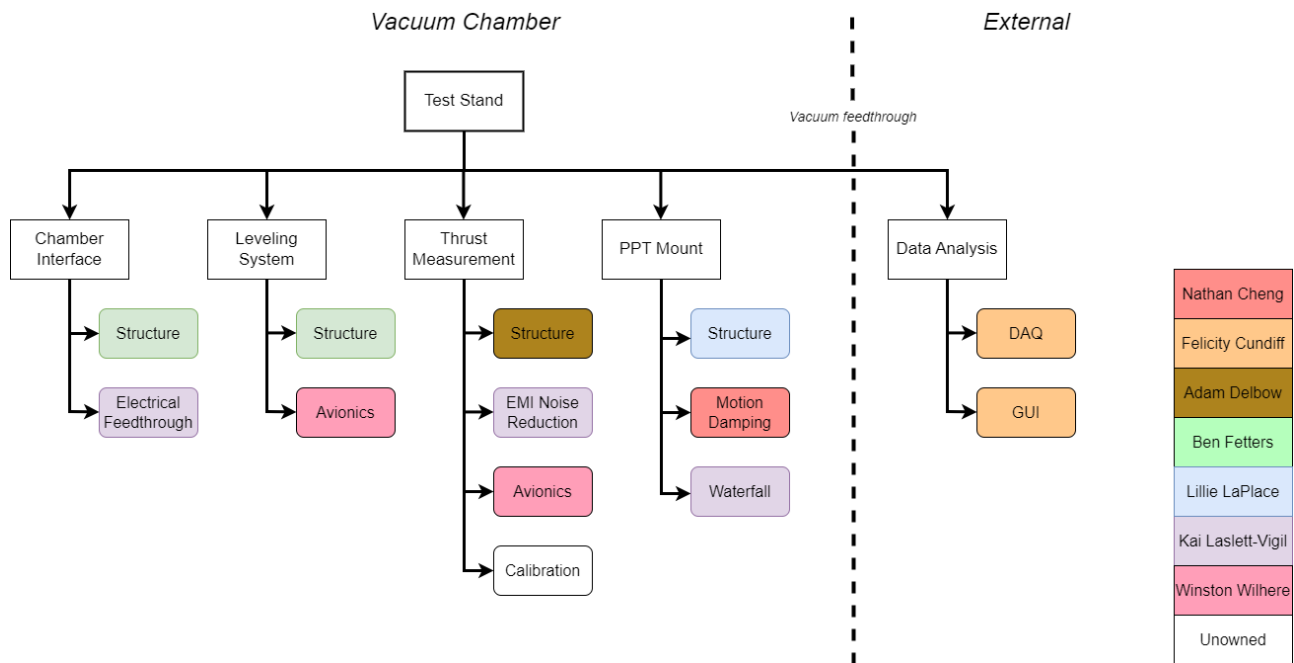
The PPT mount subsystem is where the PPT physically interacts with the thrust stand to produce displacements used to measure thrust/impulse produced by the thruster. It will be tested to ensure it is capable of supporting thrusters up to 8 kg (Sys.5) and demonstrated to accommodate an upper limit of thruster diameters of 10" and lengths of 9.1" (Sys.6). This subsystem ultimately used \$447.15 (9%) of the total budget. The subsystem is broken into three subsystem sub-blocks: Structure, motion damping, and waterfall. The structure subsystem sub-block of the PPT mount is the shelf the thruster sits on during the test that bolts to the underside of the pendulum top. It is constructed out of a Delrin thermoplastic. The motion damping subsystem sub-block is made up of 2 parts: an aluminum plate adhered to the face of the rigid pendulum frame, and opposite to it a magnet fixed in place with a housing on the pendulum. This configuration works as an eddy current brake, damping the system response such that it returns the stand to an equilibrium position on a timescale of ~30 seconds when under vacuum. The waterfall subsystem sub-block consists of the wire bundles connecting from the vacuum chamber feedthroughs to the locus clamped onto the pendulum frame and shelf. It is configured such that it produces a constant spring constant during the stand's deflection.

2.1.5 Data Analysis

Outside the vacuum chamber is the data analysis subsystem, which is responsible for receiving voltages produced by any sensors and converting them into usable data. It is broken into two subsystem sub-blocks: DAQ and GUI. Instead of utilizing a traditional DAQ system, the thrust measurement setup interfaces with an oscilloscope for data acquisition purposes. On the other hand, the GUI sub-block is responsible for displaying the information collected by the thrust measurement subsystem in a user-friendly manner. In terms of budget allocation, the data analysis subsystem accounts for \$103.81 (2%) of the total project budget.

2.2 Work Breakdown Schedule (WBS)

Work was divided among the 7 team members as follows: Nathan Cheng is the systems lead, Felicity Cundiff is the software lead, Adam Delbow and Ben Fetter are structures leads, Lillie LaPlace is the propulsion lead, Kai Laslett-Vigil is the power lead, and Winston Wilhere is the avionics lead. With regard to the system architecture, all team members contributed to all subsystem sub-blocks; Fig. 2.2.1 b organizes the team members primarily responsible for each subsystem sub-block.

**Fig. 2.2.1 a. Team Organizational Chart****Fig. 2.2.1 b. System Architecture Work Breakdown**

2.3 Schedule & Budgets

The total project budget was \$4900. \$4506.63 was spent, leaving \$393.37 remaining. Table 2.3.1 breaks down the expenditures at the subsystem level. Of all subsystems, chamber interface, leveling system, thrust measurement, Multi-subsystem went into margin (yellow), while PPT mount, data analysis, and others were above margin (green).

Subsystem	Limit	Margin	Allocated	Used	Available
Chamber Interface	\$ 200	15%	\$ 170	\$ 194.43	\$ 5.57
Leveling System	\$ 400	15%	\$ 340	\$ 356.96	\$ 43.04
Thrust Measurement	\$ 1200	30%	\$ 840	\$ 1147.05	\$ 52.95
PPT Mount	\$ 500	10%	\$ 450	\$ 430.61	\$ 69.39
Data Analysis	\$ 150	30%	\$ 105	\$ 103.81	\$ 46.19
Multi-subsystems	\$ 2250	15%	\$ 1912.5	\$ 2126.42	\$ 123.58
Other	\$ 200	15%	\$ 170	\$ 147.35	\$ 52.65
Total	\$ 4900	19%	\$ 3987.5	\$ 4506.63	\$ 393.37

Table 2.3.1. Project Cost Budget. Yellow cells represent going into margin, green cells represent staying above margin.

Items that were purchased and used in multiple subsystems were categorized into the multiple-subsystems category. These consisted of structural components among manufacturing and safety equipment. Overall, these purchases accounted for \$2126.42 (43%) of the total budget. Table 2.3.2 itemizes every purchase made during the project.

Category	Item	Cost	Total
Structure	Fiberglass screws	\$ 12.50	\$ 2126.42
	Nylon screws	\$ 13.44	
	Steel screws	\$ 29.98	
	.5" Garolite	\$ 390.26	
	.125" Garolite	\$ 98.85	
	PETG plastic	\$ 55.14	
	Vacuum epoxy	\$ 130.37	
	Nitrile gloves	\$ 26.38	
	Garolite angle, 1"	\$ 774.16	
	Garolite angle, 2"	\$ 238.98	
	Assorted nuts & bolts	\$114.24	

	Steel nozzle	\$ 29.69	
	Abrasice garnet	\$ 212.33	
			\$ 2126.42

Table 2.3.2. Multi-subsystem Budget Summary

The project schedule includes the Winter 2024 and Spring 2024 academic quarters. Weeks 1-11 of Winter 2024 encompass 1/3/2024 - 3/15/2024, while weeks 1-11 of Spring 2024 encompass 3/25/2024 - 6/4/2024. Each major section of the schedule breaks down the tasks being completed for the structure, avionics, software, and greater system. Winter quarter primarily consisted of conducting trade studies and design work, as project goals were oriented toward preliminary design review in week 4 and critical design review in week 10. Materials ordering started in Winter and carried over into Spring. Spring quarter consisted of manufacturing and testing of materials and conducting system-wide tests. Major presentations in this quarter consisted of test readiness review in week 8 and acceptance review in week 11. Figure 2.3.4. tabulates this information.

Winter 2024

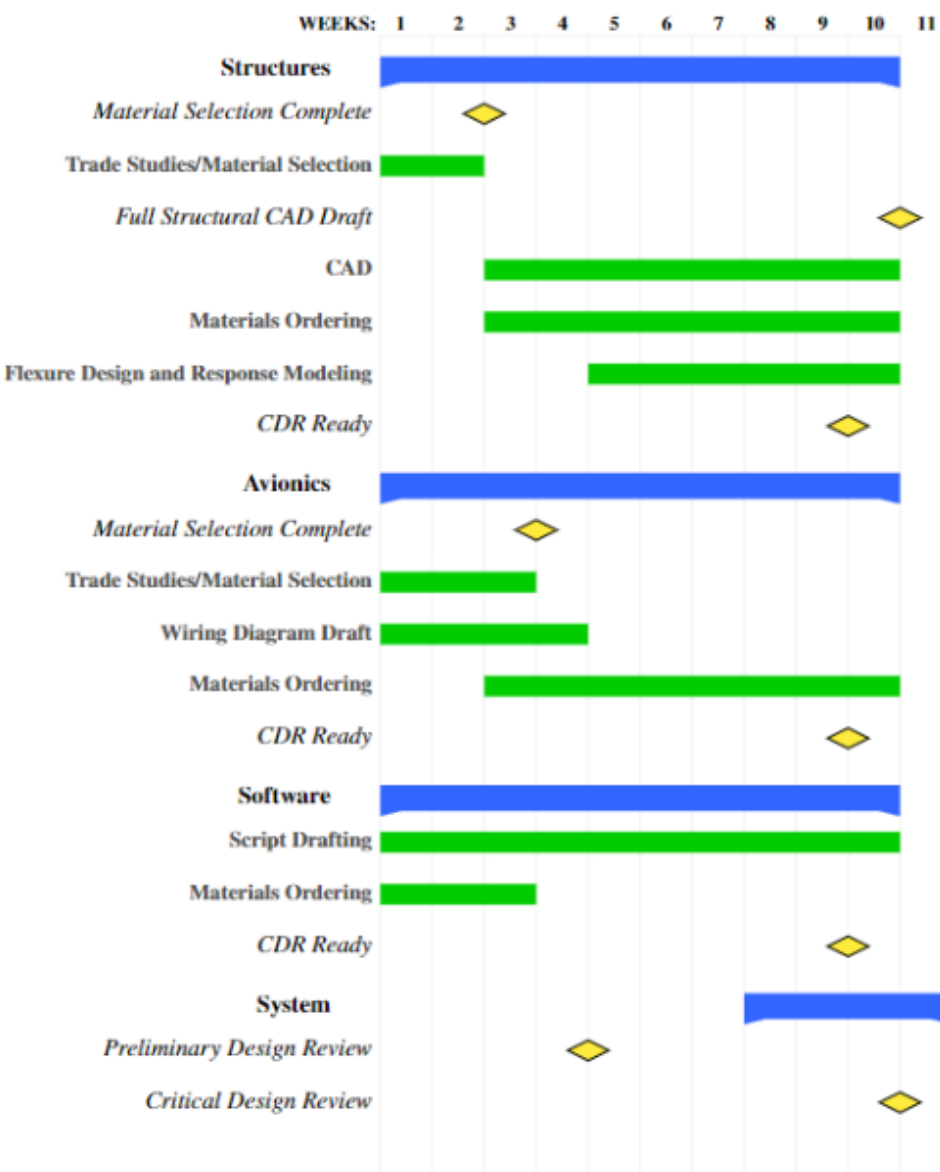


Figure 2.3.4.a. Capstone Schedule in Winter 2024

Spring 2024



Figure 2.3.4.b. Capstone Schedule in Spring 2024

3 Chamber Interface Subsystem Design

The following section will discuss the design of the chamber interface subsystem. This subsystem has components for structures and electrical feedthrough that involve how the test stand will interact with the chamber. The structure of the test stand will be in constant contact with the chamber walls, which will make for several structure requirements related to chamber

interface. Power, ground, and signal lines for the test stand sensors must pass through the chamber walls, which will make for several electrical feedthrough requirements related to chamber interface.

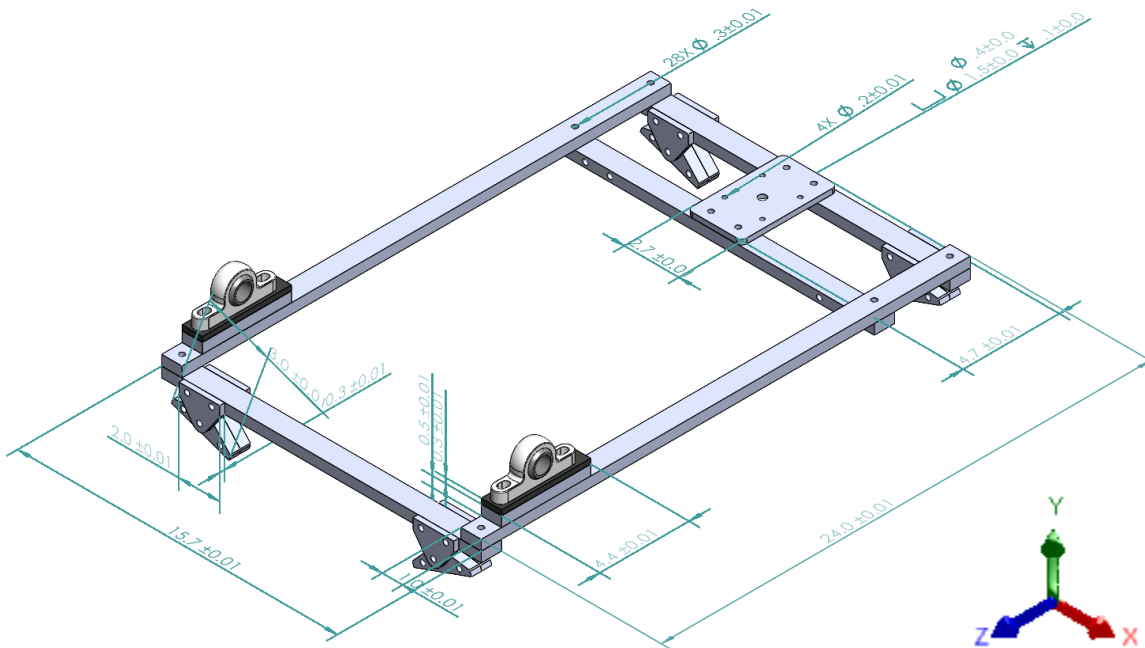
3.1 Functional Requirements

ID	Requirement	Verification Method
Ci.1	Test stand must fit inside a vacuum chamber with an 18 inch radius of curvature, and be able to adapt to a minimum radius of curvature of 15 inches.	<i>Inspection</i>
Ci.2	Chamber interface must not scratch vacuum chamber walls.	<i>Inspection</i>
Ci.3	Chamber interface must be isolated from vibrations from vacuum chamber walls in accordance with SPACE Lab standards.	<i>Inspection</i>
Ci.4	Chamber interface must not exceed 0.04 inches of deflection under the weight of overlying subsystems.	<i>Analysis</i>
Ci.5	Chamber interface assembly must have a minimum safety factor of 2.5	<i>Analysis</i>
Ci.6	Have sufficient number of connection inputs to support test stand and PPT	<i>Inspect</i>
Ci.7	Electrical feedthroughs shall be able to interface with the flanges provided by the SPACE Lab	<i>Inspect</i>

Ci.8	Ground sources shall comply with SPACE Lab standards on grounding	Test
-------------	---	------

Table 3.1.1: Chamber Interface Requirements

3.2 Design Overview

**Figure 3.2.1. Chamber Interface (all units in inches unless otherwise noted).**

The chamber interface is designed to facilitate the operation of the test stand in multiple testing environments, including VC1 and VC2. Its pivoting feet allow the stand to accommodate vacuum chambers ranging from 15-18 inches in radius. It also provides mounting surfaces on which the leveling system pivot and stepper motor actuation rod interface. Its design ensures that vibrations generated by the lab environment, including vacuum pump vibrations are damped to reduce the noise generated in the thrust measurement's system output trace.

Additionally the electrical feedthrough component of the chamber interface sub-system facilitates the transmitting of power and signals between the internal and external hardware utilized for this system.

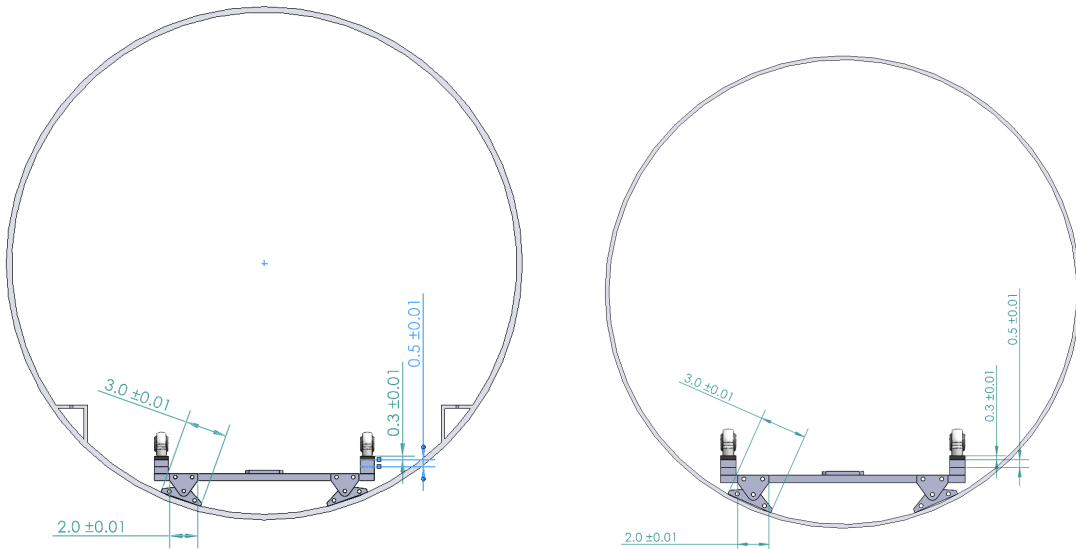


Figure 3.2.2. Chamber Interface Fit in VC1 (Left) and VC2 (Right) (all units in inches unless otherwise noted).

3.3 Budgets

Of the total budget, the chamber interface utilized \$194.43 (4%) of the total budget. Table 3.3.1. itemizes each purchase

Category	Item	Cost	Total
Structure	Buna-N Rubber	\$ 74.87	\$ 74.87
Avionics	DB 25 Connector	\$ 22.82	\$ 119.56
	High Temperature Stranded Wire	\$ 96.74	
			\$ 194.43

Table 3.3.1. Chamber Interface Subsystem Budget Summary

3.4 Chamber Interface Subsystem - Structures

The main functions of the structure subsystem sub-block of the chamber interface is to ensure the test stand fits inside the chamber, the test stand can rest on the chamber walls without causing damage to the walls, and to isolate the test stand from vibrations from laboratory equipment being transmitted through the chamber walls. The chamber interface must also be capable of supporting the weight of the pendulum, frame, thruster being tested, and the leveling system with minimal structural deflection.

3.4.1 Structures Requirements

ID	Requirement	Verification Method
Ci.1	Test stand must fit inside vacuum chamber with 18 inch radius of curvature, and be able to adapt to a minimum radius of curvature of 15 inches.	<i>Inspection</i>
Ci.2	Chamber interface must not scratch vacuum chamber walls.	<i>Inspection</i>
Ci.3	Chamber interface must be isolated from vibrations from vacuum chamber walls in accordance with SPACE Lab standards.	<i>Inspection</i>
Ci.4	Chamber interface must not exceed 0.04 inches of deflection under the weight of overlying subsystems.	<i>Analysis</i>
Ci.5	Chamber interface assembly must have a minimum safety factor of 2.5	<i>Analysis</i>

Table 3.4.1.1: Chamber interface - structures requirements

3.4.2 Interfaces

The primary interface for the chamber interface structures component is between the structure of the chamber interface system and the walls of the vacuum chamber. To avoid scratching and minimize vibrations transmitted through the chamber walls to the test stand, four rubber feet will be fitted to the part of the structure that actually contacts the chamber walls. This gives a total of four physical interface points between the structural component of the chamber interface subsystem and the vacuum chamber walls.

The second interface is with the structural component of the leveling system. The motor for the leveling system bolts to one end of the chamber interface using 4 bolts, and the threaded push rod for the leveling system passes through a hole in the chamber interface. At the opposite end of the chamber interface, the leveling system is allowed to pivot on the two nylon bushings bolted to the chamber interface. This gives a total of 3 physical interface points between the structural components of the chamber interface system and the leveling system.

The third interface is between the pendulum's waterfall wire bundle and an attachment point at the top of the vacuum chamber's inner diameter. This will be affixed as needed to the chamber walls through the use of a laminated adhesive strip. See attached Test Stand Assembly Procedures document for integration plan with avionics and the rest of the structure of the system.

3.4.3 Trade Analysis

G10 Garolite was ultimately selected for its structural rigidity and nonconductivity as the primary structural material in the chamber interface. Buna-N rubber was selected for vibrational damping, scratch-resistance at the chamber interface, and its vacuum-compatibility. It was specifically recommended by our advisor as the material currently in use within the SPACE Lab.

Material	Weight	Garolite	Carbon Fiber Filled PET-G	PLA
Machinability	0.1	0.4	0.5	1
Cost	0.2	0.5	1	1
Vacuum Compatibility	0.3	1	0.5	0.4
Density	0.2	0.75	1	0.5
Yield Strength	0.2	1	0.3	0.1
Total	1	0.79	0.66	0.54

Table 3.4.3.1 Structures Material Selection Matrix

3.4.4 Detailed Design

The chamber interface sub-system serves the purpose of providing a stable base between the test stand and vacuum chamber walls. Its primary objectives include damping vibrations from outside the vacuum chamber, ensuring proper fit within the chamber, preventing scratching of chamber walls, isolating from chamber wall vibrations, limiting deflection under load, and maintaining a high safety factor.

The subsystem comprises two major parts: feet and structural struts. The feet, constructed from Buna-N rubber and G10 Garolite, are designed to dampen vibrations from the chamber walls and conform to different diameters of vacuum chambers with pivoting feet to accommodate both VC-01 and VC-02's diameters. The chamber feet were designed based on SPACE Lab precedent, with the Buna-N rubber pad interfacing with the vacuum chamber. Their dimensions and mass are specified in the "Test Stand Technical Drawings" file. Similarly, the structural struts, made from Garolite, provide rigid structural support to the system. Their dimensions and mass are also detailed in the technical drawings.

The overall geometry of the chamber interface was determined based on limitations due to vacuum chamber geometry. Additionally, FEA conducted using SolidWorks Simulation helped find maximum deflections and stresses in parts. The FEA results indicated minimal deflection and low stress levels, with a factor of safety above 19 for all components, validating the design's structural integrity.

Detailed drawings and specifications can be found in the [Test Stand Technical Drawings](#) document, offering information on dimensions and material specifications.

3.4.5 Materials & Manufacturing

The chamber interface is composed of three materials: G10 Garolite, Buna-N rubber, and nylon screws. Initially, 3D printed materials were assessed for suitability, but due to concerns with outgassing, air entrapment and decompression under vacuum, and structural rigidity, were not ultimately selected. Garolite was selected for its structural rigidity and electrically insulating properties, as the material for both the radial and longitudinal struts and pivot. As a vacuum-rated rubber, Buna-N was selected as the material of choice for the chamber interface feet. The rubber's pliability ensured that in tandem with the rotating foot pivots, the chamber interface would conform to both VC-1 and VC-2's diameters without slippage or vibrational transfer. Nylon screws were selected for their durability under our loading conditions and non-conductivity.

A variety of manufacturing techniques were employed to produce the chamber interface's parts. Using exported .dxf files from the assembly CAD, the radial and longitudinal struts and feet were waterjetted out of 0.25" Garolite sheet stock. Similarly, the foot brackets were waterjetted out of 0.125" sheet stock. A significant challenge with this approach was the delamination of the Garolite upon attempting to pierce holes. Even with thinner sheet thickness, this issue persisted, leading to the holes in each part to be drilled manually. To drill the holes in each part, a paper .dxf template was laser cut using a Universal Laser System ILS12.75 laser cutter and aligned and taped to each part post-waterjetting to guide drilling. Each hole was either drill pressed or milled, depending on mill availability in the AA shop. Due to high demand of the AA mill from other capstones and calibration challenges, the drill press was the primary device used throughout this project.

The Buna-N sheets were planned to be cut out into rectangular pads to fit under the chamber interface feet. They were planned to be affixed using vacuum adhesive from the SPACE Lab. The upper feet were initially waterjetted, but due to a problem with the MSE department's axis leveling system, some had damage around their edges. Extra parts were cut, and those with the least damage would have been used in the full chamber interface assembly, had the system not been descoped.

Chamber Interface Structure System Manufacturing Matrix			
Part Name	Material	Manufacturing Technique	Quantity
Longitudinal Strut C2	1/2" G10 Sheet	Waterjet, drill press holes	2

Radial Strut C2	1/2" G10 Sheet	Waterjet, drill press holes	3
Chamber Interface Feet (Upper)	1/2" G10 Sheet	Waterjet, drill press holes	8
Chamber Interface Feet (Lower)	Buna-N Rubber Sheet	Not manufactured, planned to cut to size with shears	4
Chamber Interface Feet Mount	1/8" G10 Sheet	Waterjet, drill press holes	8
Chamber Interface Bearing Doubler	1/2" G10 Sheet	Waterjet, drill press holes	2
Chamber Interface Bearing Damper	Buna-N Rubber Sheet	Not manufactured, planned to cut to size with shears	4

Table 3.4.5.1. Chamber Interface Structures Manufacturing Matrix

3.4.6 Verification

Due to time constraints limiting the team's manufacturing capability, the chamber interface components were not integrated into the full system, and the chamber interface was ultimately descoped. However, the chamber interface's full integration into the test stand was simulated within the full SolidWorks assembly for the project without any interference or other visible impediments to system integration.

3.4.7 Risk Analysis

The most significant risk with the chamber interface subsystem is insufficient vibration damping from operation of the pumps. The vibrations contribute to noise in test data, which could potentially make it unusable. Additionally, the stand cannot damage the SPACE Lab vacuum chambers. The strategy put in place was to install vacuum-rated rubber (Buna-N) feet to the stand, such that the material properties of Buna-N dampen vibrations and create a flexible physical interface between the stand assembly and the vacuum chamber.

Deflection in the stand could also occur under the weight of the assembly. To mitigate this risk, the struts of the chamber interface system have been designed to accommodate a doubler at the point of deflection.

#	Risk Description	Mitigation	Likelihood	Consequence
1	Vibrational noise	Use of Buna-N rubber feet	2	5
2	Scratching chamber walls	Use of Buna-N rubber feet	1	2
3	Structural deflection	Designed for doubler installation	1	2

Table 3.4.7.1. Risk Analysis for Chamber Interface - Structure. Likelihood is scored on a scale from 1-5. Consequences are scored on a scale from 1-5.

3.5 Chamber Interface Subsystem - Electrical Feedthrough

The main purpose of the electrical feedthrough subsystem is to enable the hardware components to be powered and controlled from outside the chamber walls. Due to the large E&M fields that will be generated from the PPT, is it easier to move all of the necessary hardware and power supplies outside of the chamber than to attempt to provide all the EMI shielding that would be necessary to make the equipment operational within the vacuum chamber. Additionally this feedthrough system allows the leveling system stepper motor to be actively controlled remotely as the need occurs throughout testing.

3.5.1 Electrical Feedthrough Requirements

ID	Requirement	Verification Method
Ci.6	Have sufficient number of connection inputs to support test stand and PPT	<i>Inspect</i>
Ci.7	Electrical feedthroughs shall be able to interface with the flanges provided by the SPACE Lab	<i>Inspect</i>
Ci.8	Ground sources shall comply with SPACE Lab standards on grounding	<i>Test</i>

Table 3.5.1.1. Chamber Interface - Electrical Feedthrough Requirements

3.5.2 Interfaces

The structure of the electrical feedthrough system will be mounted to either side of the flanges that are installed into the vacuum chamber, with the flanges acting as a ground for the connectors in accordance with SPACE Lab SOP. All the necessary wire bundles used to power the internal hardware, and transmit data to the data acquisition system will be run through the electrical feedthrough system. An important note: the wire bundle that powers the PPT itself will be run through a separate electrical feedthrough system set up by the SPACE Lab.

3.5.3 Trade Analysis

The SPACE Lab requested that the connectors used for this project be BD-25 compatible, and have a body primarily made of metal. Aside from the specifications given by the customer, the electrical feedthrough system must be able to withstand the current and voltage output from the hardware. Additionally the hardware needed to be as affordable as possible, as the majority of our budget needed to be prioritized. The priority was first given to finding the most affordable option, with the next highest priority given to the current and voltage rating of the connectors. After comparing a variety of products that satisfied all of our requirements, the decision was made to move forward with the cheapest option. Thus the Amphenol Communications Solutions L717DB25P D Sub Connector was chosen.

3.5.4 Materials & Manufacturing

An Amphenol Communications Solutions L717DB25P D Sub Connector, solder, PTFE coated wire (24 gauge), (3 sets) 4-pin wire-to-wire Molex connectors were used to assemble the DB-25 electrical feedthrough. The Molex connectors were first crimped to the PTFE coated wires, after which solder was added to the joint to ensure secure attachment between the parts. Following this, the Molex connectors crimped to the wires were inserted into the D Sub Connector and soldered.

3.5.5 Detailed Design

Once the DB-25 selection was finalized, all the necessary wires were soldered onto the DB-25. To avoid the issue of soldering on wires before we know the exact length of each wire that would be needed to reach its respective hardware connection, several Molex wire-to-wire connectors were connected to the DB-25s to allow for interchangeability between wire bundles of different lengths and gauges depending on the hardware's power requirements and location within the vacuum chamber. This step of making wire bundles greatly aided in wire management.

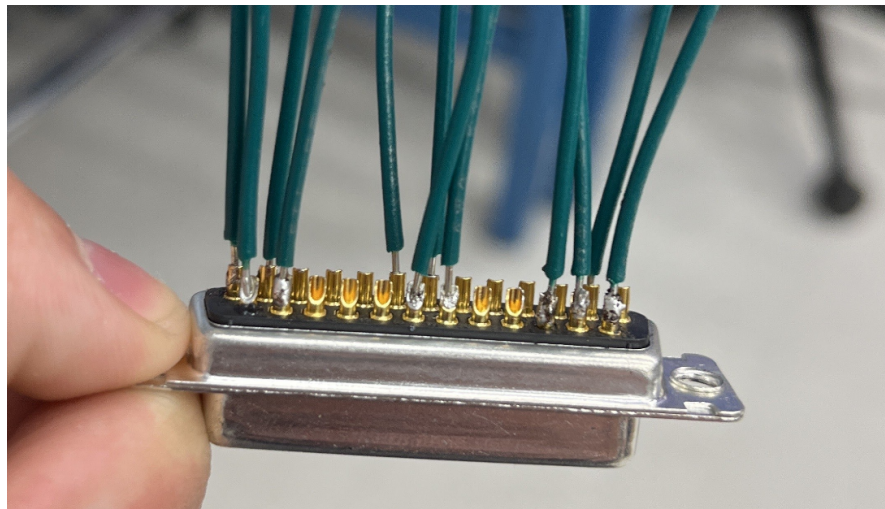


Fig. 3.5.5.1. Soldered DB-25 electrical connection

3.5.6 Verification

With the project being de-scoped due to manufacturing delays the electrical feedthrough system was never fully tested during integration. The DB-25 connectors were fully soldered and assembled but never integrated into the SPACE Lab's vacuum chambers for grounding testing. The connectors were assembled to carry twelve lines through the vacuum chamber walls, the exact amount needed for all the essential hardware within the vacuum chamber, with additional solder cups available for additional connections as needed. A DMM was used to check the connection continuity across the DB-25s through the Molex connectors. With this test the electrical feedthrough connectors were verified to have met requirements Ci.6 & Ci.7. Future testing that needs to be completed is the connection between the DB-25 and the flanges provided by the SPACE Lab to ensure proper grounding and verify requirement Ci.8.

3.5.7 Risk Analysis

The DB-25 connectors were fully, and properly, soldered and assembled however there were noted inconsistencies in the strength of the solder connections. This is likely due to manufacturing inconsistencies from human error. In future, crimp connectors would be recommended for individuals who do not have a solid soldering background and the implementation of such connectors could be beneficial for any future team looking to continue working on this project. Overall once secure connections have been established between the connectors and wires there is minimal risk. The only source of future risk is running a current or voltage that is too powerful for the DB-25 connectors to handle, as this could cause arcing between the solder cups or simply destroy the connectors. Assuming proper power cautionary measures are implemented the system is fairly secure.

#	Risk Description	Mitigation	Likelihood	Consequence
1	Poor manufacturing of the connectors	Assigning connector manufacturing to those with more experience in soldering	2	2
2	Overloading connectors, causing arcing.	Proper power safety	1	3

Table 3.5.7.1. Risk Analysis for Chamber Interface - Electrical Feedthrough. Likelihood is scored on a scale from 1-5. Consequence is scored on a scale from 1-5.

3.6 Integration Plan/Process

Structural components are to be assembled as per Test Stand Assembly Procedures. Assemblies were prototyped via 3D printing and test fit. Successful test fits ensured that the system could reasonably be mechanically assembled in accordance with design procedures.

Once ready for testing, the DB-25s will be inserted into the internal and external flange ports before connecting their respective wire bundles. Ensure a proper connection with the DB-25s and screw them into the flanges until hand tight with a screwdriver. Secure any loose wire bundles to vacuum chamber walls to avoid interference with pendulum motion or plasma plume.

4 Leveling System Subsystem Design

The leveling system was intended to raise and lower the pitch of the pendulum such that the pendulum is leveled to its stable zero position. It was designed to operate using a pivoting radial member and stepper motor actuating rod that raises and lowers the radial strut at the end of the stand opposite to the pivot.

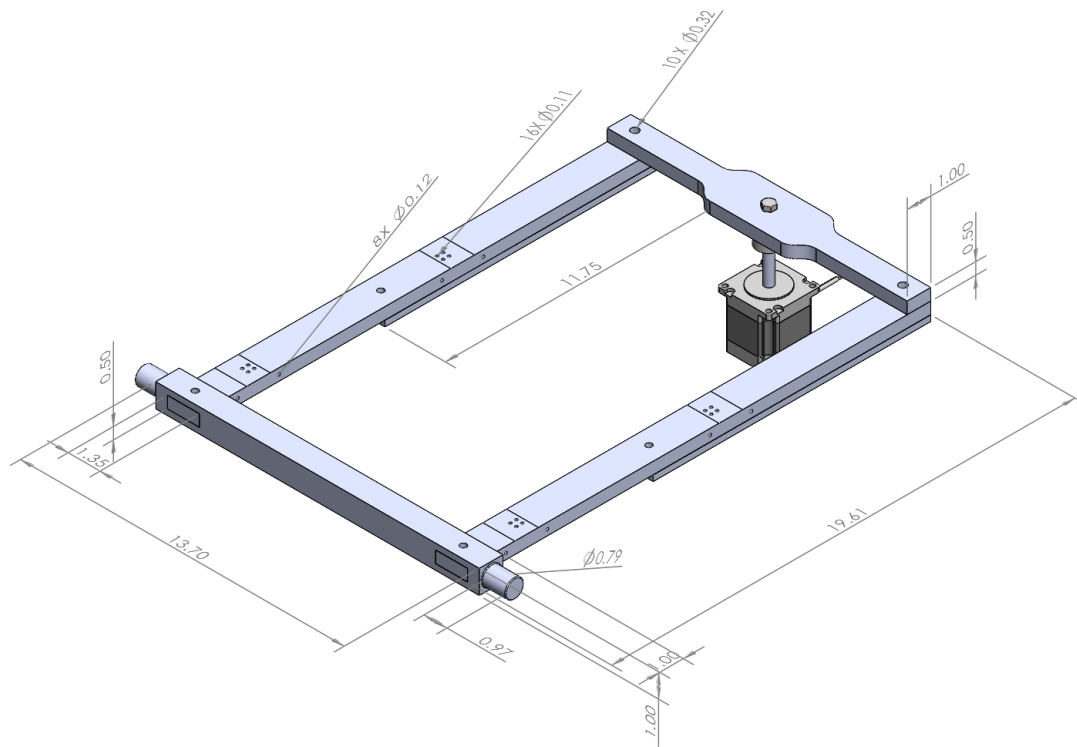


Figure 4.0.1. Leveling System Overview

4.1 Functional Requirements

ID	Requirement	Verification Method
Ls.1	Leveling system must be able to pitch across bearing axis within a range of ± 1.5 degrees	<i>Inspection</i>
Ls.2	Leveling system must not exceed 0.04 inches of deflection due to the weight of overlying subsystems.	<i>Analysis</i>
Ls.3	Leveling system assembly must have a minimum safety factor of 2.5	<i>Analysis</i>
Ls.4	Electronics/hardware must have minimal conductive	<i>Inspection</i>

	components	
Ls.5	Stepper must be able to actuate so that leveling system may pitch between ±1.5 degrees	<i>Test</i>
Ls.6	Stepper must be able to actuate so that leveling system has minimum resolution of 0.001 degrees	<i>Test</i>

Table 4.1.1: Leveling system requirements

4.2 Design Overview

The leveling system is intended to provide fine pitch control with a resolution of 0.001 degrees, pitching between ± 1.5 degrees, to level the thrust stand pendulum to its stable, undeflected zero point. The pendulum and pendulum housing are rigidly mounted to the leveling system using bolt patterns of four, which is then driven to pivot about Part CISMM1 through the use of an electric stepper motor. By commanding the stepper motor to raise and lower its actuation rod with a precision of 0.00035" per step using a GUI system detailed in Section 7.5, the leveling system's length allows the specified resolution of 0.001 degrees to be achieved.

4.3 Budgets

By the end of the project, the leveling system used \$356.96 (7%) of the total budget. Table 4.3.1 itemizes the purchases below.

Category	Item	Cost	Total
Structure	Ball bearing	\$ 20.47	232.47
	Vibration damping sandwich mount	\$ 7.00	
	Vibration damping sandwich mount 2	\$ 7.29	
	Bubble level	\$ 32.88	
	2" Garolite	\$ 140.88	
	Delrin Rod	\$ 23.95	
Avionics	Linear Stepper Motor	\$ 51.19	\$ 123.59
	Digital Stepper Driver	\$ 20.86	
	24 V Power Supply	\$ 16.99	
	Multicolored Dupont Wire	\$ 6.98	
	Bud Industries CU-478 Box	\$ 26.90	
	Switch	\$ 0.67	
			\$ 163.66

Table 4.3.1. Leveling System Subsystem Budget Summary

4.4 Leveling System Subsystem - Structures

The main functions of the structures component of the leveling system is to ensure the test stand is able to be leveled from outside the vacuum chamber. The test stand will be manually leveled after installation of the stand into the vacuum chamber, but shifting due to the installation of the thruster onto the test stand, the connection of all power and signal wire connections, and the pump down process will need to be corrected in order to gather data effectively. The leveling system must also be capable of supporting the weight of the pendulum, frame, and thruster being tested with minimal structural deflection.

4.4.1 Structures Requirements

ID	Requirement	Verification Method
Ls.1	Leveling system must be able to pitch across bearing axis within a range of ± 1.5 degrees	<i>Inspection</i>
Ls.2	Leveling system must not exceed 0.04 inches of deflection due to the weight of overlying subsystems.	<i>Analysis</i>
Ls.3	Leveling system assembly must have a minimum safety factor of 2.5	<i>Analysis</i>

Table 4.4.1.1. Leveling system - structures requirements

4.4.2 Interfaces

The structures component of the leveling system subsystem has an interface with the structures component of the chamber interface subsystem through the nylon bushings of the chamber interface structure. There is one large square rod with both ends cut into cylinders that allows the leveling system to pivot on the nylon bushings. This gives two physical interface points between the structures component of the leveling system and the chamber interface subsystems.

The structures component of the leveling system also interfaces with the structural component of the thrust measurement subsystem. Each of the 4 legs of the pendulum of the thrust measurement subsystem is bolted to the structures component of the leveling system using 4 bolts each. Each leg of the frame that goes around the pendulum also has physical interfaces with the structure component of the leveling system. Each of the 4 legs of the frame attaches to the structure component of the leveling system using two bolts each. This means there are 8 total physical interface points between the structures component of the leveling system and the structures component of the thrust measurement subsystems.

The structures component of the leveling system has an interface with the avionics component of the leveling system. The leveling of the test stand is done by the avionics component of the leveling system through the use of a stepper motor. The stepper motor is controlled by the software system and acts on a threaded actuator rod. This rod has a rubber isolator on the end that pushes on the structure of the leveling system. This gives one physical

interface point between the structures component of the leveling system subsystem and the avionics component of the leveling system subsystem.

4.4.3 Trade Analysis

Making the same material considerations as the chamber interface (outlined in Table 3.4.3.1), the material of choice selected for the leveling system was G10 Garolite. The leveling system sustains similar loads to the chamber interface, as later confirmed through finite element analysis, and during the initial design stage of the project, was a logical conclusion to make. Later on in the design, as detailed in Section 4.4.4, this proved to be a challenge due to issues with the machinability of Garolite.

4.4.4 Materials & Manufacturing

Similarly to the chamber interface, Garolite was selected as the material of choice for the leveling system's longitudinal and radial struts. The stepper motor mounting plate was originally intended to be produced out of Garolite, but due to the inset hole, this was delayed to reassess the design and ultimately descoped. All components were first waterjetted, then had all hole features drilled using a combination of a drill press and mill using a laser-cut guide.

The leveling system pivot was intended to be lathed to produce its cylindrical ends, then milled to create the remaining interior features. The only suitable Garolite stock available was an inch larger in cross section than needed. Garolite, as a brittle material, was not well-suited to this manufacturing approach, particularly with the risk of delamination throughout both lathing and cutting such large features into it. In future iterations of this project, the leveling system pivot should be redesigned for simpler manufacturing, or should be made from aluminum stock. This part was ultimately descoped, as was the remainder of the leveling system.

Leveling System Structures Manufacturing Matrix			
Part Name	Material	Manufacturing Technique	Quantity
LS Longitudinal Strut C2	1/2" G10 Sheet	Waterjet, drill press holes	2
LS Radial Strut C2	1/2" G10 Sheet	Waterjet, drill press holes	1
LS Pivot	2" G10 Bar Stock	N/A, planned to lathe ends, mill holes	1
Stepper Motor Mount	1/2" G10 Sheet	N/A, planned to waterjet, drill press holes, mill inset	1
LS Doubler	1/8" G10 Sheet	Waterjet, drill press holes (double to reach 1/4" thickness)	4
Leveling Bracket	1/8" G10 Sheet	Waterjet, drill press holes	4

Table 4.4.4.1: Leveling system structures manufacturing matrix

4.4.5 Detailed Design

The leveling system sub-system gives both a stable structure in which the pendulum is mounted on, and a pivoting base that can be used to reset the orientation of the pendulum.

The subsystem comprises three major sections: the stepper motor mount, the pivoting body, and structural struts. The stepper motor mount is made of Garolite, and was cut out using a waterjet. CAD of the stepper motor was available online, allowing a mounting plate to easily be designed that would interface with the motor. The ends of the pivot for this system were intended to be turned on a lathe out of a 1 inch X 1 inch X 24 inch square stock of Garolite. The square body would then have been machined using a mill to cut channels in which the struts would fit. This section was never machined, but a scaled prototype proved that the manufacturing plan was feasible. Finally, the struts of this system followed similar design principles to those in the chamber interface. There is very little force acting on the system, so FEA was used to model simulated loads. Under maximum loading conditions, small deflections were predicted. In order to mitigate this, doublers were added to the struts experiencing the most deflection.

Detailed drawings and specifications can be found in the [Test Stand Technical Drawings](#) document, offering information on dimensions and material specifications.

4.4.6 Verification

All of the components except for the main pivot were manufactured, but left unassembled due to time constraints. Regardless, the requirements of the system were tentatively validated through CAD and FEA. Fig. 4.4.6.1 shows the angular range being met in CAD. Fig. 4.4.6.2 shows mechanical properties of the assembly being analyzed through FEA.

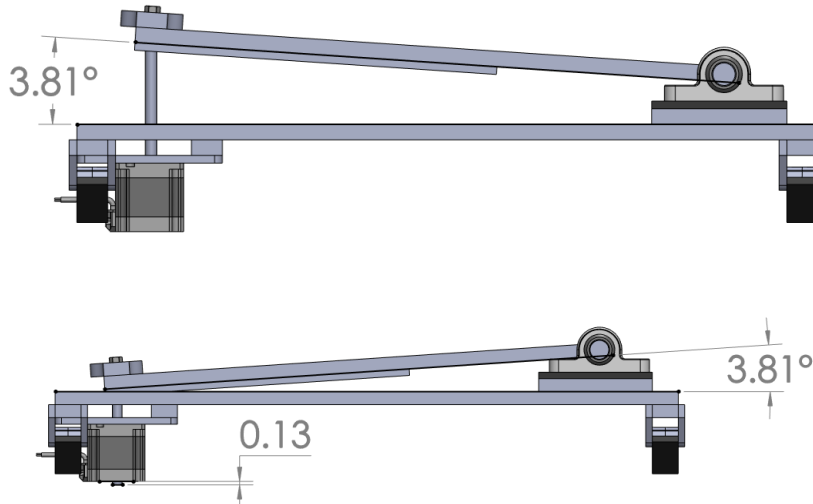


Fig. 4.4.6.1: CAD indicating the maximum deflection of the leveling system. Beyond this point, plastic deformation of the rubber isolator was predicted according to manufacturer specifications.

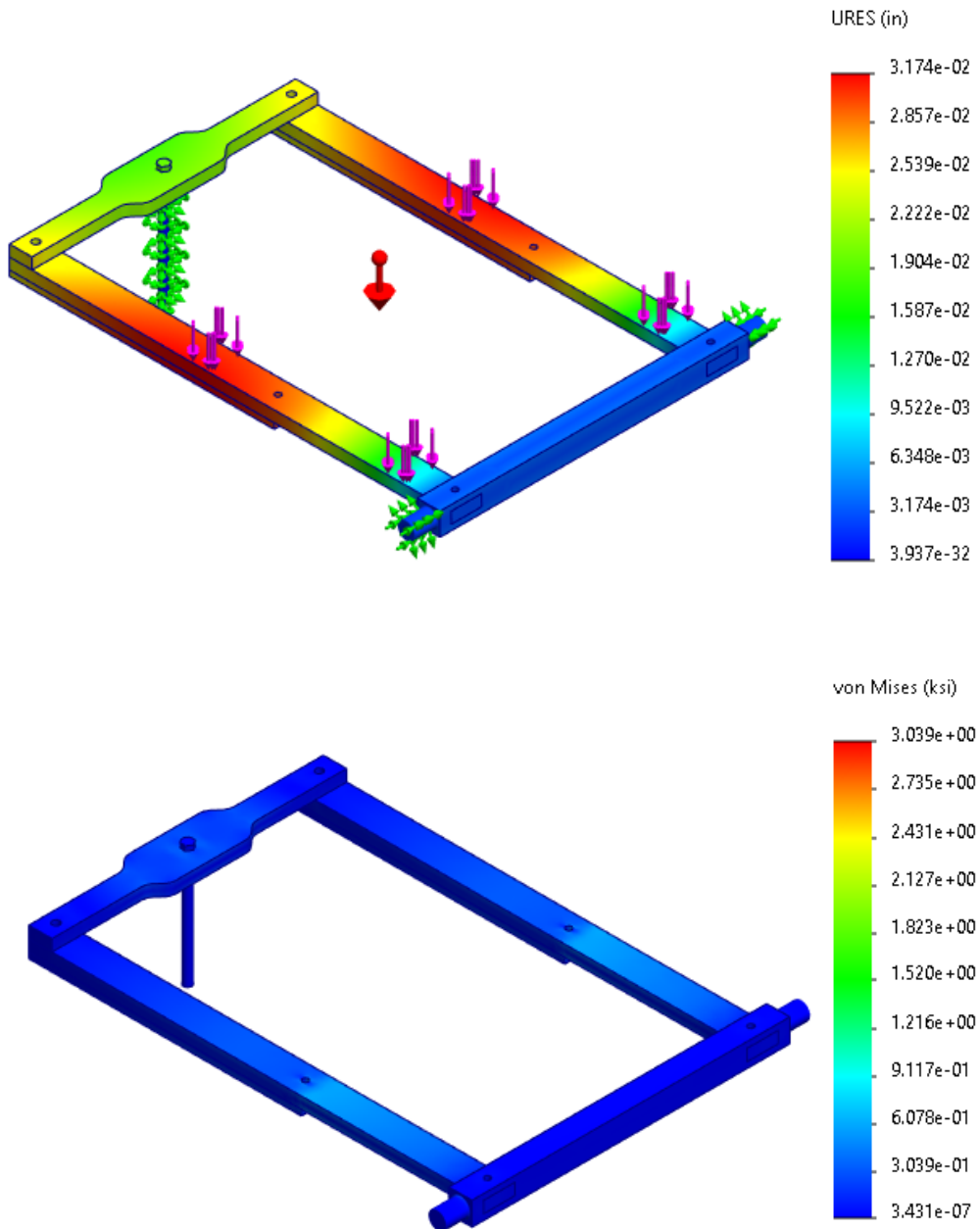


Fig. 4.4.6.2: FEA results showing deflection and stresses meeting subsystem requirements. Max deflections and stresses were 0.0032 and 3.029 ksi, respectively.

4.4.7 Risk Analysis

A concern of the leveling system structure is excessive deflection of its struts under the weight of the thrust measurement, PPT Mount, and PPT during operation. This could potentially lead to stability issues, rendering the stand unusable. To account for this, a “half doubler” design

was implemented in order to reduce potential deflection. This design could be upgraded to a full doubler if it does not provide enough rigidity to support the assembly weight.

#	Risk Description	Mitigation	Likelihood	Consequence
1	Structural deflection	"Half doubler" design	1	4

Table 4.4.7.1. Risk Analysis for the leveling system structure. Likelihood is scored on a scale from 1-5. Consequence is scored on a scale from 1-5.

4.5 Leveling System Subsystem - Avionics

The avionics of the leveling system drive the systems structure to level the pendulum between tests. A stepper motor is driven by a motor controller, which is in turn controlled by an Arduino. Connections between the stepper motor and motor controller are shielded, and the motor controller and Arduino are contained within a grounding box to prevent EMI from affecting subsystem function.

4.5.1 Avionics Requirements

ID	Requirement	Verification Method
Ls.4	Electronics/hardware must have minimal conductive components	<i>Inspection</i>
Ls.5	Stepper must be able to actuate so that leveling system may pitch between ±1.5 degrees	<i>Test</i>
Ls.6	Stepper must be able to actuate so that leveling system has minimum resolution of 0.001 degrees	<i>Test</i>

Table 4.5.1.1: Leveling system - avionics requirements

4.5.2 Interfaces

The wiring for the leveling system starts inside the vacuum chamber at the motor mounted onto the structure. A wire bundle runs to a DB-25 connector on a vacuum electrical feedthrough. From there, another wire bundle connects to a DB-25 connector on the atmosphere side of the same electrical feedthrough and runs to the control box, as shown in Fig. 4.5.2.1.

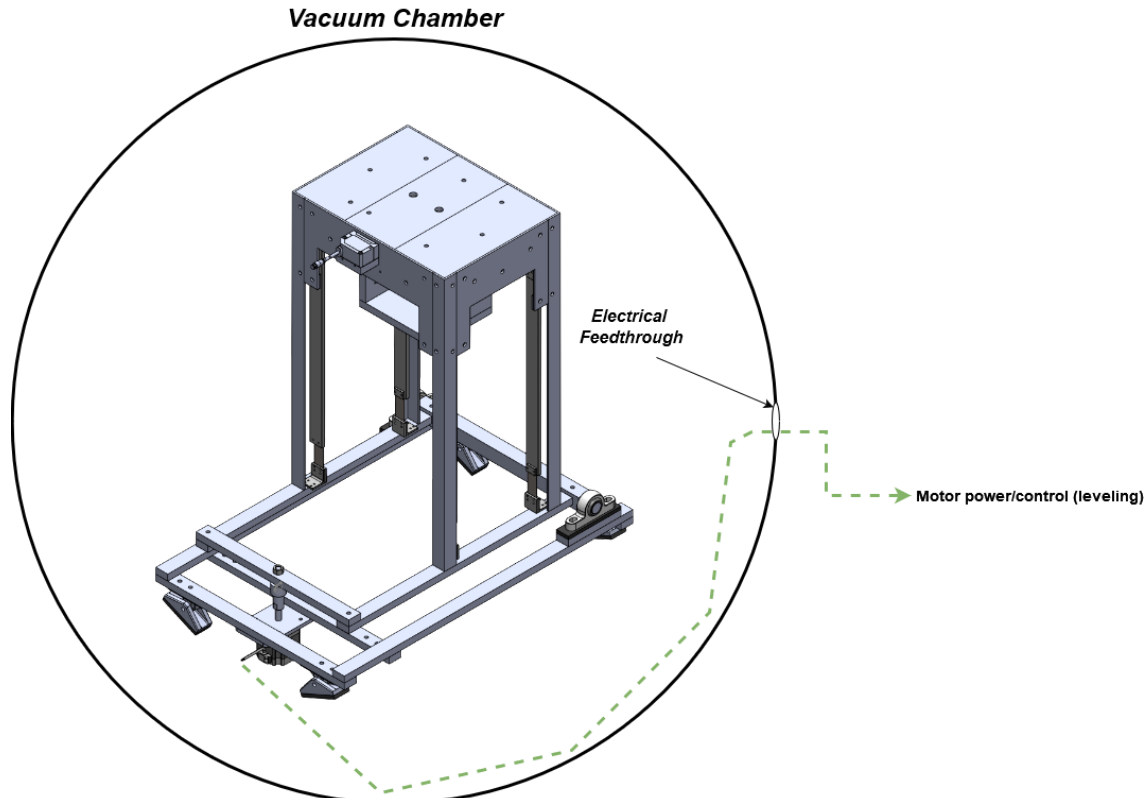


Fig. 4.5.2.1: Wiring harness location for leveling system avionics.

4.5.3 Trade Analysis

Stepper motors were chosen to be used for stand actuation due to their ability to be precisely located and output high amounts of torque. Two different types of stepper motor bodies were considered for the leveling actuation of the stand. First, a captive linear actuator motor was considered but not chosen due to extremely high cost and large vertical profile. Second, non-captive linear actuators were considered. These types of motors are cheaper and have a much smaller vertical footprint compared to the other option, which is quite beneficial when designing for small diameter vacuum chambers. The Nema 23 motor variant was chosen for its high step resolution and power requirements, which fit within the requirements of the system overall.

4.5.4 Detailed Design

The leveling system was designed such that the test stand could be leveled to its zero-point of deflection between thruster fires without the operator being physically in the vacuum chamber. This allows for an increased testing rate since the stand can be leveled while still under vacuum. A Nema 23 linear actuator motor model 2315HS300AW-OB is mounted to the leveling system structure such that the actuator rod displays vertically. The rod was cut down from the factory length in order to satisfy the clearance requirements to the bottom of the vacuum chamber. A DM556T driver is employed to drive the motor. This device converts a digital input signal at a low voltage level, to a high voltage and current signal at the proper timing to drive the motor and variable step size and power. The motor driver is powered with a 24VDC 5.6A wall plug power supply. An Arduino Uno Rev. 3 is used to generate the signals to control the motor driver from a computer running python. The wiring for the described system is shown in Fig. 4.5.4.1. The complete wiring diagram may be found in Appendix A.

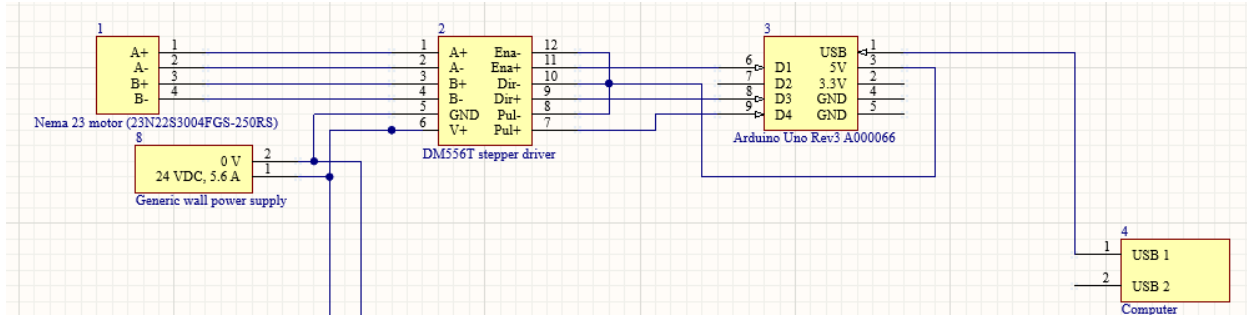


Fig. 4.5.4.1: Leveling system avionics wiring diagram.

The Arduino and DM556T driver are mounted within the overall control black box with a USB input and power input respectively. The Nema 23 motor was chosen specifically for its high holding torque that fit within the overall power budget of the system. It was also a solid option when considered from a budget perspective and physical footprint. The plastic shell of the motor and small diameter actuator screw satisfies the Ls.4 requirement that all electronic hardware should have minimal conductive components where possible. The DM556T driver was chosen for use as it is a commonly accepted highly compatible driver designed for use specifically with this type of motor. The Nema 23 motor is rated at 200 motor steps per full revolution of the actuator rod. With a lever arm of twenty inches from pivot to actuator rod, trigonometry may be employed to demonstrate an angular resolution of 4.41E-5 degrees per revolution. This shows that theoretically the motor may be actuated at an even finer resolution by stepping the motor in only partial revolutions, therefore Ls. 6 is satisfied. Since the length of the actuator rod is 4 inches and the length of the motor body is 2.20 inches, which results in an actuating length of 1.8 inches, then by employing a similar use of trigonometry as previously, it can be shown that the leveling system is able to actuate between positive and negative 1.5 degrees, which satisfies the Ls.5 requirement.

4.5.5 Materials & Manufacturing

An early concern with the implementation of a stepper motor was the presence of a metal actuating rod during testing. To circumvent the EMF that would ostensibly be produced by this component, early prototyping included 3D printing an actuation rod out of PLA. This piece was printed vertically to avoid sagging in a horizontal print. Some sagging still occurred along the screw thread. The idea was further discussed with our faculty advisor and ultimately

descoped, as the EMF produced by the original metal component could be assumed to be small and far away enough from any sensing equipment to be negligible.

A control box was assembled to house the arduino and stepper driver units in an easy to use way. An aluminum enclosure was purchased and various connectors attached. This included a USB-USB connector so that the arduino could be connected to from outside the enclosure, a DC voltage power barrel plug connector to power the stepper driver and motor, a power switch to control the power to the stepper driver, and an open through-hole for the wire bundle from the driver to the motor to pass through. The power switch was installed in order to allow the motor to be powered off when not in use to prevent the motor from overheating in vacuum. The driver and arduino were mounted on a plywood backing which is held in place by set screws.

Wires were soldered from the various connectors to the required locations as defined in the wiring diagram. Some wires were left with ends open to allow connection to clamp connectors.

Leveling System Avionics Manufacturing Matrix			
Part Name	Material	Manufacturing Technique	Quantity
CU480	Aluminum	Drilled through holes	1

Table 4.5.5.1: Leveling system avionics manufacturing matrix

4.5.6 Verification

The leveling system motor and controller unit were verified during system testing. By using the bubble level designated for initial system leveling, the angular movement of the stand was characterized for incrementally steps of the motor, yielding an angular resolution within the system requirements.

4.5.7 Risk Analysis

The main risk associated with this subsystem is the case of the holding torque of the motor being overcome by the torque associated with the weight of the stand. For this reason, the motor model chosen was a high torque variant. This gives the motor extra holding power at the cost of a larger physical footprint. At the time of purchase, the pendulum and frame models were not complete so only an applied torque estimate could be achieved. For that reason, a motor able to provide a margin of torque much greater than the estimated requirement was chosen.

#	Risk Description	Mitigation	Likelihood	Consequence
1	Insufficient torque to drive motor	Purchasing a higher torque motor	1	3

Table 4.5.7.1. Risk Analysis for Leveling System - Avionics. Likelihood is scored on a scale from 1-5. Consequences are scored on a scale from 1-5.

4.6 Integration Plan/Process

Avionics CAD files were mated to structural assemblies in SolidWorks, and no clearance or other functional interference issues were detected. However, as the leveling system did not ultimately get built, this was the furthest integration of the leveling system progressed.

5 Thrust Measurement Subsystem Design

The following section will discuss the design of the thrust measurement subsystem. This subsystem has components for structures, EMI noise reduction, avionics, and calibration. The structural component of the thrust measurement subsystem is the pendulum itself, which means there will be several critical structural requirements of the thrust measurement subsystem. The data taken will be extremely sensitive to EMI interference, meaning the EMI noise reduction component will also have several critical requirements. The avionics component of the thrust measurement subsystem is responsible for accurately measuring the displacement of the test stand pendulum, so requirements for avionics will be critical to stand function. And finally, the test stand must be calibrated before any thrust measurements can be taken, meaning there will also be critical calibration requirements in the thrust measurement subsystem.

5.1 Functional Requirements

ID	Requirement	Verification Method
Tm.1	Flexure spring constants must allow for 2.25 μlbf*s to 22.5 mlbf*s (10 μ N*s to 100 mN*s) impulses to be tested	<i>Test</i>
Tm.2	Flexures must be replaceable/interchangeable	<i>Inspection</i>
Tm.3	Provide 35 dB of attenuation to for signal frequencies between 5 MHz to 250 MHz	<i>Test</i>
Tm.4	DAQ must be capable of sampling at least 40x the natural frequency of the test stand	<i>Demonstration</i>
Tm.5	DAQ must have sufficient memory to collect data for a timescale 10x the period of the test stand	<i>Demonstration</i>
Tm.6	Rangefinder must have minimum resolution of half the minimum stand deflection	<i>Test</i>
Tm.7	Calibration procedure must be completable under	<i>Demonstration</i>

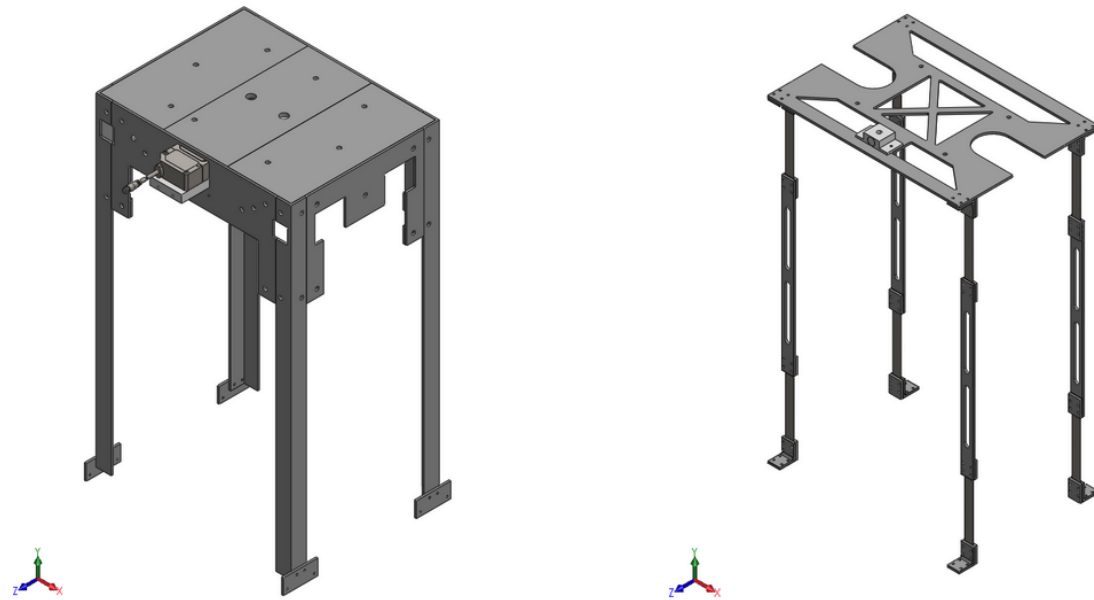
	vacuum	
Tm.8	Stand configuration must not change between calibration and testing	<i>Demonstration</i>

Table 5.1.1: Thrust measurement requirements

5.2 Design Overview

The thrust measurement subsystem is broken down into 4 main components: structures, EMI shielding, avionics, and calibration.

The structural component of the thrust measurement subsystem is further broken down into 2 major parts: the pendulum frame and the pendulum, which are shown in the figures below.



Pendulum frame limits travel of pendulum to 0.191 inches and provides mounting for laser rangefinder

Pendulum moves in response to thruster impulse and provides mounting for laser rangefinder target and damping system magnet housing

Fig. 5.2.1: Pendulum frame(right) and pendulum(left)

The pendulum frame, shown above on the left, goes over the pendulum to provide a stop to prevent the pendulum from moving more than 0.191 inches in either direction. Additionally, the frame gives a mounting point for the laser rangefinder. The top panels of the frame are removable to give access to the top of the pendulum to adjust the magnetic damping system. Half inch holes are drilled in the center of the top frame panel so hooks can be used to pull the panel off the frame, making removal easier. The laser rangefinder is mounted at a hole in the frame that looks onto the pendulum top where the target for the rangefinder is located. The frame securely bolts to the leveling system using 4 brackets at the base of each leg. A detailed drawing of the pendulum frame can be found below.

The pendulum, shown above on the right, moves in response to thruster impulse or steady state thrust. The target for the laser rangefinder is located on top of the pendulum as part of the magnetic damping system magnet housing. The pendulum has 8 removable spring steel flexures, 2 on each leg, that can be swapped out as a set to provide more or less spring resistance depending on the output of the thruster being tested.

The EMI shielding is incorporated into the system to cover all hardware that will be transmitting data, and their respective analog signal lines. This will take the form of a faraday shield around the IL-030, and wire sheaths encasing the analog signal lines from the IL-030 and an unspecified plasma diagnostic probe to be situated inside the plasma plume of the PPT.

The analog output of the laser rangefinder is fed into the IL-1000 for noise filtering and amplification. This signal is then sent to an oscilloscope for digitization and is analyzed in post-processing.

The test stand will be calibrated using an electrostatic comb provided by the SPACE Lab. Test stand design has incorporated spaces on the frame and PPT mounting shelf to mount the two halves of the electrostatic comb. Details of the operation of the electrostatic comb will be left to grad students working in SPACE Lab, this team is merely providing a location for each piece of the comb as well as wiring. Mounting locations for electrostatic combs are shown below.

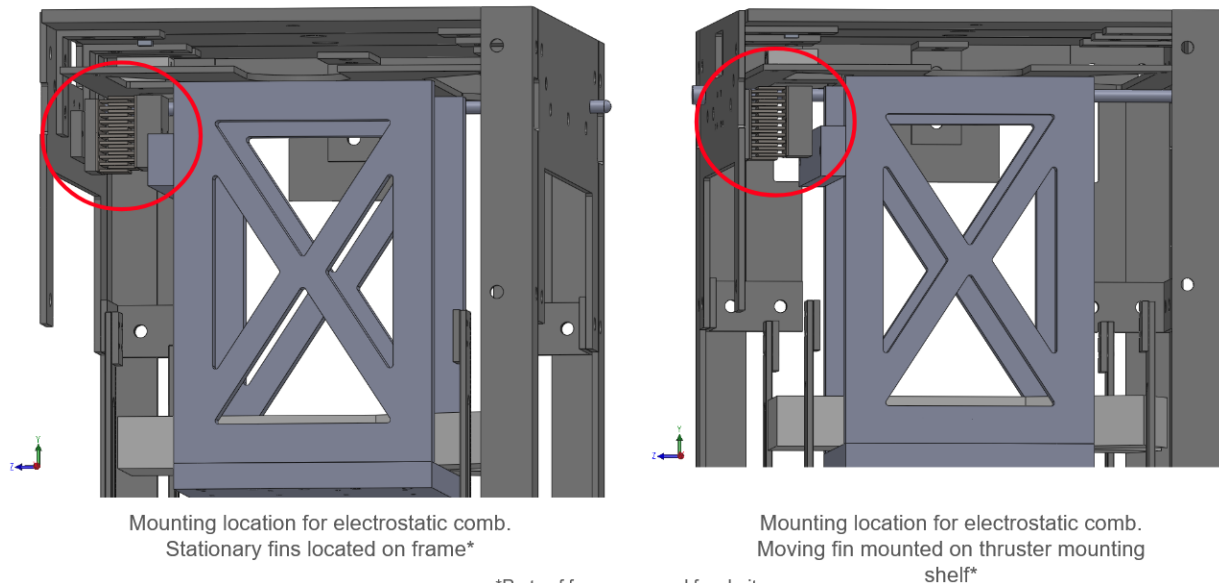


Fig. 5.2.2: Electrostatic comb location on frame(left) and on thruster shelf(right)

5.3 Budgets

By the end of the project, the thrust measurement subsystem utilized \$1147.05 (24%) of the total budget. Table 5.3.1. itemizes the purchases.

Category	Item	Cost	Total
Structure	Spring Steel 0.01",	\$ 120.58	\$ 265.02

	0.02", 0.005"		
	Tempered Spring Steel 0.01", 0.015", 0.02", 0.025"	\$ 144.44	
Avionics	IL - 30 Laser	\$ 348.25	\$ 882.03
	IL - 1000 Transducer	\$ 238.00	
	DAQ	\$ 62.00	
	Connectivity AMP Connectors	\$ 22.60	
	Keyence Wire Adapter	\$ 12.90	
	TI DC-DC Converter	\$ 49.00	
	Digikey M8 Cable	\$ 29.99	
	Keyence NIB OP	\$ 12.90	
	Female 10 Pcs 12V 5.5mm x 2.1mm DC Power Jack Connector	\$ 7.49	
	3pcs XL4015 5A DC to DC CC CV Lithium Battery	\$ 10.49	
	M8 Connector	\$ 4.35	
	Assorted Connectors	\$ 93.06	
			\$ 1147.05

Table 5.3.1. Thrust Measurement Subsystem Budget Summary

5.4 Thrust Measurement System - Structures

The main functions of the structures subsystem of the thrust measurement system is to ensure the test stand is able to respond to micronewton impulses in a measurable way, while maintaining stability of the pendulum, as well as be able to damp out oscillations caused by thruster impulse within a 6 second time frame. This offers the ability to not only measure small impulses, but also the ability to take several impulse measurements over a short period of time.

5.4.1 Structures Requirements

ID	Requirement	Verification Method
Tm.1	Flexure spring constants must allow for full range of impulse to be tested 10 $\mu\text{N}^*\text{s}$ to 100 mN*s	<i>Test</i>
Tm.2	Flexures must be replaceable/interchangeable	<i>Inspection</i>

Table 5.4.1.1: Thrust measurement - structures requirements

5.4.2 Interfaces

The structure component of the thrust measurement subsystem has an interface with the structures subsystem sub-block of the leveling system through 4 brackets at the base of the pendulum and four brackets at the base of the frame. These brackets are connected to the leveling system with bolts in order to keep the thrust measurement system stationary at the base. This gives 8 physical interface points between the structures subsystem of the thrust measurement system and the structures subsystem of the leveling system.

The structures subsystem of the thrust measurement system has an interface with the structures subsystem of the PPT mount system. The sides of the thruster support shelf are both bolted to the top of the pendulum with two bolts each, holding it rigidly in place so the impulse from the thruster is transmitted to the pendulum. This gives 2 physical interface points between the structures subsystem of the thrust measurement system and the structures subsystem of the PPT mount system.

The structures subsystem of the thrust measurement system has an interface with the EMI shielding subsystem of the thrust measurement system. The wire shielding for all wires for the avionics and calibration subsystems of the thrust measurement system will be taped to the frame of the test stand. The wire mesh around the laser rangefinder is bolted to the pendulum frame. This gives physical interface points between the structures subsystem of the thrust measurement system and the EMI shielding subsystem of the thrust measurement system.

The structures subsystem of the thrust measurement system has interfaces with the avionics subsystem of the thrust measurement system. The laser rangefinder is physically mounted to the frame of the test stand with a 3D printed mount bolted to the surface opposite the thruster plume. The target for the laser rangefinder will be located on the top of the pendulum. This gives 1 physical and 1 electrical interface between the structures subsystem of the thrust measurement system and the avionics subsystem of the thrust measurement system.

The structures subsystem of the thrust measurement system has an interface with the calibration subsystem of the thrust measurement system. The stationary side of the electrostatic comb is mounted on the test stand frame. This gives 1 physical interface between the structures subsystem of the thrust measurement system and the calibration subsystem of the thrust measurement system.

The structures subsystem of the thrust measurement system has interfaces with the motion damping subsystem of the PPT mount system. The magnet housing for the motion

damping subsystem is mounted to the top of the pendulum and the non-magnetic plate that interacts with the magnet is mounted on the frame. This gives 2 physical interfaces between the structures subsystem of the thrust measurement system and the motion damping subsystem of the PPT mount system.

5.4.3 Trade Analysis

A trade study was conducted to choose the best material for the pendulum and frame. 5 figures of merit were considered in the trade study, and weights were assigned to each figure. Each material was evaluated for the figures of merit, and a score of 0-1 was given to each material. The total score for each material was given based on the material's score for each figure of merit multiplied by the score.

The figure of merit with the highest weight was vacuum compatibility. Given that the stand has to function within a vacuum chamber, high vacuum compatibility and low outgassing under vacuum is necessary. Vacuum compatibility was given a weight of 0.3 for this trade study. Given that Garolite has the highest vacuum compatibility according to NASA outgassing table, it was given a score of 1.

The next highest weighted figure of merit was cost. Working with a fixed budget required cost to be considered in all material selections. Cost was given a weight of 0.2 for this trade study. Both 3D printer filaments were significantly less expensive than Garolite, so each of them received a score of 1.

The next highest weighted figure of merit was density. Density had to be considered because the test stand has to fit in a finite space, and ultimately the weight of the test stand has a huge impact on its performance. Density was given a weight of 0.2 for this trade study. Carbon fiber filled PETG had the lowest overall density, so it was given a score of 1.

The next highest weighted figure of merit was yield strength. In addition to being lightweight, the stand also has to be strong in order to support the weight of the heavier thrusters to be tested. Yield strength was given a weight of 0.2 for this trade study. Garolite has a yield strength far above that of the filaments, so it was given a score of 1.

The last figure of merit considered was machinability. A consideration has to be given to machinability to avoid expensive machining and potential problems with tolerances of the design. Machinability was given a weight of 0.1 for this trade study. PLA filament is by far the easiest material to work with of the three, so it was given a score of 1.

The results of this trade study are shown in table 5.4.3.1 below.

Material	Weight	Garolite	Carbon Fiber Filled PET-G	PLA
Machinability	0.1	0.4	0.5	1
Cost	0.2	0.5	1	1
Vacuum Compatibility	0.3	1	0.5	0.4
Density	0.2	0.75	1	0.5
Yield Strength	0.2	1	0.3	0.1
Total	1	0.79	0.66	0.54

Weighted decision matrix for pendulum and frame materials

Table 5.4.3.1: Weighted decision matrix for pendulum and frame materials

Based on the results of this trade study Garolite was chosen as the material to build the test stand and frame. Spring steel flexures had to be used on the pendulum in order to have flexures that could produce predictable, repeatable results, so no trade study was conducted for flexure material.

5.4.4 Detailed Design

The flexures for the pendulum structure were sized based on the equations shown in Fig. 5.4.4.1, more information on these equations can be found in references for beam spring equations and impulse response equations where the MATLAB ode89 solver is used to yield a transient response to the rotational equation of motion. The code may be referenced in Appendix A. The overall spring constant for the pendulum is calculated by first finding the bending spring constant of each flexure by itself, treating the flexure like an ideal beam and assuming that both ends of the beam remain planar. Then each arm of the pendulum, with two flexures on it, is treated as two springs in series and the four total arms are treated as four springs in parallel. The torsional spring constant of the stand is then found by calculating the torque applied by the springs per unit of rotation, minus the torque applied by the weight of the stand, allowing for any arbitrarily low value of the spring constant to be obtained.

$$I_p \ddot{\theta} + c\dot{\theta} + k_{rad}\theta = \tau$$

$$k = \frac{3EI}{l^3}$$

$$k_{eff} = 4 * (\frac{1}{k} + \frac{1}{k})^{-1}$$

$$k_{rad} = k_{eff}L^2 - mgL_{cg}$$

$$c = 2\zeta\sqrt{I_p k_{rad}}$$

$$\theta(t) = \frac{I_b L}{I_p \omega_n} \left[\frac{1}{\sqrt{1 - \zeta^2}} e^{-\zeta \omega_n t} \sin(\omega_d t) \right]$$

$$\dot{\theta}(t) = \omega_d e^{-\zeta \omega_n t} \cos \omega_d t - \zeta \omega_n e^{-\zeta \omega_n t} \sin \omega_d t$$

$$t_{peak} = \frac{\pi}{2\omega_d}$$

$$\omega_n = \sqrt{\frac{k_{rad}}{I_p}}$$

$$\omega_d = \omega_n \sqrt{(1 - \zeta^2)}$$

Fig. 5.4.4.1: Equations used to model pendulum dynamics.

Different flexure dimensions, limited by what can fit within the constraints of the stand, are then iterated through with two major limiting conditions. First, the flexure must not buckle within a certain safety factor given the weight of the stand and the thruster on it. Second, the spring constant must be positive, so that the pendulum does not go unstable. In the case where both conditions are satisfied, the response of the pendulum with the given spring constant to a given impulse is solved for. The peak displacement of the plot is the most important data point for resolving impulse measurements, so the code then determines if that value is above or below the minimum resolution set for the data collection system. At this point, there are still a number of flexure options available, so the group is filtered down even further by adding two more metrics for evaluation. First, the ratio of energy per unit displacement in the bending direction to the energy per unit displacement in the twisting direction, as described by the ideal beam equations, must be very high. This way energy is more likely to be stored in the bending direction, the direction of the pendulum's movement, so that the pendulum does oscillate in a twisting manner and instead translates in a straight path. A rule of thumb was determined that this ratio should be on a similar order of magnitude to 1000. Second, the natural frequency modes of each flexure must be sufficiently high such that pumps and other low frequency sources in the lab do not create a resonance in the flexure, causing it to twist on itself. Again, these values were calculated using ideal beam equations. Since external frequency sources in the lab space are on the order of one to ten Hertz, a natural frequency of hundreds to thousands of Hertz on its first mode is sufficient for flexure design.

Given these constraints, the final dimensions of the flexure were chosen to maximize displacement at the minimum impulse value of the system requirements. Since this also results in an extremely low spring constant value, which is dependent on the mass of the system, ballasts were introduced so that any test for a given thruster should be conducted with a total weight for what each flexure is rated for. These dimensions set the width and length of the

flexure sets, but varying thicknesses of flexures were then used to account for increased thruster weights and power.

5.4.5 Materials and Manufacturing

G10/FR4 Garolite was chosen as the primary structural material for both the pendulum and the frame. It was chosen because of its non-conductivity, vacuum compatibility, and high strength. A variety of machining techniques were used to manufacture the Garolite components. First, dxf files were created and sent to the MSE department's Omax 2652 waterjet where the basic shape was cut out of 0.125 inch thick Garolite sheets. Delamination was a concern for any interior geometries such as bolt holes or weight saving cut-outs, so those had to be done by hand. Paper stencils were made using a Universal Laser System ILS12.75 laser cutter. These stencils were then taped to the water jetted parts for drilling holes and dremelling weight saving cut-outs.

Holes for the pendulum parts were drilled using an Atlas 863 drill press in the AA machine shop with a 15/128" drill bit. Parts that were able to fit on a mill were drilled using a Bridgeport Series 1 with a 15/128" drill bit. The mill was used for higher accuracy of hole location. On the mill one hole was drilled using the paper stencil, then all other holes were drilled relative to that hole, with the stencil kept in place in order to ensure hole location was as accurate as possible.

Similar methods were used for drilling holes for the frame components. Stencils were used for drilling holes, and parts that could fit on the lathe were drilled on the Bridgeport Series 1 mill, otherwise they were drilled on an Atlas 863 drill press. Initial pilot holes were drilled to 15/128", then holes were sized up to 17/64". The legs of the pendulum were cut from 36" long, $\frac{1}{8}$ " thick G10/FR4 Garolite 1" outside width angle stock on a Doall DBW-12B band saw. The brackets holding the frame together were cut from $\frac{1}{8}$ " thick G10/FR4 Garolite 2" outside length angle stock.

Weight saving cut outs were cut using a Dremel 332-5 rotary cutting tool. A laser cut stencil was used as a guide for cutting. Once the shape of the cut out was cut, a sanding wheel on the Dremel 332-5 rotary cutting tool to smooth out the cut outs.

Nylon fasteners were chosen in order to minimize test stand conductivity. Almost all fasteners are nylon, with the exception of the fasteners that secure the spring steel flexures to the pendulum arms. Those fasteners were chosen to be 18-8 stainless steel because the durability and reusability of nylon fasteners was considered too low for the repeated removal and replacement of the flexures.

The spring steel flexures come in thicknesses of 0.010", 0.015", 0.020", and 0.025". Each set of flexures was cut from sheets of blue tempered 1075 spring steel. Dxf files were created for the general geometry of the flexures to be laser cut. They were cut on a Perfect Laser 500c Fiber Laser Cutting Machine Model PE-F500-3015 laser cutter at Vashon Aircraft. The laser cutter was unable to cut all the way through the 0.025" flexures, which had to be finished using a Dremel 332-5 rotary cutting tool.

Due to limitations on precision from using a drill press for adding hole features and Dremel to add lightening features, several parts' designs should be reconsidered in future integrations. Using more external weight-saving shaping for the VC1/VC2 arms rather than internal holes alone would have been simpler to manufacture. Additionally, having access to a larger footprint mill than currently offered in the AA shop would have allowed for more parts to be both cut to size and have their holes drilled in one go, rather than having tolerance issues accumulate from changing machines throughout their manufacturing. Fastener placement, type,

and quantity should have been considered more from the start, as attempting to secure as many fasteners with both a nut and bolt as were called for in the design was challenging and tedious.

Thrust Measurement System Structures Manufacturing Matrix			
Part Name	Material	Manufacturing Technique	Quantity
VC1 Arms	1/8" G10 Sheet	Waterjet, drill press holes, Dremel lightening slots	4
VC2 Arms	1/8" G10 Sheet	Waterjet, drill press holes, Dremel lightening slots	4
Bracket Connector	1/8" G10 Sheet	Waterjet, drill press holes	8
Corner Bracket	1/8" Thick 1x1" G10 Angle Stock	Drill press holes, bandsaw individual brackets	8
Flexure (F1)	0.010" Spring Steel Sheet	Laser cut	8
Flexure (F2)	0.015" Spring Steel Sheet	Laser cut	8
Flexure (F3)	0.020" Spring Steel Sheet	Laser cut	8
Flexure (F4)	0.025" Spring Steel Sheet	Laser cut, Dremel to release partially cut flexures	8
Housing Leg (Front)	1/8" Thick 1x1" G10 Angle Stock	Bandsaw to length, drill press holes, dremel access tabs	2
Housing Leg (Back)	1/8" Thick 1x1" G10 Angle Stock	Bandsaw to length, drill press holes, dremel access tabs	2
Frame Top (Side)	1/8" G10 Sheet	Waterjet, drill press holes	2
Frame Top (Center)	1/8" G10 Sheet	Waterjet, drill press holes	1
Frame Side (Back)	1/8" G10 Sheet	Waterjet, drill press holes	1
Frame Side (Front)	1/8" G10 Sheet	Waterjet, drill press holes	1
Frame Side (Side)	1/8" G10 Sheet	Waterjet, drill press holes	2
Pendulum Top	1/8" G10 Sheet	Waterjet, drill press holes, dremel lightening slots	1
Bracket	1/8" Thick 2x2" G10 Angle Stock	Drill press holes, bandsaw individual brackets	12

Table 5.4.5.1: Thrust measurement structures manufacturing matrix

5.4.6 Verification

Verification of requirement Tm.1 - Flexure spring constants must allow for full range of impulse to be tested 10 $\mu\text{N}^*\text{s}$ to 100 mN*s, was done through testing. The procedure for this test can be found [here](#), the test plan for this test can be found [here](#). For 0.010", 0.015", and

0.020" thick flexures all became unstable with no load on them other than the mass of the pendulum itself. As will be discussed in section 8.3.3, the estimated minimum impulse the test stand can resolve is 44.5 micronewton seconds, which is above the minimum impulse required in requirement Tm.1. These means that requirement Tm.1 is not verified by the test stand as built.

Verification of requirement Tm.2 - Flexures must be replaceable/interchangeable, was done through inspection. Cut outs were designed in all 4 sides of the pendulum frame, as shown below, to give easier access to the bolts that hold the flexures to the pendulum arms.

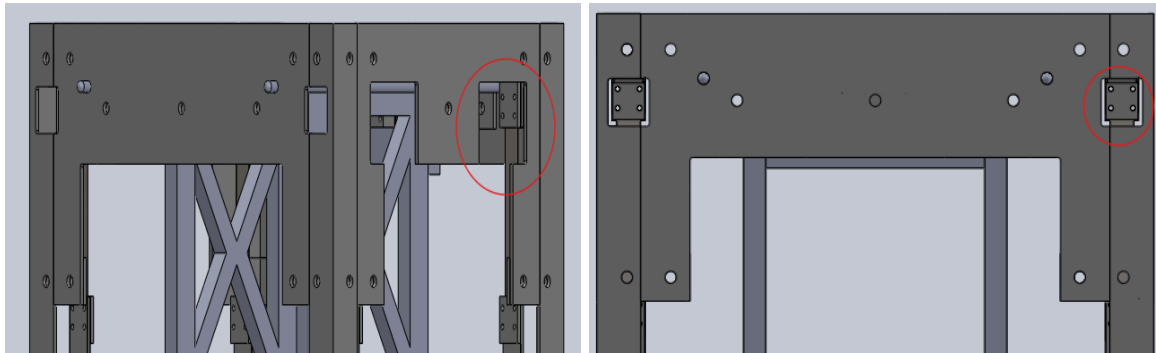


Fig. 5.4.6.1: Cut-outs for access to flexure fasteners

Inspection of the pendulum shows that requirement Tm.2 is verified.

In addition to the cut outs, holes were made for 0.25 inch pins to fit in to support the pendulum top, as shown below. These pins are designed to be 10 inches long and fit all the way across the pendulum frame, fitting under the pendulum top.

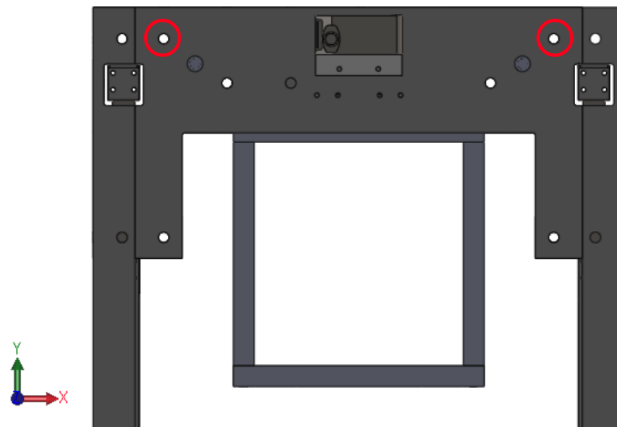


Fig. 5.4.6.2: Pin locations for supporting pendulum top during flexure change

The validity of the model developed for flexure design will be verified during system testing. Different masses and impulses will be applied to the pendulum with the corresponding flexure sizes installed and the experimental results will be compared to the theoretically derived ones. For more detail on system testing, please review the system test plan document.

5.4.7 Risk Analysis

The primary risks for the structures component of the thrust measurement subsystem were the flexures buckling under the weight of the stand and the thruster being tested, the structure being too heavy, the structure have an excess of conductive components, and the structure not being accurately machined.

#	Risk Description	Mitigation	Likelihood	Consequence
1	Flexure buckling	Use analysis and optimization to find the right balance of strength and flexibility	3	4
2	Structure being too heavy	Utilize weight saving cut-outs and lightweight materials	3	4
3	Structure being too conductive	Use non-conductive hardware where possible	2	2
4	Structure not accurately machined	Use laser cut stencils and machine on the mill	4	3

Table 5.4.7.1. Risk Analysis for Thrust Measurement - Structure. Likelihood is scored on a scale from 1-5. Consequences are scored on a scale from 1-5.

According to our analysis of the flexure design we chose, the flexures should have been able to support the thrusters that were anticipated to be tested. Unfortunately it turned out that our flexures could support the weight of the thrusters, but couldn't stay stable while supporting them. Only the thickest flexures could remain stable with any amount of weight put on the stand.

Garolite was used as the primary material for the test stand because of its high strength to weight ratio. Even so, the stand needed to be as light as possible, so weight saving cut-outs were used all over the pendulum structure. A large amount of weight was saved with little effect on the overall strength of the components. This risk was successfully mitigated.

In order to make the stand as minimally conductive as possible nylon fasteners were used where possible. We decided to use metal fasteners to hold the flexures on to ensure they could be tightly secured without having to replace the fasteners every time the flexures needed to change. The fasteners that hold the pendulum frame to the lower structure of the test stand were also made out of metal to clamp them down tighter than could be done with nylon fasteners. These were considered acceptable use of conductive materials and the overall effect on stand function was minimal. This risk was successfully mitigated.

Because Garolite was the primary material used in stand construction, machining was difficult. There were very few precision machining equipment available on campus that could reliably cut holes into the Garolite, regardless of the thickness. In an effort to mitigate this risk, paper stencils were cut using a laser cutter and taped to the Garolite pieces and holes were

drilled using a drill press or, when available, a mill. This risk was largely mitigated, though there are some parts that will need to be re-machined using more precise methods.

5.5 Thrust Measurement Subsystem - EMI Noise Reduction

The purpose of this sub-system was to reduce any uncertainty in our displacement data that might originate from induced currents due to the large E&M fields the PPT would be offputting as it fires. All the necessary hardware that would be transmitting or generating analog signals needed to be shielded, both the hardware themselves and their data lines. An initial study on the strength and frequency of the E&M fields generated by the Dawgstar PPT was conducted using a fast-fourier-transform of collected Rogowski coil that was obtained during previous experiments when the Dawgstar was fired at full power. This data was then analyzed to determine the specifications of this sub-systems driving requirement.

5.5.1 EMI Noise Reduction Requirements

ID	Requirement	Verification Method
Tm.3	Provide 35 dB of attenuation for signal frequencies between 5 MHz to 250 MHz	<i>Test</i>

Table 5.5.1.1: Thrust measurement - EMI noise reduction requirements

5.5.2 Interfaces

As determined through an initial inspection of the design concept early on into development, EMI shielding (specifically a faraday cage) would be needed to cover the IL-030 including its output signal wire, and to an unspecified plasma characterization probe to be attached to the pendulum via the waterfall wire bundle. Additionally, an aluminum control box was used to house our external hardware which provided some EMI shielding but the exact shielding applications of the control box were never quantified, and its exact specifications will not be explored in depth within this section.

5.5.3 Trade Analysis

For shielding the wires an initial multi-layered concept of a conductive wire sheath plus a secondary conductive foil or tape to be wrapped around the wires was explored. However, upon consulting with our customer and advising team it was decided that this approach was overly complicated and overkill for the aforementioned application. Ultimately for the wires a simple tinned-copper wire sheath was decided upon that would entirely cover any analog data lines within and outside of the vacuum chamber. This choice allows for easy and simple installation of the wire shielding, as wire sheaths can be specifically purchased to provide the exact shielding

a customer is looking for. The specific product chosen was DigiKey's Techflex MBN0.50SV50. For the IL-030 the team decided to move forward with the copper mesh concept, as copper mesh is cheap, effective, and easy to obtain. A calculation of the thickness and aperture size requirement for the copper mesh was conducted to determine the exact mesh number to be used for satisfying the driving requirements. The team ordered several square feet of BOEGGER's Copper Mesh size #16. With the vacuum chamber providing some amount of EMI shielding, the control box was selected with EMI shielding as a secondary thought but was chosen to be thick enough that it was estimated to provide an excessive amount of shielding.

5.5.4 Detailed Design

Each wire bundle was to be fed through the wire sheaths, with a focus of shielding the analog signal wire from the IL-030 and the unspecified plasma characterization probe. This shielding would additionally continue outside the vacuum chamber until the lines reached the control box or their respective data collection cache. The copper mesh was to be cut and folded so it fully wrapped the IL-030. Kapton tape was then to be used to hold the copper mesh securely in place.

5.5.5 Materials & Manufacturing

Due to the project being de-scoped due to manufacturing delays, which made it extremely improbable that testing would be conducted with an actual PPT within a vacuum chamber, manufacturing and assembly of the EMI shielding hardware was never completed. Were the project to have continued without a time budget the manufacturing process for the wire sheaths was to cut them to length to shield the bundles, then insert the bundles through the sheaths before being soldered onto their respective hardware or connectors. Regardless of delays, the wire sheaths that were ordered never arrived and could not be tested. For the copper mesh, the manufacturing plan entailed cutting and folding the copper mesh to entirely surround the IL-030 as it sits atop the laser mount.

5.5.6 Verification

Due to project delays and testing equipment availability, testing for the EMI hardware was never completed. Had more time been provided, the testing plan would have consisted of setting up an RF antenna to mimic the frequencies output by the Dawgstar and placing several sets of wires in front of the antenna. A bare wire would have been set up, a wire with the braided sheath, and a wire wrapped by the braided sheath with a section in the middle being only covered by the copper foil. A previous analysis was performed to show that the purchased EMI shielding hardware was able to provide the shielding needed with a comfortable factor of safety ranging from 2 to 10, virtually Tm.3.

5.5.7 Risk Analysis

The analysis performed by the team on the shielding capabilities of the EMI shielding hardware showed that the wire sheath and copper mesh were able to provide more than sufficient shielding, however with no testing being performed this leaves room for error. Any personnel who wish to carry on this project, would be strongly advised to perform the aforementioned testing to fully verify the sub-systems ability to satisfy Tm.3. Additional risks included the coverage of EMI shielding at the connection joints between hardware and wire, and within the electrical feedthrough connections to the vacuum chamber. The team was advised

that any small gaps in shielding should have a minimal effect on the uncertainty of our data, but further testing should be performed.

#	Risk Description	Mitigation	Likelihood	Consequence
1	Insufficient shielding testing	Conducting tests when with access to vacuum	1	3

Table 5.5.7.1. Risk Analysis for Thrust Measurement - EMI Noise Reduction. Likelihood is scored on a scale from 1-5. Consequences are scored on a scale from 1-5.

5.6 Thrust Measurement Subsystem - Avionics

5.6.1 Avionics Requirements

ID	Requirement	Verification Method
Tm.4	DAQ must be capable of sampling at least 40x the natural frequency of the test stand	<i>Demonstration</i>
Tm.5	DAQ must have sufficient memory to collect data for a timescale 10x the period of the test stand	<i>Demonstration</i>
Tm.6	Rangefinder must have minimum resolution of half the minimum stand deflection	<i>Test</i>

Table 5.6.1.1: Thrust measurement - avionics requirements

5.6.2 Interfaces

The laser output is carried by a wire bundle along the external frame of the pendulum down to the pivot of the leveling system. There the wire bundle is attached to the internal DB-25 connector on the electrical feedthrough vacuum flange. An external wire bundle carries the laser signal to the IL-1000 in the control box where it is amplified. This is shown in Fig. 5.6.2.1.

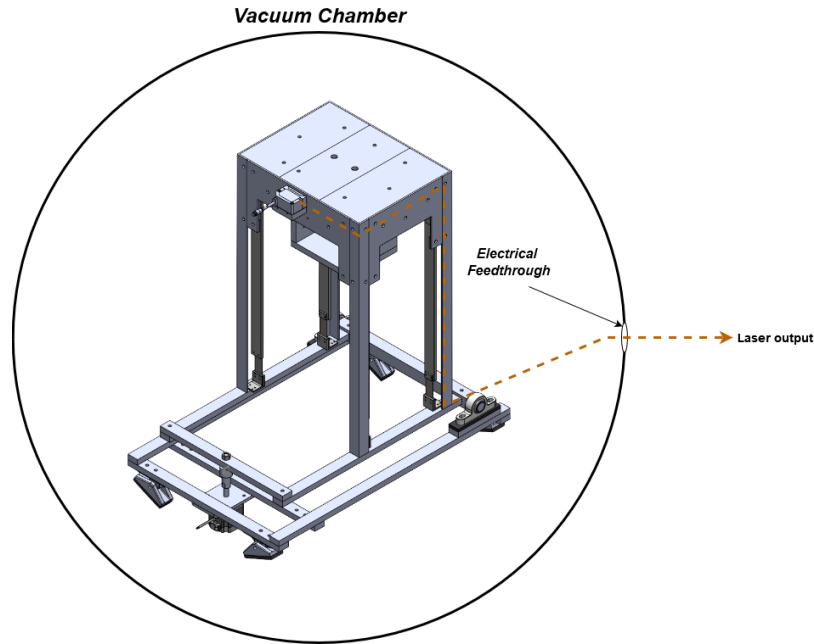


Fig. 5.6.2.1: Wiring harness location for laser output signal.

5.6.3 Trade Analysis

KEYENCE laser devices were chosen for use in the deflection measurement of the pendulum primarily because they are already in use in the SPACE lab, this means that they will be able to better integrate with other hardware that could be potentially used in parallel to this test stand for future experiments. Also the KEYENCE devices have been verified to work well within SPACE lab operating procedures. The IL-030 was specifically chosen for its high resolution of 10 micron. This allows the motion of the test stand to be resolved at a much lower impulse as compared to a different laser unit. The IL-1000 was chosen because it is a required component to be used in series with the IL-030 for proper function of the device.

5.6.4 Detailed Design

The electronic hardware for thrust measurement consists of three components. The IL-030 laser rangefinder, the IL-1000 laser amplifier unit, and an oscilloscope. The IL-030 is able to resolve a range of displacements at a distance between 0.75 inches and 1.75 inches, therefore the rangefinder body must be at least one inch away from the target in all testing cases, and no more than three inches away. The rangefinder has a measurement resolution of ten micron, which sets the limiting case of the thrust stand deflection in order to satisfy the Tm. 6 requirement. Since the minimum projected deflection of the pendulum is just over twenty microns, this requirement is satisfied. For a bottom case testing scenario, the stand should move at least two increments of the minimum resolution so that a measurement can be determined with an uncertainty of fifty percent as defined by the system requirements.

The rangefinder is placed on the test stand frame inside the vacuum chamber. A wire bundle carries the signal generated by the laser outside the vacuum chamber to the control box, where the IL-1000 is located. The IL-1000 is powered by the same power supply as the leveling system, but a $100\ \Omega$ current-limiting resistor is placed in series with the positive voltage signal to prevent damage from current surges. The IL-030 is powered by the IL-1000 through the same bundle that carries the laser signal. The wiring for the described system is shown in Fig. 5.6.4.1.

The complete wiring diagram may be found in Appendix A. The rangefinder signal bundle interfaces with the IL-1000 using a KEYENCE crimp connector designed for this application. The IL-1000 outputs a voltage from either 0 to 5 V or -5 to 5 V depending on its setting. For use with the scope, 5 to -5 is preferable to yield higher voltage resolution per unit deflection. If the IL-1000 were to be interfaced with an arduino unit of some sort to take data, then the 0 to 5 V setting would be used, with 2.5 V used as the zero point.

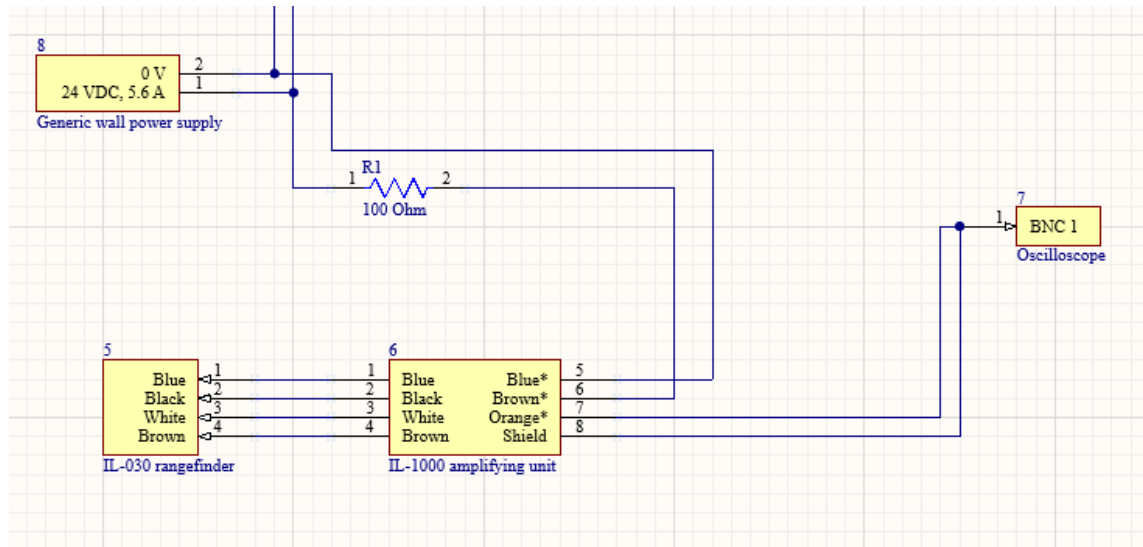


Fig. 5.6.4.1: Thrust measurement avionics wiring diagram.

The oscilloscope, or scope, is used to measure the voltage output of the IL-1000 over the duration of a test. Scopes can capture data for extended periods of time continuously. With a projected minimum natural frequency of the pendulum at 0.028 Hz (or a period of approximately forty seconds) in any test case stated by the system requirements, and an expected test length of ten periods until a one-percent settling point, the data collection capacity of any common scope should be sufficient to capture all data required by an operator of the test stand. Any standard scope will also be capable of collecting data at a sampling rate of at least 1 MHz, so the requirements Tm. 4 and Tm. 5 will be satisfied.

5.6.5 Materials & Manufacturing

The IL-1000 was installed to the control box that also houses the avionics for the leveling system. The power of the IL-1000 was connected to the same power input connector as the stepper driver, with the 100 Ohm resistor in between. The output of the IL-1000 was connected to a BNC connector which can be connected to an oscilloscope. The wire bundle from the IL-030 to the IL-1000 was fed in the same through-hole as the wire bundle from the stepper driver to the motor. The IL-1000 was attached to a small section of DIN rail, which was mounted to the plywood backing in the control box.

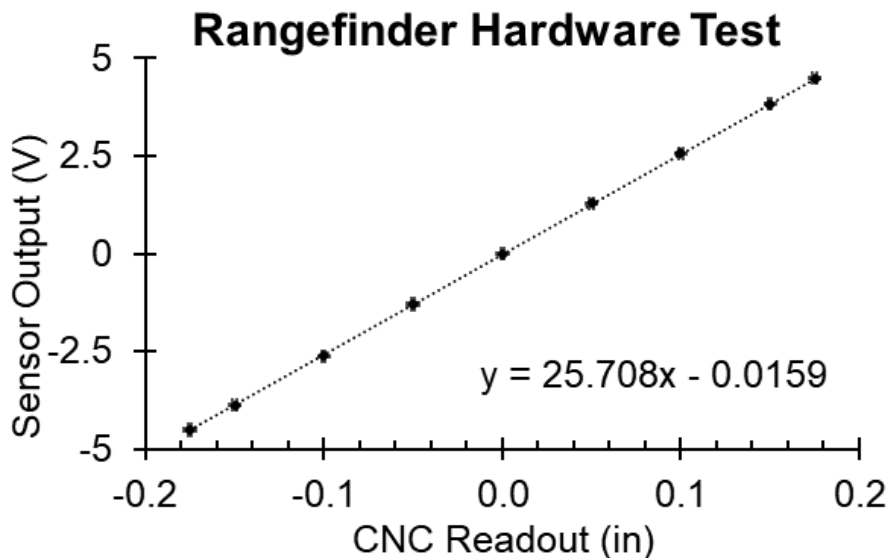
The rangefinder mount was designed to interface with the IL-030's two fastener holes, then attach to the pendulum housing frame's front surface. It was laser cut out of Delrin sheet stock, after which its holes were drilled and tapped using a laser cut paper guide.

Part Name	Material	Manufacturing Technique	Quantity
Rangefinder Mount	1/2" Delrin Sheet	Laser cut, drill press holes, tap holes	1
Control Box	Aluminum	Drill through holes	1
DIN Rail	Aluminum	Band saw	1

Table 5.6.5.1: Thrust measurement avionics manufacturing matrix

5.6.6 Verification

The resolution and linearity of the laser was verified in accordance with the laser verification test plan. In short, the laser was mounted on the table of a 3-axis CNC mill. A flat bit was placed in the mill and used as a stationary target for the laser as the laser was translated in well-defined increments. The voltage at each target location was recorded, and the procedure was repeated three times to determine some amount of standard deviation error. The results demonstrated that the response of the laser is highly linear, with low repeatability error. The minimum resolution was also confirmed to be 10 micron as stated in the device specifications. The test results are shown in Fig. 5.6.6.1. The minimum expected deflection of the stand is 22 micron, so this rangefinder resolution validates the satisfaction of requirement Tm. 6.

**Fig. 5.6.6.1: Rangefinder signal compared to CNC mill location averaged over three trials.**

5.6.7 Risk Analysis

The largest risk when considering data quality is the effect of EMI on the signal. For this reason, the wire bundle carrying the laser signal is shielded with an external metal braid that is grounded to act as a Faraday cage. The positive voltage and reference ground signals of the laser wire bundle are twisted to form a twisted pair signal in order to reduce net noise gain when exposed to any amount of EMI.

#	Risk Description	Mitigation	Likelihood	Consequence
1	Excessive noise in data	Implementation of twisted pairs	1	5

Table 5.6.7.1. Risk Analysis for Thrust Measurement - Avionics. Likelihood is scored on a scale from 1-5. Consequences are scored on a scale from 1-5.

5.7 Thrust Measurement Subsystem - Calibration

The thrust measurement subsystem's calibration functionality was designed to accommodate the SPACE Lab' electrostatic comb test devices. The electrostatic combs function through a current flowing through the fins attached to the pendulum frame from outside the vacuum chamber and generating a static charge, against which the opposite fins generate an opposing force to create a capacitive actuation. The thrust measurement subsystem was therefore dimensioned to accommodate the two fin components, illustrated below in Figure 5.7.0.1.

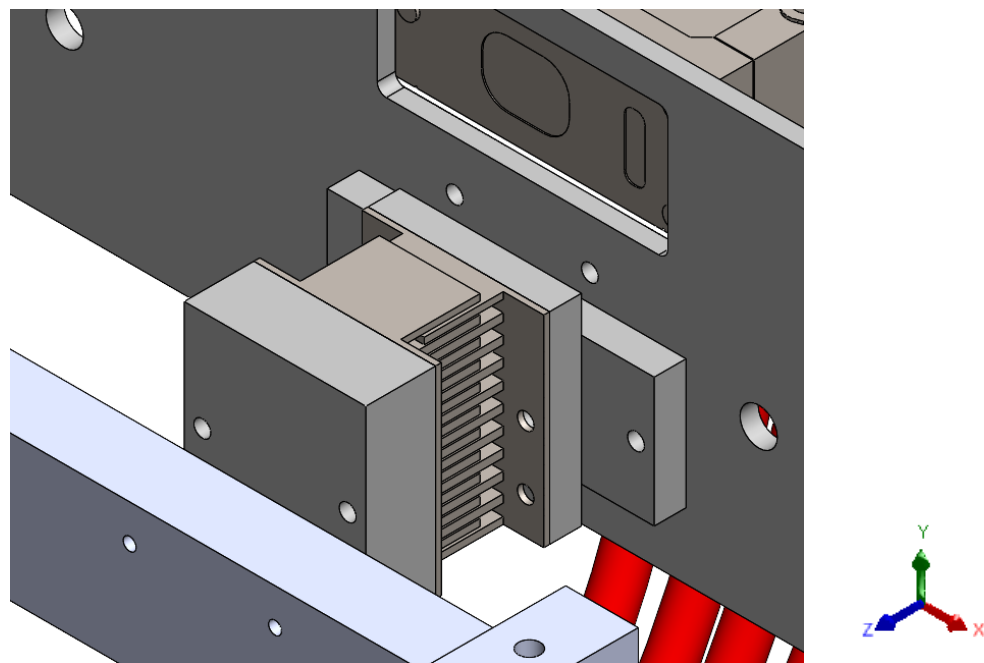


Figure 5.7.0.1. Electrostatic Comb Integration into Stand

5.7.1 Calibration Requirements

The electrostatic comb was intended to function through providing a known calibration force or impulse, from which a displacement could be measured, to create a model from which expected displacements for a given steady state or impulse thrust could be determined. These combs were expected to be able to provide steady state forces and impulses over the full range of expected thruster performance, from 10 $\mu\text{N}\cdot\text{s}$ -100 mN*s

5.7.2 Interfaces

The calibration system interfaces with several systems. Its wires were designed to pass under the pendulum frame's back (on the same face as the laser rangefinder) and out of the vacuum chamber along with the thruster waterfall bundle. The comb-mount assemblies illustrated in Figure 5.7.0.1 are mounted to the pendulum frame (on Part FS3, see Drawing Package) on one side and the pendulum mount strap (on Part SR1, see Drawing Package) on the other using two ostensibly 1/32" screws.

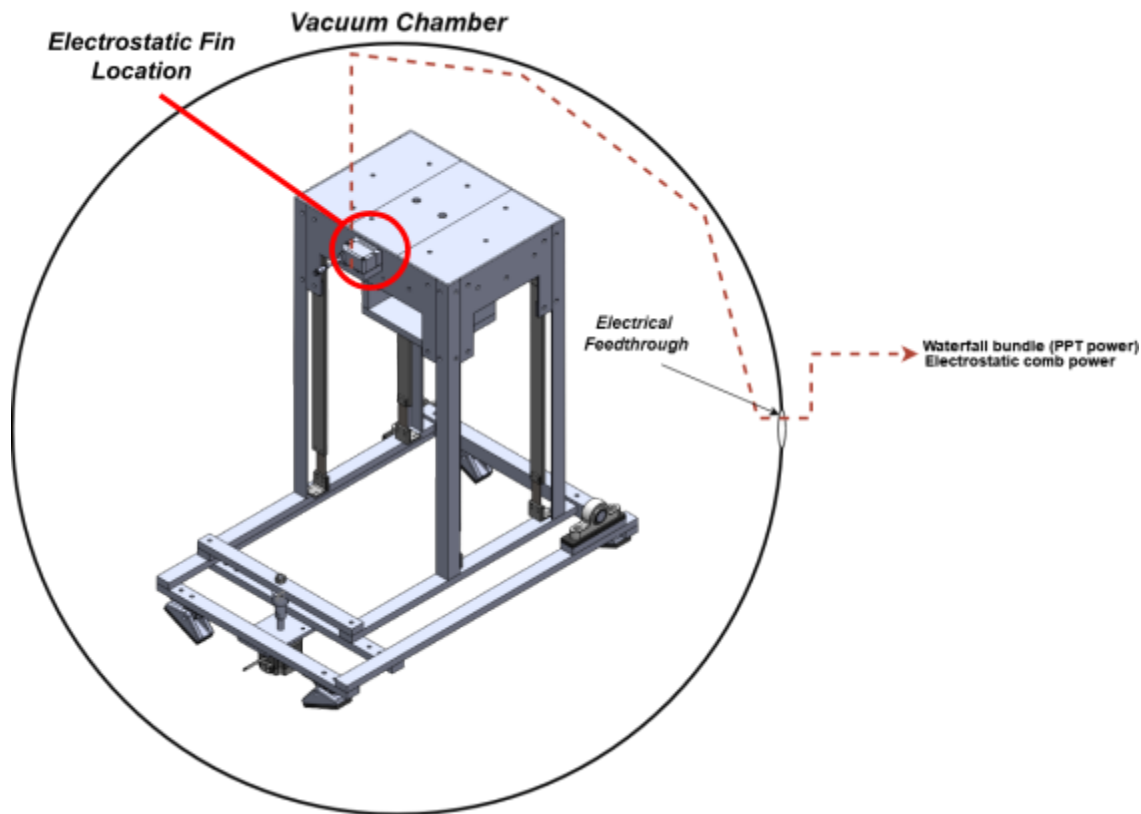


Fig. 5.7.2.1: Wiring harness location for calibration power

5.7.3 Trade Analysis

Several options for calibration were considered prior to the selection of electrostatic fins. First, a mass impacting the stand was considered for impulse characterization. The team had prior experience with this approach from electric propulsion coursework, which made it appealing thanks to the lab procedure documentation already on hand and familiarity from direct experience. A significant drawback to this approach is that the striking object's mass is not easily set in small increments, and cannot generate impulses on the order of $\mu\text{N} \cdot \text{s}$. However, upon being informed that the SPACE Lab had an electrostatic comb system potentially available for use, this shifted the team's focus to integrating this much more finely controlled system into our design, as it could theoretically characterize our full range of thrusts and impulses. The thrust calibration system was designed around this assumption, and though we were not ultimately able to test with the electrostatic combs and instead took our original proposed approach, the stand retains this capability for future use.

5.7.4 Detailed Design

Calibration is a critical process for ensuring the accuracy of thrust measurements for the pulsed plasma thruster. Initially, confirm that the DAQ device and associated sensors are correctly connected and recognized by the computer, using Python along with various packages such as PySerial, NI-DAQmx, and SciPy. Zero the sensors to account for any initial offsets by recording a baseline measurement with the thruster inactive. Incrementally apply known impulses to the displacement sensor, recording the corresponding data outputs to establish the precise relationship between the sensor reading and the force exerted. This data is then utilized to generate a calibration curve through regression analysis.

5.7.5 Verification

After generating the calibration curve and deriving the calibration constant, a series of test firings were intended to be conducted with the DawgStar pulsed plasma thruster. To further ensure accuracy, in Appendix A (Deflection Data Analysis code) the Python script prints the calibration constant in the terminal during each measurement session. For each recorded data file, the maximum voltage (V_{max}) was computed and printed in the Python terminal. This procedure verifies that the script is correctly reading the data files and extracting the correct numbers for analysis.

5.7.6 Risk Analysis

As the calibration system has remained nebulous throughout the entire project scope, there is significant risk in both integration and operation of the system. It is recommended that communication and aid from SPACE Lab staff be imperative to the success of calibrating the test stand under vacuum.

#	Risk Description	Mitigation	Likelihood	Consequence
1	Lack of access to calibration system	Communication from SPACE Lab	5	3
2	Calibration system operation	Aid from SPACE Lab	2	4

Table 5.7.6.1. Risk Analysis for Thrust Measurement - Calibration. Likelihood is scored on a scale from 1-5. Consequences are scored on a scale from 1-5.

5.8 Integration Plan/Process

The calibration process is integral to the test stand's setup, ensuring accuracy in thrust measurements throughout the day's testing. Continuous monitoring during testing, facilitated by the Python script, tracks the calibration constant and V_{max} values for each data file generated. At the day's end, a repeat calibration verifies measurement consistency, with all adjustments documented. This integrated approach safeguards reliability and repeatability in our thrust measurements, vital for accurate data analysis and experimental success.

6 PPT Mount Subsystem Design

The following section will discuss the PPT mount subsystem. This subsystem has components for structures, motion damping, and waterfall. The structures component must be able to support a variety of thruster sizes and mass, as well as being vacuum compatible, so there will be several critical structure requirements in the PPT mount subsystem. The motion damping component will be responsible for bringing the pendulum to equilibrium after each test while having minimal effect on the sensitivity of the stand, so there will be critical motion damping requirements in the PPT mount subsystem. The waterfall will reduce the impact of the wires needed to power the PPT on the effective spring constant of the steel flexures. This will be a critical requirement of the waterfall component of the PPT mount subsystem.

6.1 Functional Requirements

ID	Requirement	Verification Method
Pm.1	Structure must be able to support thrusters with mass up to 17.6 lbs (8kg)	<i>Test</i>
Pm.2	Test stand must be able to accommodate thrusters up to 10 inches wide	<i>Inspection</i>
Pm.3	Structure must be non-conductive and outgas in accordance with NASA standards for ASTM E595 outgassing testing	<i>Analysis</i>
Pm.4	PPT mount structure must keep thrusters centered to within 10% of vacuum chamber radii	<i>Analysis</i>
Pm.5	Damper system must not affect stand equivalent spring constant.	<i>Test</i>

Pm.6	Damper system must provide a constant damping factor during the entire system response.	<i>Test</i>
Pm.7	Damper system must settle stand motion to 2% within a timescale of 5x the period of the test stand.	<i>Test</i>
Pm.8	Waterfall shall minimize effective spring constant of wires connecting to pendulum.	<i>Test</i>

Table 6.1.1: PPT mount requirements

6.2 Design Overview

The PPT mount subsystem is broken down into 3 main components: structures, motion damping, and waterfall.

The structural component of the PPT mount is the mounting shelf the thruster will sit on for testing. There will be two different designs for the mounting shelf: one for the metal vacuum chamber (VC-01) and one for the crystal vacuum chamber (VC-02). The shelf for the metal vacuum chamber will be shorter than the shelf for the crystal chamber, in order to keep the thrust of the Dawgstar centered within 10% of the radius of either vacuum chamber. Both shelf designs are illustrated below in Figure 6.2.1.

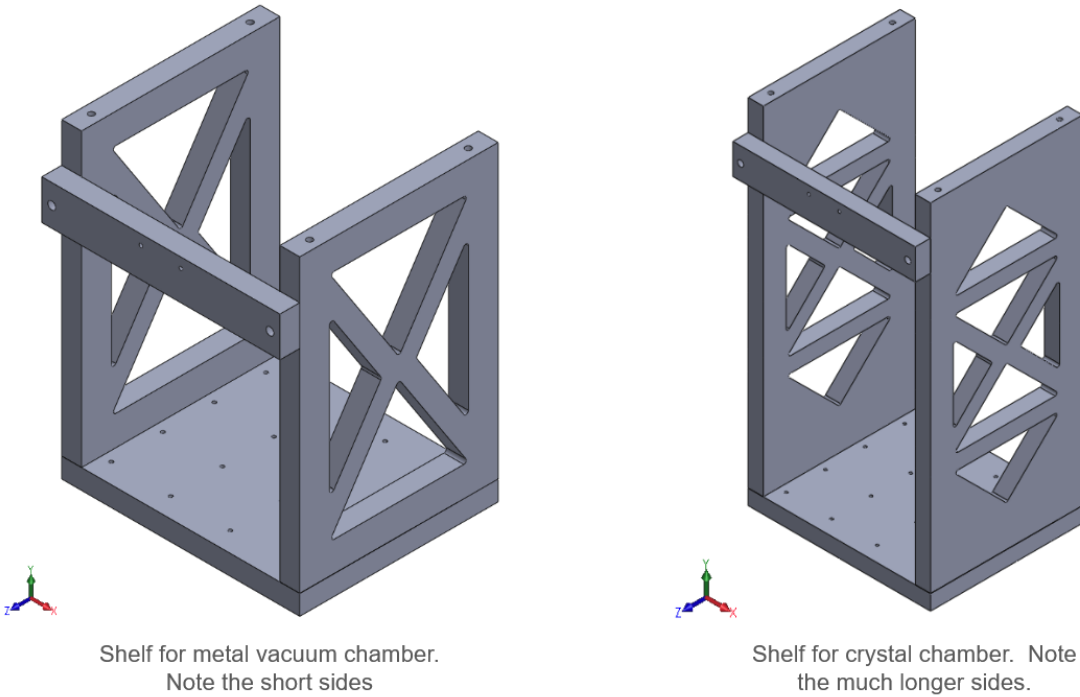


Fig. 6.2.1: Thruster shelf designs for metal vacuum chamber(left) and crystal chamber(right)

The difference between the two designs shown above is the length of the sides. The radius of the metal vacuum chamber is 36 inches, so the test stand top sits much lower in the chamber, meaning the sides of the thruster shelf (shown on the right) have to be shorter to center the thrust of the Dawgstar in the chamber. The radius of curvature of the crystal chamber is 30 inches, so the test stand top sits higher in the vacuum chamber, meaning the sides of the thruster shelf (shown on the left) have to be longer to center the thrust of the Dawgstar in the chamber.

Both designs have a width at the bottom of 5 inches, as well as the strap between the sides toward the top to add structural stability as well as a mounting point for the electrostatic comb. Holes drilled into the bottom of the shelf allow for ballast to be hung from the shelf as needed for increasing stand sensitivity for lower impulse PPTs.

The waterfall exists to limit the effective spring constant of any wires/lines that need to be connected to a piece of hardware that resides on the pendulum. The waterfall wire bundle interfaces directly with the thruster shelf and the laser mount. This interface is defined by passing the four power and data transmission wires through two waterfall wire clamps, which hold each wire securely in place using an inserted screw.

Deflecting a pendulum in vacuum without a damper elicits a settling time in excess of 15 minutes. An eddy current damper was therefore chosen to reduce settling time, with minimal conductive elements introduced as an acceptable compromise for its associated decrease in settling time. This system offers a solution that is passive, produces a consistent damping ratio without affecting spring constant, is accessible within the stand assembly, and cost effective. This system consists of 3 parts: a magnet, magnet housing, and conducting aluminum plate.

6.3 Budgets

This subsystem ultimately used \$447.15 (9%) of the total budget. Table 6.3.1. itemizes these purchases.

Category	Item	Cost	Total
Structure	Magnet	\$ 0.58	\$173.40
	Aluminum plate	\$ 7.08	
	.5" Delrin	\$ 165.74	
Avionics	4 Pin Connector kit	\$ 7.35	\$ 273.75
	4 Pin Connector kit (2)	\$ 16.54	
	M8 circular mount	\$ 11.89	
	PTFE Stranded Wire	\$ 97.91	
	Delrin Rod	\$106.08	
	M8 Female Connector	\$33.98	
			\$ 447.15

Table 6.3.1. PPT Mount Subsystem Budget Summary

6.4 PPT Mount Subsystem - Structures

The main functions of the structures subsystem of the PPT Mount measurement system is to ensure the test stand is able support the mass of a variety of thrusters without collapsing, as well as accommodating a variety of thruster widths and lengths, and ensure that materials used in test stand design will not outgas at a rate that would compromise vacuum chamber pressure.

6.4.1 Structures Requirements

ID	Requirement	Verification Method
Pm.1	Structure must be able to	Test

	support thrusters with mass up to 17.6 lbs (8kg)	
Pm.2	Test stand must be able to accommodate thrusters up to 10 inches wide	<i>Inspection</i>
Pm.3	Structure must be non-conductive and outgas in accordance with NASA standards for ASTM E595 outgassing testing	<i>Analysis</i>
Pm.4	PPT mount structure must keep thrusters centered to within 10% of vacuum chamber radii	<i>Analysis</i>

Table 6.4.1.1: PPT mount - structures requirements

6.4.2 Interfaces

The structures component of the PPT mount subsystem has a physical interface with the structures component of the thrust measurement system. The PPT mount bolts directly to the top of the thrust measurement pendulum top using 4 plastic #10 bolts. Each vertical wall of the PPT mount is in direct contact with the pendulum top, giving the structures component of the PPT mount subsystem two physical interfaces with the structures component of the thrust measurement subsystem.

The structures component of the PPT mount subsystem also has a physical interface with the waterfall component of the PPT mount subsystem. A waterfall clamp will be bolted to the PPT mount to provide the necessary power to the PPT being tested. The wiring of the waterfall will also have a physical effect on the motion of the pendulum through the PPT mount. This gives the structural component of the PPT mount subsystem 2 physical interfaces with the waterfall component of the PPT mount subsystem.

6.4.3 Trade Analysis

A trade study was conducted to choose the best material for the PPT mount. 5 figures of merit were considered in the trade study, and weights were assigned to each figure. Each material was evaluated for the figures of merit, and a score of 0-1 was given to each material. The total score for each material was given based on the material's score for each figure of merit multiplied by the weight.

The figure of merit with the highest weight was machinability. In order to design a shelf that can meet the requirement for keeping thrust centered in the vacuum chamber, the material

had to be easy to work with, otherwise the mount would need excessive amounts of material and an overcomplicated design. Machinability was given a weight of 0.3 for this trade study. The fact that Delrin can be easily and reliably threaded made it so the design of a Delrin mount would be far simpler than a Garolite mount and would use less material, so it was given a score of 1.

The next highest weighted figure of merit was vacuum compatibility. Given that the test stand will ultimately be operated inside a vacuum chamber, vacuum compatibility had to be a consideration. Vacuum compatibility was given a weight of 0.3 for this trade study. Both Delrin and Garolite perform very well under vacuum according to NASA outgassing standards. Both materials were given a score of 1.

The next highest weighted figure of merit was density. Density had to be considered because the test stand has to fit in a finite space, and ultimately the weight of the test stand has a huge impact on its performance. Density was given a weight of 0.2 for this trade study. Garolite has a slightly lower density than Delrin, so it was given a score of 1.

The next highest weighted figure of merit was yield strength. In addition to being lightweight, the stand also has to be strong in order to support the weight of the heavier thrusters to be tested. Yield strength was given a weight of 0.1 for this trade study. Garolite has a yield strength greater than Delrin, so it was given a score of 1.

The last figure of merit considered was cost. Given that the project has a fixed budget cost was a significant consideration, but given that the mount is a relatively small part of the stand it was given a lower weight. Cost was given a weight of 0.1 for this trade study. The cost of Garolite is slightly lower than that of Delrin for a similarly sized piece of material, so it was given a score of 1.

The results of this trade study are shown in the table below.

Material	Weight	Garolite	Delrin
Machinability	0.3	0.3	1
Cost	0.1	1	0.8
Vacuum Compatibility	0.3	1	1
Density	0.2	1	0.75
Yield Strength	0.1	1	0.5
Total	1	0.79	0.88

Weighted decision matrix for PPT mount materials

Table 6.4.3.1: Weighted decision matrix PPT mount materials

Based on the results of this trade study Delrin was chosen as the material to build the PPT mount.

6.4.4 Detailed Design

The final design of the PPT Mount was to create a bolt pattern that SPACE Lab personnel could use to create custom PPT Mounts depending on the thruster being tested. For system testing, the initial plan was to test the stand with the Dawgstar Ablative PPT. Two separate designs were created in order to keep the DawgStar centered in both VC-01 and VC-02. The components were laser cut from Delrin, after which their feature holes were drilled and tapped to accommodate fasteners.

Technical drawings and part specifications, can be found in the [Test Stand Technical Drawings](#) document.

6.4.5 Materials & Manufacturing

The PPT mount subsystem was primarily composed of Delrin 0.5" sheet stock. This material was selected for its vacuum compatibility and machinability. To ensure that the mount would not sag or otherwise deflect when testing different mass thrusters, a thickness of 0.5" was chosen. The shelf components were all cut out of the Delrin sheet using a Universal Laser System ILS12.75 laser cutter. After their perimeters were cut, laser cut paper guides were used to drill each hole using a drill press. Then, each hole was tapped to accommodate threaded nylon fasteners #10-32x0.75" that held the shelf together and attached it to the pendulum top. The Delrin received was denser than anticipated, and in future iterations of this project, should be reconsidered as a primary structural material, as the PPT mount's weight was a significant challenge to the operation of the stand without buckling.

Part Name	Material	Manufacturing Technique	Quantity
VC1 Shelf Side	1/2" Delrin Sheet	Laser cut, drill press holes, tap holes	2
VC2 Shelf Side	1/2" Delrin Sheet	Laser cut, drill press holes, tap holes	2
Shelf Bottom	1/2" Delrin Sheet	Laser cut, drill press holes, tap holes	1

Table 6.4.5.1: PPT mount structures manufacturing matrix

6.4.6 Verification

Verification of requirement Pm.1 - Structure must be able to support thrusters up to 17.6 lbs (8 kg), was done through testing. The test procedure for buckling can be found [here](#), the test plan can be found [here](#). Validation of Pm.1 was done on the 0.025" flexure set with the larger PPT mounting shelf used for the crystal vacuum chamber installed. The results of the buckling test for the 0.025" flexure set can be seen below.

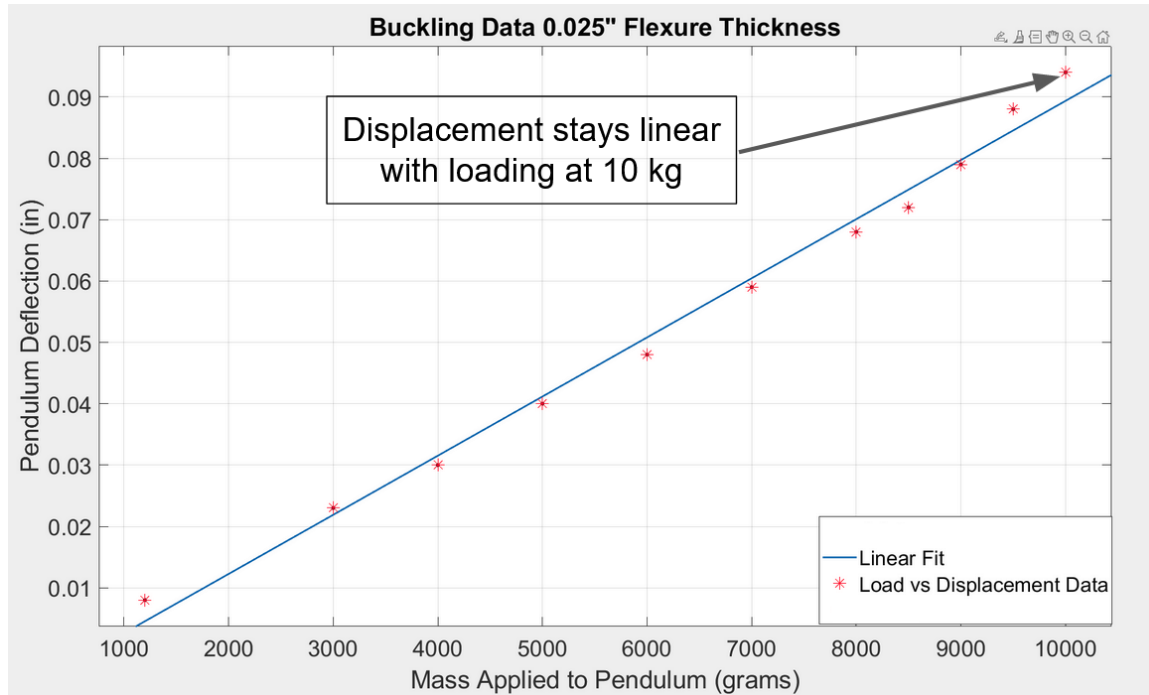


Fig. 6.4.6.1: Buckling data for 0.025" flexures

Buckling is indicated when the change in vertical displacement becomes non-linear relative to the change in applied loading. This test never reached the point where the change in vertical displacement never became non-linear because the overall displacement was large and potential plastic deformation of the flexures due to buckling needed to be avoided because there was only one set of 0.025" flexures that was successfully made. The results of this test showed that the flexures could support 8 kg of loading in addition to the thruster mounting shelf with a minimum factor of safety of at least 1.25. It was not noticed until system testing that the stand becomes unstable when loaded above 1.27 kg. This means that while the flexures didn't buckle with a 10 kg load, the test stand becomes unusable above 1.27 kg. While the requirement Pm.1 was verified as written, the mission objective related to supporting a variety of masses was not validated due to the stand not being operational at that loading.

Verification of requirement Pm.2 - Test stand must accommodate thrusters up to 10 inches wide, was done through inspection. In accordance with the expectations of SPACE Lab, the PPT mounting shelf designed by this capstone group did not have to accommodate a 10 inch wide thruster, but the design of the pendulum itself had to allow for future development of a shelf that could accommodate such thrusters. The pendulum was designed in SolidWorks to have a gap of 10.52 inches between pendulum legs, which would allow for the design of future mounting systems for thrusters up to 10 inches wide. Consideration must be given to center of gravity in these future thruster mounts. A thruster who's center of gravity is not below the pendulum top will cause the test stand to become unstable. Measurements of the constructed pendulum found that the distance between pendulum legs is 10.5 inches. This means that requirement Pm.2 has been verified through inspection.

Verification of requirement Pm.3 - Structure must be non-conductive and outgas in accordance with NASA standards for ASTM E595 outgassing standards, was done through analysis. Delrin is a non-conductive material with a surface resistivity of 1×10^{13} ohms per centimeter [source]. NASA outgassing tables, found [here](#), were used to determine outgassing standards. According to the tables, Delrin has a Collected Volatile Compressible Material

(CVCM) was found to be 0.01 and the Total Mass Loss (TML) was found to be 0.28%. The criteria for vacuum compatibility is that CVCM must be below 0.1 and TML must be less than 1%, meaning that Delrin is vacuum compatible.

Extension of requirement Pm.3 to the Garolite structure was also done. According to NASA outgassing tables, Garolite has a CVCM of 0.00 and a TML of 0.27%. This means that both the PPT mount shelf and the Garolite structure of the test stand both meet requirement Pm.3.

Verification of requirement Pm.4 - PPT mount structure must keep thrusters centered to within 10% of vacuum chamber radius, was done through inspection. CAD models, constructed in SolidWorks, were used to validate that the Dawgstar PPT thrust would be centered within 10% of each chamber radius. These models are shown below.

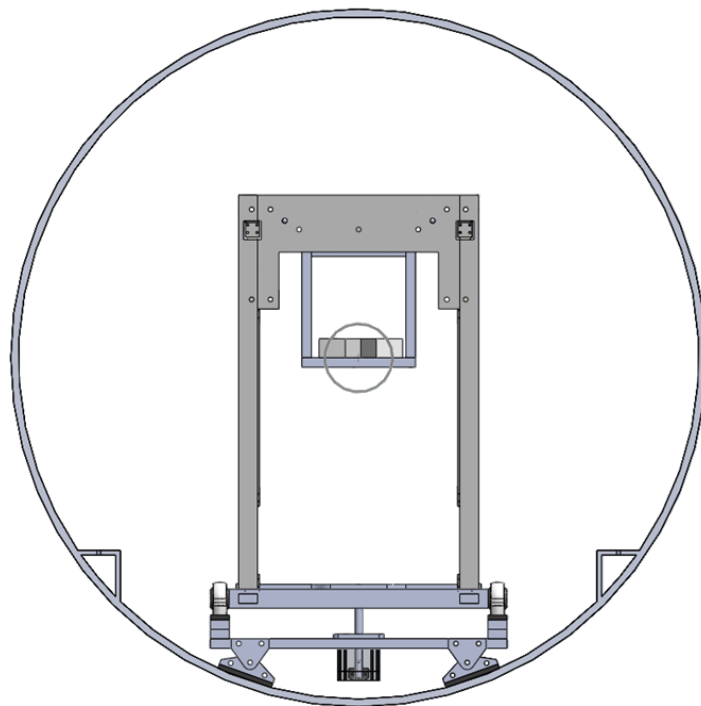


Fig. 6.4.6.2: Thruster shelf centers thruster plume within 10% of the metal chamber radius

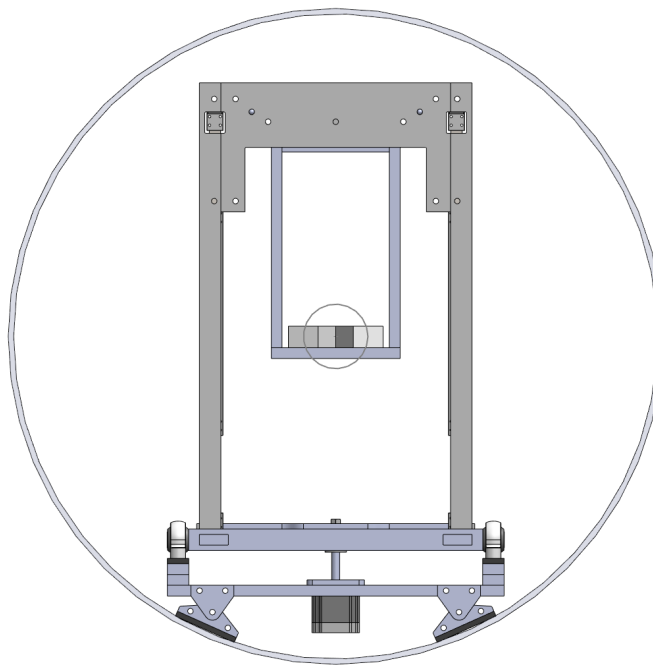


Fig. 6.4.6.3: Thruster shelf centers thruster plume within 10% of the crystal chamber radius

6.4.7 Risk Analysis

The primary risks for the structures component of the PPT mount subsystem were difficulty of manufacturing, accommodation of a variety of thrusters, and excessive weight. The breakdown of the risks in terms of likelihood and consequence severity is shown in the table below.

#	Risk Description	Mitigation	Likelihood	Consequence
1	Difficulty of manufacturing	Make out of Delrin instead of Garolite	4	2
2	Can't accommodate a variety of thrusters	Provide a means of mounting custom thruster mounts	4	1
3	Shelf contributes excessive weight to overall stand weight	Use lightweight material	3	3

Table 6.4.7.1. Risk Analysis for PPT Mount - Structure. Likelihood is scored on a scale from 1-5. Consequences are scored on a scale from 1-5.

When Garolite was chosen as the material for stand construction, the size and shape needed for the PPT mount was going to be difficult to machine. Delrin was chosen early as an alternative to Garolite as an easy to work with material. The downside being that it was more expensive.

When designing the PPT mount one large concern was that it would be hard to design a mount that could accommodate all the thrusters that could be tested. Through discussion with Peter Thoreau at SPACE Lab we decided to make a known bolt pattern on the pendulum top that could be used for custom mounting systems.

The size the thruster shelf needed to be in order to center the thruster plume in the chamber caused concern over the weight of the shelf. We thought this concern was not very likely based on analysis of the flexures. Unfortunately our analysis was incorrect, causing the shelf to be too heavy for use with the 0.10", 0.015", and 0.020" thick flexure sets. The problem of excessive weight will be mitigated through the use of custom built PPT mounts designed and constructed by SPACE Lab. The shelf that was designed and built for this project can be used with certain thruster sizes, but it will have a much narrower use than originally thought.

6.5 PPT Mount Subsystem - Motion Damping

Deflecting a pendulum in vacuum without a damper elicits an unreasonable settling time of 15+ minutes. An eddy current damper is required to reduce settling time without affecting spring constant.

6.5.1 Motion Damping Requirements

The motion damping system was intended to damp the pendulum's oscillations to a reasonable settling time, >20 s, but up to 60 s for lower impulse thrusters.

6.5.2 Interfaces

The motion damping system's parts are mounted to two components: the pendulum top and frame housing top. The magnet housing is fixed to the pendulum top using two 1/32" nuts and bolts. Figure 6.5.2.1 illustrates where the frame housing top is installed when the pendulum top is removed.

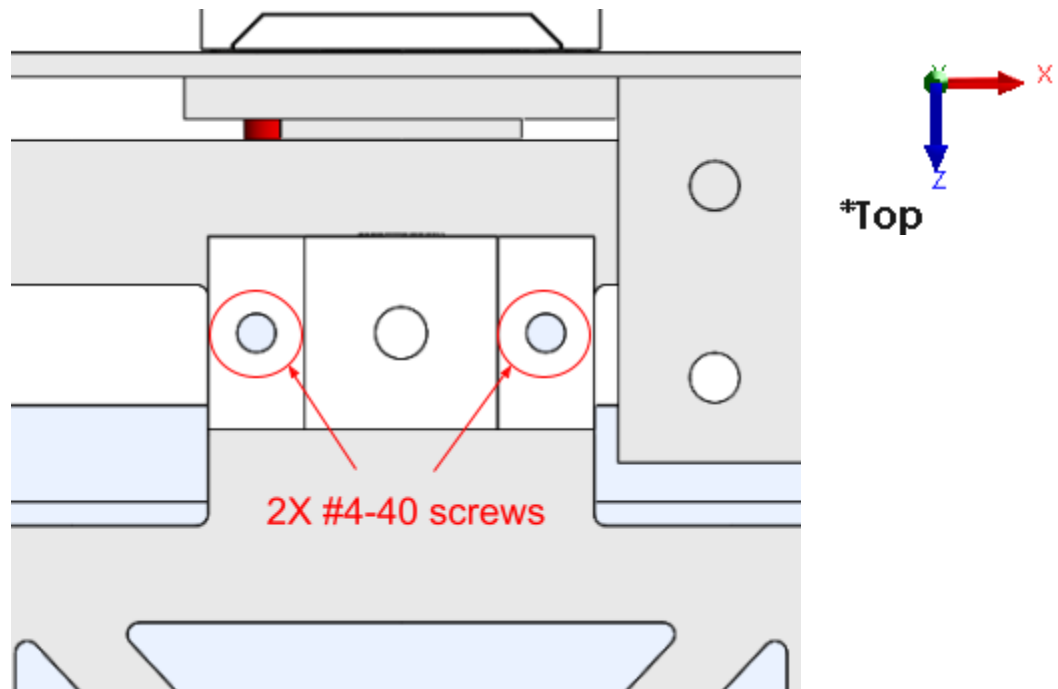


Figure 6.5.2.1. Magnet Housing Screws

The aluminum plate is mounted to the pendulum top using Vac-Seal vacuum-safe adhesive. For testing purposes, the magnet housing and aluminum plate were only temporarily affixed to the test stand using masking tape to ensure testing could be completed for configurations both with and without the damping system.

6.5.3 Trade Analysis

Analysis was conducted for the optimal damping system with emphasis on passivity, damping ratio, ζ , consistency, location of operation, and cost. The systems under consideration were: an eddy current damper, mechanical damper, and linear variable differential transformer (LVDT) operated voice coil damper. In the decision matrix, the 5 figures of merit were considered, and weights were assigned to each figure. Each material was evaluated for the figures of merit, and a score of 0-1 was given to each material. The total score for each material was given based on the material's score for each figure of merit multiplied by the score.

Passivity was the figure with the greatest weight with a score of 0.4, as having a passive system allows users to continue using the damping system without the need for an external power source, making it more reliable and easier to maintain. The eddy current damping scored full points in this section, as the geometrical configuration of the system is the primary driver in meeting requirements. The mechanical damper and LVDT voice coil damper scored lower, as their systems require a power source and electrical input to operate.

Damping ratio, ζ , was also heavily weighted with a score of 0.3 since it directly impacts the system's effectiveness in reducing oscillations. Consistency was important to ensure that the system's performance remains stable over time and under different operating conditions, in addition to producing compatible data. The eddy current system uses a permanent magnet, which possesses a constant magnetic field to damp motion, giving full points. The LVDT voice coil system also scored full points, as its damping force is controlled using a computer generating a measurable current. The mechanical damping system scored 0.9 points, as while they are consistent, they could potentially lose consistency due to operational friction.

The location of operation considered the ease of access to the system for changes and maintenance, in the event that the user wants to manipulate damping strength. The eddy current and LVDT voice coil systems both earned 0.7 points, as their installation location on the top of the pendulum frame would be easy to access by opening the pendulum top. The mechanical system only earned 0.5 points because its location of operation would create a physical connection between the moving pendulum frame and rigid pendulum shell. This is undesired because the connection point could adversely affect impulse resolution by affecting the system's effective spring constant.

Cost was the last consideration, such that the project doesn't overspend on what would otherwise be a simple system. The eddy current damper system only requires a magnet and conducting plates, making it incredibly cost effective. This earns it 0.8 points. The mechanical system is the most affordable as they are usually <\$20 and are ready to be installed from the box. This earns it full points. Lastly, the LVDT voice coils are the least cost-effective, as they are on the magnitudes of 100s of dollars and will require an electrical feedthrough and python script to operate. This earns it 0.6 points.

Overall, the eddy current damping system was the preferred choice and was used in the project. It earned 0.92 points in total, while the mechanical and LVDT coil systems earned 0.79 and 0.54 points respectively. The results are tabulated in Table 6.5.3.1.

Damping Method	Weight	Eddy Current	Mechanical	Linear Variable Differential Transformer
Passivity	0.4	1	0.8	0.1
ζ consistency	0.3	1	0.9	1
Location of operation	0.2	0.7	0.5	0.7
Cost	0.1	0.8	1	0.6
Total	1	0.92	0.79	0.54

Table 6.5.3.1. Weight decision matrix for damping system selection

6.5.4 Detailed Design

The damping system for the test stand utilizes an eddy current damper configuration. A magnet is installed onto the top of the moving pendulum, while a small conducting aluminum plate is installed on the rigid face opposite to it. Since the plate is located inside the magnetic field, the relative motion between the displacement of the pendulum (with the magnet on it) and rigid frame (with the conducting plate) will induce a current that in turn induces an electromotive force that resists motion. Fig. 6.5.4.1 details the installation of these 2 components. During operation, MH1 and MA1 are located 0.2" from each other, such that the conducting plate is in the magnetic field.

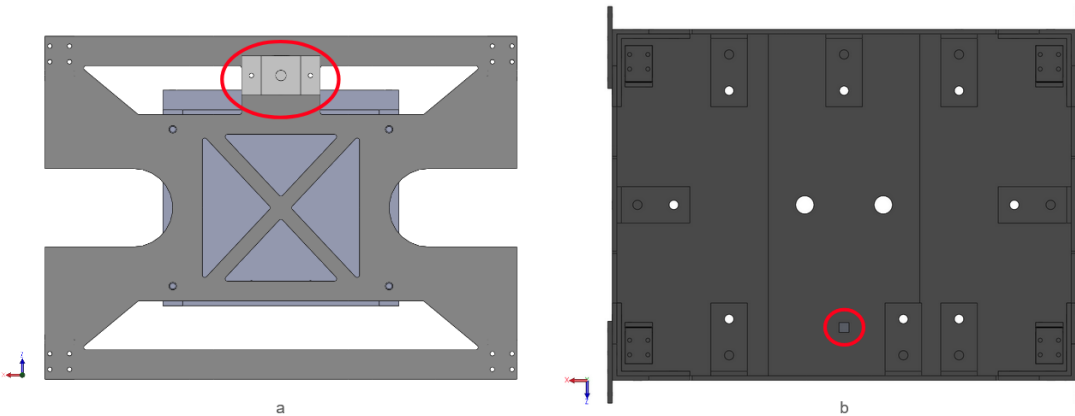


Fig. 6.5.4.1.a. Magnet housing installation on pendulum top. 6.5.4.1.b. conducting aluminum plate installation on removable pendulum frame

The magnet is housed inside a magnet housing printed out of carbon fiber-reinforced PETG (part name MH1). There is a slot for the magnet, which will be held in place with a set screw. There are also bolt holes to install the housing onto the pendulum top. The conducting aluminum plate is installed onto the rigid pendulum top, and is made out of aluminum 6061 (part name MA1).

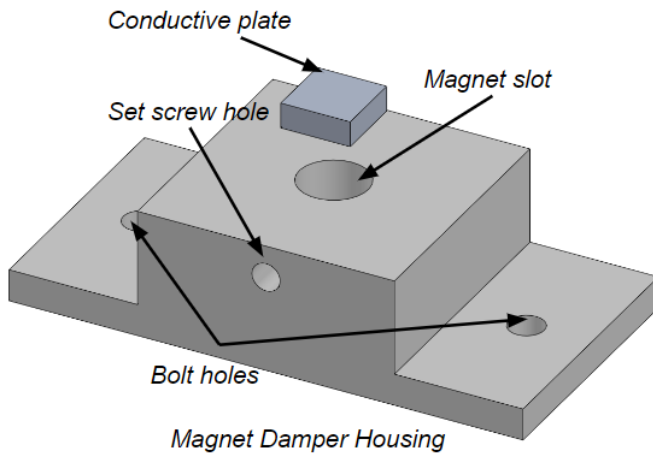


Fig. 6.5.4.2. Annotated magnet housing (MH1) and conducting plate (MA1).

This system utilizes Lenz's Law to operate. Lenz's law states that an induced electromotive force will always act in the direction opposite to the change in the magnetic field. As the magnet and conductive plate move against each other, the induced current resists the motion, providing a consistent damping. Fig. 6.5.4.3 contains equations used to derive the strength of the system's damping ratio. The system, in theory, will produce a damping ratio of 0.47.

$$F_d = \frac{vB^2At}{\rho}$$

$$F_d = \zeta v$$

$$\zeta = \frac{B^2At}{\rho}$$

F_d = Damping force
 v = Pendulum velocity
 B = Magnetic field
 A = Magnet face area
 t = Plate thickness
 ρ = Plate resistivity

Fig. 6.5.4.3. Damping ratio derivation

6.5.5 Materials & Manufacturing

The motion damping system consisted of two manufactured components: the magnet housing and damping sheet. The magnet housing was made of carbon fiber-reinforced PETG filament in one iteration and PLA in the next, and was 3D printed using an Ender 3 and Prusa i3 MK3S printer, respectively. The 0.125" diameter permanent magnet was friction fit into the magnet housing.

Part Name	Material	Manufacturing Technique	Quantity
Magnet Housing	Carbon Fiber-Reinforced PETG Filament / PLA	3D printing	1
Damping Sheet	0.1" Aluminum 6061 Sheet	Cut to size with shears	1

Table 6.5.5.1: PPT mount motion damping manufacturing matrix

6.5.6 Verification

Lack of access to a vacuum chamber meant that all damping system tests were completed at atmospheric pressure. During these tests, an impulse was supplied to the pendulum through releasing a 20 g mass and striking the pendulum. After processing the rangefinder voltage data to produce displacement vs. time plots, it was found that the damping system did not appreciably affect the damping time of the pendulum.

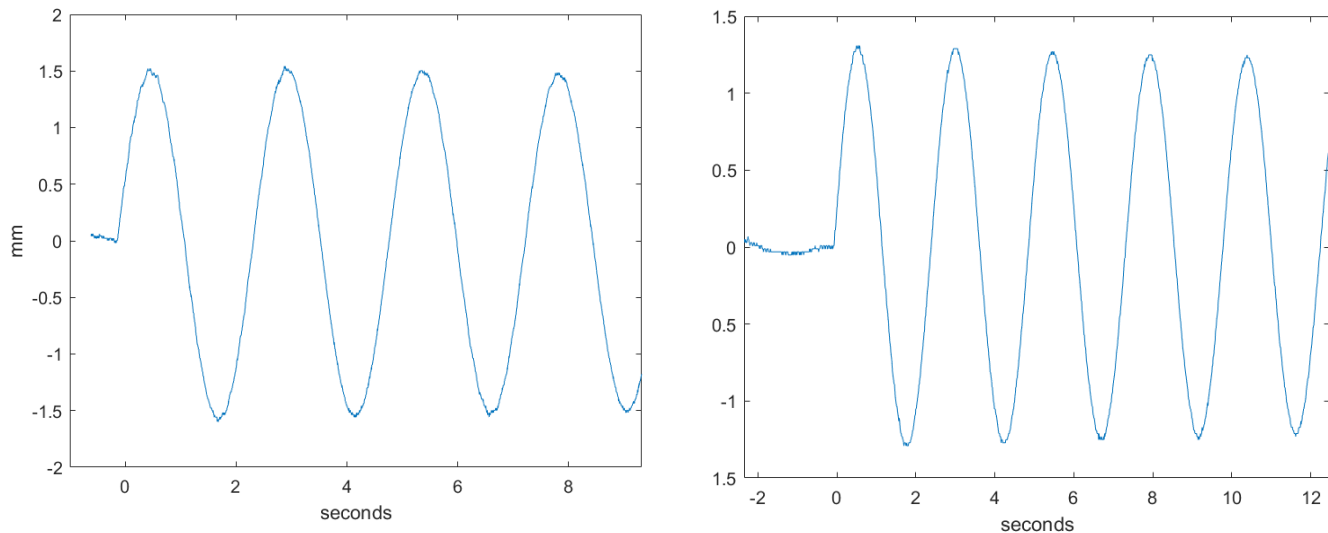


Figure 6.5.6.1. Pendulum Oscillation a) Without Damper (left), b) With Damper (right)

As the damping effects of this system are very weak compared to air resistance, with no discernible change in the stand's settling time, the damping system's performance could not be verified through testing.

6.5.7 Risk Analysis

This system could not be verified through the testing methods available to the team. For atmospheric pressure operations, this does not pose a risk, as the system's effects are negligible. For any vacuum testing, the characterization of this system's performance would be necessary for the proper function of the test stand.

#	Risk Description	Mitigation	Likelihood	Consequence
1	Lack of testing under vacuum	Testing was conducted at atmospheric pressure	4	1

Table 6.5.7.1. Risk Analysis for PPT Mount - Motion Damping. Likelihood is scored on a scale from 1-5. Consequences are scored on a scale from 1-5.

6.6 PPT Mount Subsystem - Waterfall

The waterfall subsystem exists to minimize the effective spring constant of the wires that are connected to the pendulum. For this system, the lines that are to be connected to the pendulum include: power lines to the PPT, power line to the electrostatic comb, and power/analog signal line to and/or from an unspecified plasma diagnostics probe.

6.6.1 Waterfall Requirements

ID	Requirement	Verification Method
Pm.8	Waterfall shall minimize effective spring constant of wires connecting to pendulum.	Testing

Table 6.6.1.1: PPT Mount - Waterfall driving requirements.

6.6.2 Interfaces

The waterfall wire bundle originates from two separate flanges, the high voltage PPT power line originating from a separate flange as the plasma sensor analog signal line due to EMI noise concerns, before running along the vacuum chamber wall and dropping down from above the stand. The waterfall is attached to the stand via two waterfall clamps, one sitting on the far end of the laser sensor mount, and the other attached to the none-plasma facing side of the thruster mount as seen in Fig. 6.6.2.1 and Fig. 6.6.2.2.

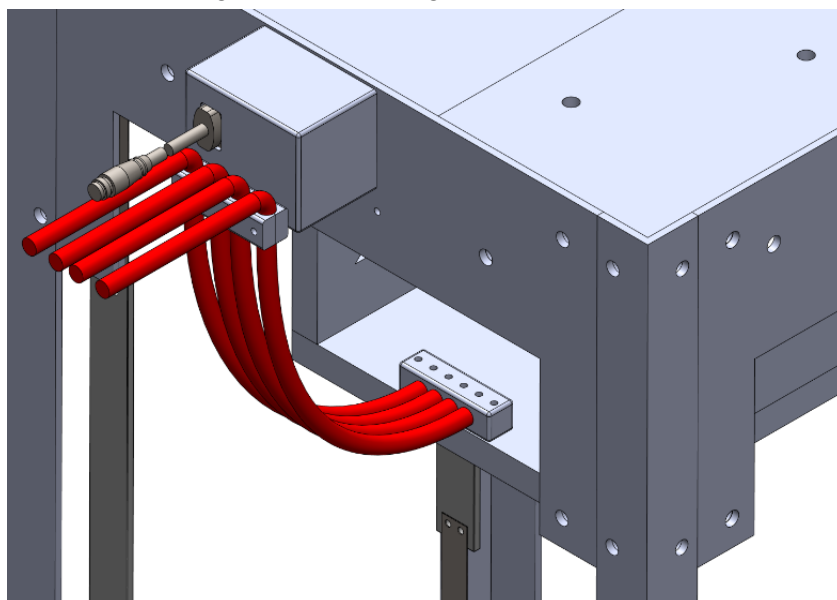


Fig. 6.6.2.1: Close up of waterfall clamp locations

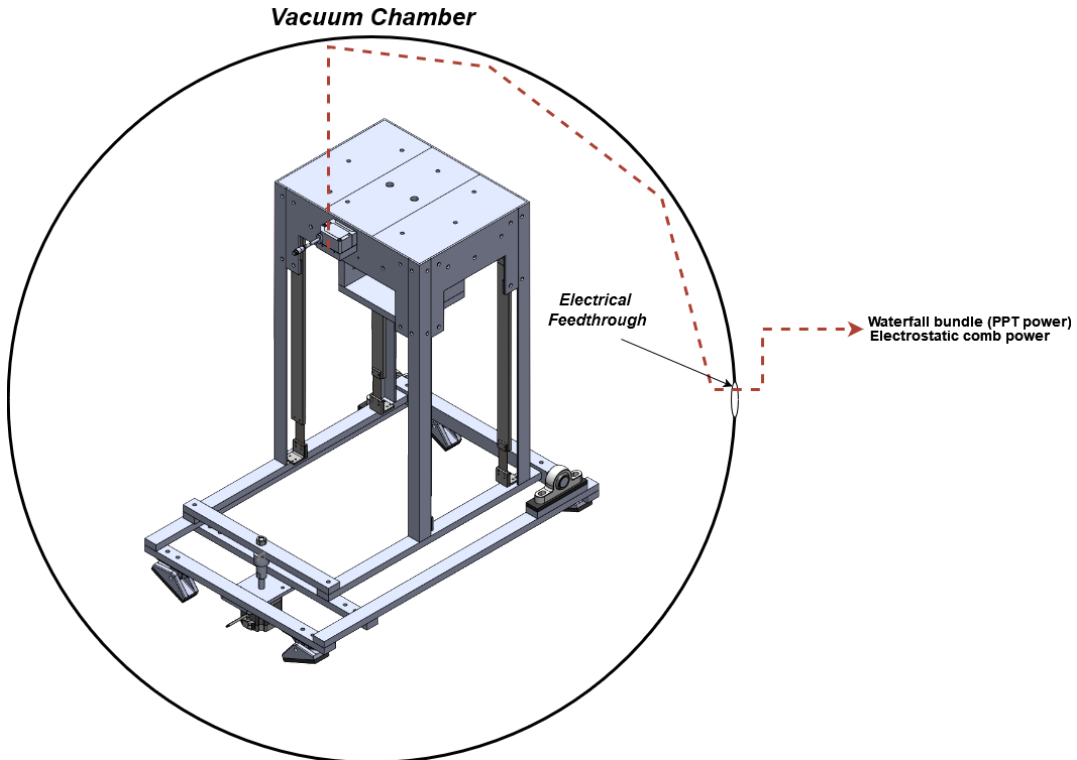


Fig. 6.6.2.2: Waterfall wiring diagram

6.6.3 Trade Analysis

The waterfall clamps were selected to be made out of carbon-fiber reinforced PETG filament to allow for easy iteration and to ease the manufacturing of such a small, detailed piece.

6.6.4 Detailed Design

The waterfall was designed with thermal expansion, and the vector direction of the spring force of the wires in mind. The two clamps were mounted perpendicularly to ensure that any thermal expansion would be perpendicular to the pendulum's direction of motion. The mounting points of the waterfall clamps were specially placed along the pendulum's axis of symmetry (i.e. in line with the PPTs firing direction) such that the waterfall's restoring force wouldn't create torsional oscillations in the pendulum's motion. Additionally the clamp locations were chosen to be surrounded by as much free space as possible, so nothing could make contact with the wire bundle during firing. Lastly the waterfall needed to be long enough relative to the flexibility of the wires, as to minimize the restoring force of the waterfall when the pendulum was in its centered "neutral" position.

The clamps themselves were designed as two symmetrical halves that were to be screwed together. The holes for the wires were designed to fit a maximum wire size of 0.25" inner diameter, with four separate wire pass-throughs. A set of through holes tapped to 4-40 were placed directly in the center of the wire pass-throughs to allow for the hand tightening of the wires in place.

6.6.5 Materials & Manufacturing

The waterfall clamps were printed using carbon-fiber reinforced PETG filament. This design uses two symmetrical halves with two screws to hold the clamp together and fasten the two sets of clamps to the PPT mount shelf bottom and laser rangefinder mount. These halves were 3D printed using a Prusa i3 MK3S printer. Four sets of screws for each wire were then screwed into the wire pass-throughs to hold them securely in place throughout thruster operation.

Part Name	Material	Manufacturing Technique	Quantity
Waterfall Clamp	Carbon-Fiber Reinforced PETG Filament	3D printing, drill press, tap holes	4
Wire Bundles	24 AWG PTFE Wire		3

Table 6.6.5.1: PPT Mount Waterfall Manufacturing Matrix

6.6.6 Verification

The “Impulse Response Prediction Code” script, as seen in App. A, was used to determine the effective spring constant of the waterfall using data collected from the SPACE Lab Capstone System Test Procedure. The base spring constant for the pendulum with the 0.025” flexures installed was measured to be 33.4 N/m, then with the waterfall attached the pendulum’s effective spring constant was measured to average out at 60.6 N/m, or a direct contribution from the waterfall of 27.2 N/m. However a second waterfall test was run with a wire of the exact same gauge and waterfall length, but a different brand, which resulted in a measured waterfall effective spring constant of 14.8 N/m. Thus depending just solely on the brand of wire, the waterfall’s spring constant can vary widely by at least a factor of two.

6.6.7 Risk Analysis

With the effective spring constant of the waterfall varying so wildly based on wire brand, without gauge or waterfall length being tested, this makes calibration of the system extremely important prior to testing. Such a variance in waterfall spring constant can cause major design complications for any future iterations of this project, and subsequently additional research is recommended to better understand waterfall behavior.

#	Risk Description	Mitigation	Likelihood	Consequence
1	Inconsistencies in spring constant	Individualized testing of waterfall wires before usage	3	4

Table 6.6.7.1. Risk Analysis for PPT Mount - Waterfall. Likelihood is scored on a scale from 1-5. Consequences are scored on a scale from 1-5.

6.7 Integration Plan/Process

For mechanical integration into the system, see attached Assembly Procedure file. Electric propulsion devices generate such little thrust that thrusters can be held in place on the pendulum shelf with friction alone. The shelf is simply bolted to the top of the pendulum using four nylon bolts. The waterfall clamp attached to the PPT shelf has two sets of holes drilled through the PPT mount to allow the clamps to be bolted to the shelf using nylon bolts, with an additional clamp located on the rangefinder mount, also attached using two nylon bolts.

7 Data Analysis Subsystem Design

7.1 Functional Requirements

The system must convert deflection measurements to impulse and steady-state thrust values within specified ranges of $\pm 1.125 \mu\text{lbf}$'s and $\pm 11.2 \mu\text{lbf}$ respectively. Additionally, it is required to record raw deflection data from the rangefinder at a sampling rate ranging from 100 to 1000 Hz. These functionalities ensure precise measurement conversion and accurate data recording, critical for the system's overall performance. The software is designed to display deflection measurements and corresponding uncertainties graphically at a rate of 100 to 1000 Hz, facilitating real-time visualization of data trends and variations. Additionally, the software will allow figures and raw data to be exported and processed externally.

7.2 Design Overview

The main task of the data analysis subsystem is to process raw deflection data, which is stored in an external hard drive. The calibration of the pulsed plasma thruster (PPT) before and after testing sessions is critical to maintain consistency and accuracy of measurements. Calibration entails stepping through different test conditions to create a model of expected deflections for a given impulse or steady state thrust input. Completing the calibration procedure before and after testing sessions enables the system to account for any variations in the PPT's performance. This approach to calibration ensures that data collected accurately represents the impulses and steady state thrusts generated throughout the stand's operation.

7.3 Budgets

The data analysis subsystem used \$103.81 (2%) of the total project budget. Table 7.3.1. itemizes all purchases made for the subsystem.

Category	Item	Cost	Total
Software	1 TB Hard Drive	\$ 63.15	\$ 103.81
	USB to USB A Cable	\$ 6.06	
	Arduino	\$ 27.60	

	Arduino 2.0 USB Cable	\$ 7	
			103.81

Table 7.3.1. Data Analysis Subsystem Budget Summary

7.4 Data Analysis Subsystem - DAQ

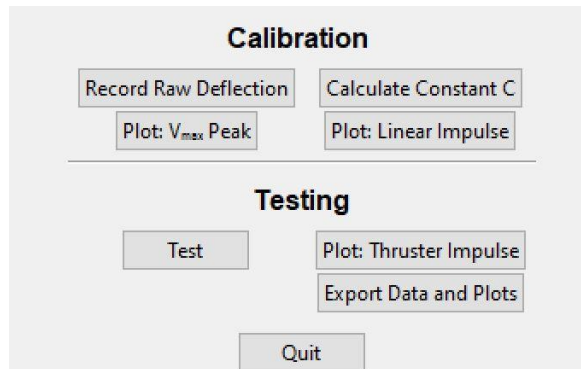
The purpose of the DAQ subsystem is to record raw voltage data from the laser rangefinder, and record it to an external drive for processing via the GUI code. It must convert the deflection measurements from the laser from impulse and steady-state configurations and their corresponding uncertainties.

7.4.1 DAQ Requirements

ID	Requirement	Verification Method
Da.1	Software will convert deflection measurements to Impulse measurements and corresponding uncertainties in the range of $\pm 1.125 \mu\text{lbf*s}$ ($5 \mu\text{N*s}$) . As well as steady state and corresponding uncertainties in the range of $\pm 11.2 \mu\text{lbf}$ (0.05 mN)	<i>Analysis</i>
Da.2	Software will record raw deflection data from the rangefinder at a sampling rate of 100 to 1000 Hz	<i>Analysis</i>

Table 7.4.1.1: Data Analysis - DAQ Requirements

7.4.2 Interfaces

**Fig. 7.4.2.1: Data analysis - DAQ Graphical User Interface**

7.4.3 Trade Analysis

The trade analysis involved the integration of the code with the avionics system. The system needed to be designed such that the DAQ could communicate effectively with the laptop running the GUI. It also includes a calibration system to test the dynamic characteristics of the stand both before and after testing.

7.4.4 Detailed Design

The detailed design for the NI-DAQmx Driver software involves several key steps. First, it is essential to verify that the Data Acquisition (DAQ) device is recognized by the computer. This step involves installing the necessary drivers and using diagnostic tools to confirm that the DAQ device is properly interfaced with the computer. Ensuring the hardware is correctly connected forms the foundation for all subsequent data acquisition tasks.

Next, Python is integrated with the NI-DAQmx Driver and PySerial to facilitate seamless data handling. This integration leverages Python's versatility and extensive libraries, enabling efficient communication with the DAQ device and other serial devices. The PySerial library, in particular, is utilized for serial communication, ensuring reliable and accurate data transmission between devices. A crucial aspect of the design is the implementation of a TTL trigger to initiate the firing sequence of the pulsed plasma thruster. This trigger mechanism provides precise timing control, which is vital for the thruster's operation. The TTL trigger ensures that the activation of the thruster is synchronized with data acquisition processes, allowing for the capture of all relevant data during the firing sequence.

For recording deflection data, the function `record_deflection()` is employed to read raw deflection data from the DAQ. This function is designed to handle large volumes of data efficiently, ensuring no data is lost during the acquisition process. The recorded data is then processed to extract meaningful insights. To improve the quality of the data, a low pass filter is applied. This filter smooths out high-frequency noise and fluctuations, making the data more suitable for detailed analysis and interpretation. The sampling clock configuration is another critical component of the detailed design. The read rate for deflection data from the rangefinder is set between 100 and 1000 Hz, using the `timing.cfg_samp_clk_timing` method. This range is chosen to balance the need for high-resolution data with the limitations of data processing and storage capabilities. The mode for the sampling clock is set to continuous, allowing for uninterrupted data acquisition over extended periods. This continuous mode is essential for capturing dynamic changes in deflection data, providing a comprehensive dataset for analysis.

7.4.5 Verification

The “Deflection Data Analysis code” in App. A, will calculate the calibration constant accurately, which is vital for converting raw data into meaningful, calibrated data. This process ensures that the measurements are both accurate and reliable. The NI-DAQmx software is responsible for saving both the calibrated and raw data correctly, which is critical for data analysis and future reference. Proper data management ensures that any discrepancies can be traced back and that data integrity is maintained throughout the process.

The NI-DAQmx software also facilitates the correct display of both calibrated and raw data in plots. This visualization is crucial for analysis and interpretation, allowing users to easily understand the data and make informed decisions based on the visual representation. The ability to visualize data accurately helps in identifying patterns, trends, and anomalies that might not be apparent in raw numerical data.

7.4.6 Risk Analysis

The greatest risk to the calculation of calibration constants was a lack of access to the electrostatic fins required for the nominal calibration process. Because these fins were produced by SPACE Lab graduate students and were regularly used for testing, availability was limited. Additionally, the Python code written was not compatible with the NI-DAQmx software or DAQ. This led to the DAQ system being descoped, with the oscilloscope used in lieu. As a result, the calibration process was only completed using a mass striking the pendulum as detailed in Section 8.

#	Risk Description	Mitigation	Likelihood	Consequence
1	Electrostatic Fin Access	Ensure SPACE Lab does not have testing scheduled during planned test stand verification testing	3	4
2	Non-functional code	Use an oscilloscope instead of a DAQ	5	5

Table 7.4.6.1. Risk Analysis for Data Analysis - DAQ. Likelihood is scored on a scale from 1-5. Consequences are scored on a scale from 1-5.

7.5 Data Analysis Subsystem - GUI

The DAQ GUI records raw deflection data from the DAQ and conducts tests accurately. It displays plots for the Linear Impulse, V_{max} Peaks, and Thruster Impulse. Additionally, it provides options to export all data and plots. The Arduino GUI allows for precise step up and step down adjustments for the leveling system. It displays the stepper motor displacement, enabling corrections if the motor displaces itself again.

7.5.1 GUI Requirements

ID	Requirement	Verification Method
Da.3	Software will display deflection measurements and corresponding uncertainties recorded at a rate of 100 to 1000 Hz graphically	<i>Demonstration</i>
Da.4	Software will allow for the export of produced figures and raw data	<i>Demonstration</i>

Table 7.5.1.1: Data Analysis - GUI Requirements

7.5.2 Interfaces

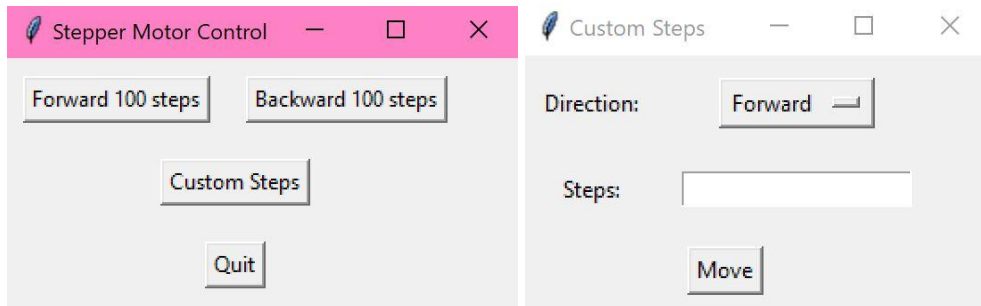


Fig. 7.5.2.1: Data analysis - Leveling System Interfaces

7.5.3 Trade Analysis

Several factors were considered throughout trade analysis in terms of the applications to both the leveling system stepper motor and DAQ interfaces. Human factors were a significant consideration, as the systems were ultimately designed to have the simplest and most straightforward interfaces possible. The stepper motor control GUI needed to provide fine control over both upward and downward motion of the actuation rod while also displaying the total displacement from the actuation rod's zero point. The control needed to actuate the stepper motor, at minimum, in step increments of 0.00035", while also providing the option to step in larger increments. The DAQ was designed to have functionalities fulfilling both calibration and testing needs. It was intended to feature a dedicated testing window and a separate calibration window.

7.5.4 Detailed Design

The Arduino is programmed to receive commands via PySerial, instructing it on how to control the stepper motor. This control allows the system to adjust up to $\pm 3^\circ$ as desired. Data transmission to the serial port is facilitated by the sendData function. GUI integration is achieved through Tkinter, enabling the design of GUI elements. A plot is provided for visual adjustment of the stepper motor displacement between tests. Buttons such as *RotateClockwise()* and *RotateAnticlockwise()* enable step up and down movements, with an option to quit to close the command window.

For the DAQ component, a TTL trigger firing sequence is implemented to all thruster avionics. Deflection data from the rangefinder is recorded at a rate of 1000 samples per second using the NI-DAQmx, stored in the global variable *deflection_data*. Calibration involves finding the V_{max} peak, calculating the constant 'c', and plotting both the V_{max} peak and V_{max} vs Known Impulse. Testing encompasses Thruster Impulse & Uncertainties and V_{max} peak plot generation. GUI integration for this component is also facilitated via Tkinter, with dedicated sections for Calibration and Testing. Export options include both figures (as .png) and raw data (as .csv), satisfying Da.3 and Da.4 of the system requirements.

7.5.5 Verification

The DAQ and Arduino GUIs were ultimately decoupled. Rather than using a GUI for the DAQ, oscilloscope traces were recorded instead, then analyzed. However, the Arduino GUI was tested following the steps outlined in the Leveling System Test Procedure and its ability to move the stepper motor actuation rod in increments of 0.00035 inches +/-50% per step was verified.

7.5.6 Risk Analysis

Table 7.5.6.1, below, highlights several potential risks associated with the data analysis subsystem. An additional risk is the failure to display plots correctly or at all. Another concern is the inability to store data on the hard drive.

#	Risk Description	Mitigation	Likelihood	Severity
A	Plot display	Test sample data prior to system testing and if needed, edit GUI to ensure proper function during full system test	2	3
B	Data storage	Manually check that files store properly by accessing hard drive through laptop prior to moving to next steps in testing	3	4

Table 7.5.6.1. Risk Analysis for Data Analysis - GUI. Likelihood is scored on a scale from 1-5. Consequences are scored on a scale from 1-5.

7.6 Integration Plan/Process

The integration process of the data acquisition subsystem into the pulsed plasma thruster (PPT) stand will involve several key steps to ensure seamless functionality and reliability. Firstly, the hardware components, such as the rangefinder and DAQ device, will be physically integrated into the structure of the PPT stand. This integration will involve mounting and securing the components in their designated positions within the stand, ensuring proper alignment and connectivity.

Concurrently, the software components, including the data acquisition software and associated drivers, will be installed and configured on the computing platform designated for the PPT stand. This step will involve installing the necessary software packages, setting up communication protocols, and configuring system parameters to ensure compatibility and optimal performance. Following hardware and software integration, a series of rigorous testing procedures will be conducted to validate the functionality and interoperability of the data acquisition subsystem. Verification tests will be performed to confirm proper communication between the software and hardware components, ensuring that data can be accurately transmitted and received. Calibration procedures will also be carried out to validate the accuracy of measurement conversion and data recording, ensuring that the system can produce reliable and consistent results.

Once integration and testing are successfully completed, the data acquisition subsystem will be fully integrated into the PPT stand, ready for operational use. To maintain the system's reliability and accuracy over time, regular maintenance and calibration routines will be established. These routines will include periodic checks and adjustments to ensure that the system continues to meet performance requirements and remains calibrated to produce accurate measurements. Throughout the integration process, comprehensive documentation will be maintained to track integration steps, testing results, and any adjustments made. This documentation will serve as a reference for troubleshooting, system maintenance, and future

upgrades, ensuring transparency and accountability in the system's operation. By following this detailed integration plan, the data acquisition subsystem will be effectively integrated into the PPT stand, supporting its overall functionality and performance.

8 System Conclusions

This project aimed to design, build, and test an impulse and thrust measurement stand for use in the SPACE Lab. The project was intended to resolve thrusts from 10 $\mu\text{N}^*\text{s}$ to 100 mN*s with an inverted pendulum-style stand by correlating displacements measured by a laser rangefinder to an impulse or steady state thrust. Though several mission objectives were met, several key functionalities of the test stand were not built or did not function as intended based on the results obtained from testing. This resulted in the descoping of several systems including the data acquisition system GUI, leveling system, and chamber interface.

8.1 Integration Plan/Process

Regarding the test stand assembly inside the chamber, all structural components are connected with an array of nuts and bolts. The pendulum assembly of the thrust measurement subsystem uses #4 size bolts installed using a wrench. All other components of the test stand are structurally held together using 1/4"-20 nylon bolts.

Regarding the electrical connections, all wires are to be connected in accordance with the wiring diagram, utilizing soldered connections as seen in App. A.

8.2 System Risk Analysis

#	Risk Description	Mitigation	Likelihood	Severity
A	Deflection Model Validity	Pendulum testing and design iteration	4	4
B	Manufacturing Quality	More team members must be AA shop trained to complete required manufacturing to specifications	4	3
C	Waterfall Spring Constant	Perform additional testing to fully characterize waterfall spring constant contribution under different conditions	3	3

8.3 Validation Analysis

Below is a table of system requirements along with the status of whether they have been met or not. Green boxes indicate the requirement is met, red indicate the requirement is not met, and gray indicates the requirement has been descoped.

- Requirement Met
- Requirement Not Met
- De-Scoped

ID	Requirement	Verification Method	Met?
Sys.1	Test stand must be an inverted pendulum style	<i>Inspection</i>	Yes
Sys.2	Test stand shall minimize the use of conductive materials	<i>Inspection</i>	Yes
Sys.3	Test stand must be able to resolve a minimum stand deflection of half the lowest predicted deflection such that impulse bits ranging from 10 $\mu\text{N*s}$ to 100 mN*s $\pm 5 \mu\text{N*s}$ can be measured	<i>Analysis/Test</i>	No
Sys.4	Test stand must be able to resolve a minimum stand deflection of half the lowest predicted deflection such that steady-state thrusts ranging from 0.1 mN to 0.1 N ± 0.05 mN can be measured	<i>Analysis/Test</i>	Yes
Sys.5	Test stand must be able to support thrusters up to 8 kg without buckling	<i>Test</i>	Yes
Sys.6	Test stand must accommodate thruster diameters up to 10.0 in, and thruster lengths up to 9.1 in	<i>Inspection</i>	Yes
Sys. 7	Test stand shall be able to be horizontally leveled to within ± 0.05 degrees	<i>Demonstration</i>	
Sys.8	Test stand must return thruster to 0.002 ± 0.001 degrees of zero-point between tests	<i>Test</i>	

Sys.9	The stand must be installed, securely operated, and safely removed from the vacuum chamber without causing any structural or cosmetic damage to the chamber wall	Demonstration	
-------	---	---------------	--

Table 8.3.1: System Requirements Status

System requirement 1 states that the test stand must be an inverted pendulum type stand. This requirement was made because SPACE Lab specified they wanted this test stand to be an inverted pendulum style. This requirement was verified through inspection.

The test stand was designed and constructed as an inverted pendulum type test stand as requested by SPACE Lab. This means that requirement Sys.1 was verified as met through inspection. Furthermore, the part of the mission objective stating the stand must be an inverted pendulum type has been validated.

System requirement 2 states that the test stand shall minimize the use of conductive materials. This requirement was made because electric thrusters can generate their own electric and magnetic fields that can interact with a stand made of conductive materials, which could have an impact on the performance of the test stand by increasing the signal to noise ratio in the laser sensor output. This requirement was verified through inspection, with the number and locations of conductive parts included below in Table 8.3.2.

Inspection of the test stand after construction found a number of conductive materials that were deemed necessary to the project. A table of these materials can be found below. The flexures were chosen to be metallic because spring steel is the best material for flexures due to its high resilience and high yield strength. Several fasteners needed to be made of steel in order to provide the strength needed for repeated use and reliability, as with the flexure and leveling bracket fasteners. The damper magnet and damper sheet both needed to be conductive in order to utilize the eddy currents needed for a damping system. The laser sensor is an electronic device, so it also had to be conductive. All of these conductive materials were deemed necessary by the team, so the amount of conductive material used in the stand was kept to a minimum. This means that requirement Sys.2 was verified as met through inspection. Furthermore, the part of the mission objective stating the stand must be minimally conductive has been validated.

Part	Material	#	Minimum Distance to Shelf Surface (cm)
Flexures	1075 Steel	8	8.7
Flexure Bolts	Stainless Steel	64	14.9
Flexure Nuts	Stainless Steel	64	14.9
Damper Magnet	Neodymium	1	20.3
Damper Sheet	Aluminum	1	21.5

Leveling Bracket Bolts	Stainless Steel	16	35.4
Leveling Bracket Nuts	Stainless Steel	16	35.4
IL-030	Various Metals	1	19.8

Table 8.3.2: Conductive Material Quantities & Locations

The natural frequency of the pendulum was derived under various loading conditions to change the overall effective spring constant of the pendulum. The pendulum was applied with some mass which was defined as the value of the mass of the PPT mount shelf combined with the mass of known increments in 100 g. These loading conditions of the applied mass were chosen so that the effective spring constant would be noticeably different, but still stable. A known impact mass was then swung on a separate pendulum to contact the PPT mount shelf. For each trial, it was determined visually from the trace if the pendulum hit the frame, if it did, then the data for that trial was retaken. The damped impulse response of the stand was used to derive this value. A damping coefficient of 0.0113 was calculated from the peak to peak change of the stand due to atmospheric pressure. Fig. 8.3.1 shows the derived flexure spring constant effect for eight 0.025" flexures under various loading conditions. The code used to generate this plot can be found in Appendix A. Only 0.025" flexures were tested because thinner flexures were found to be unstable under any loading condition. Therefore, all following data presented will be relevant only to flexures of 0.025" unless specifically stated otherwise. The spring constant of the flexures should be a constant value, so the error in the measurements is attributed to the use of an 8-bit scope for data collection. Since the natural frequency of the stand was found by locating peaks in the response, low bit resolution resulted in non-exact locations for peak timing. The eight 0.025" flexures were found to apply a total spring constant of 33.4 ± 0.5 N/m. This value is useful because it can now be used to compare the predictions made by the design model to the data collected during system testing.

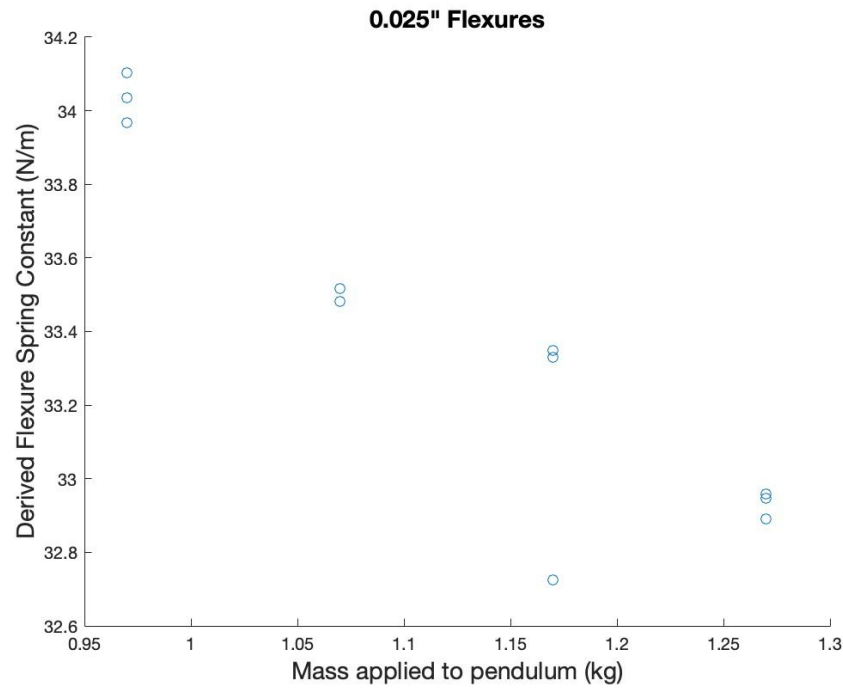


Fig. 8.3.1: Spring constant effect for eight 0.025" flexures.

Since the originally intended calibration device used to create extremely small values of impulse was not functional during the time of testing, impulse testing could not effectively be completed. For that reason, the stand was then tested under steady state conditions by using a known hanging mass to apply a known force to the pendulum. Masses of 1 gram, 2 grams, and 3 grams were used to create forces of 9.8 mN, 19.6 mN, and 29.4 mN. In this test setup, a mass was applied to the pendulum PPT mount shelf but now a piece of fishing wire with a known mass attached to the end was taped to the shelf and run over a fixed piece of Garolite so that the gravitational force of mass was in plane with the direction of motion of the pendulum. Garolite was used in this case to minimize the effect of friction on the applied force to the pendulum, but frictional effects were not accounted for in any other way. The mass of the fishing wire was determined to be negligible based on a mass per unit length of 0.2 g/m, and only eight centimeters of fishing wire was used. The steady state deflection of the stand for ten trials at each force was recorded and averaged over ten trials to account for any out-of-plane alignment of the force vector as well as any effects of slight offset in the pendulum zero pointing between trials. The model used to design the pendulum showed a predicted response 1.114 ± 0.033 times that of the empirically collected data. The predicted vs measured steady state response of the pendulum is shown in Fig. 8.3.2. The code used to generate this plot can be found in Appendix A.

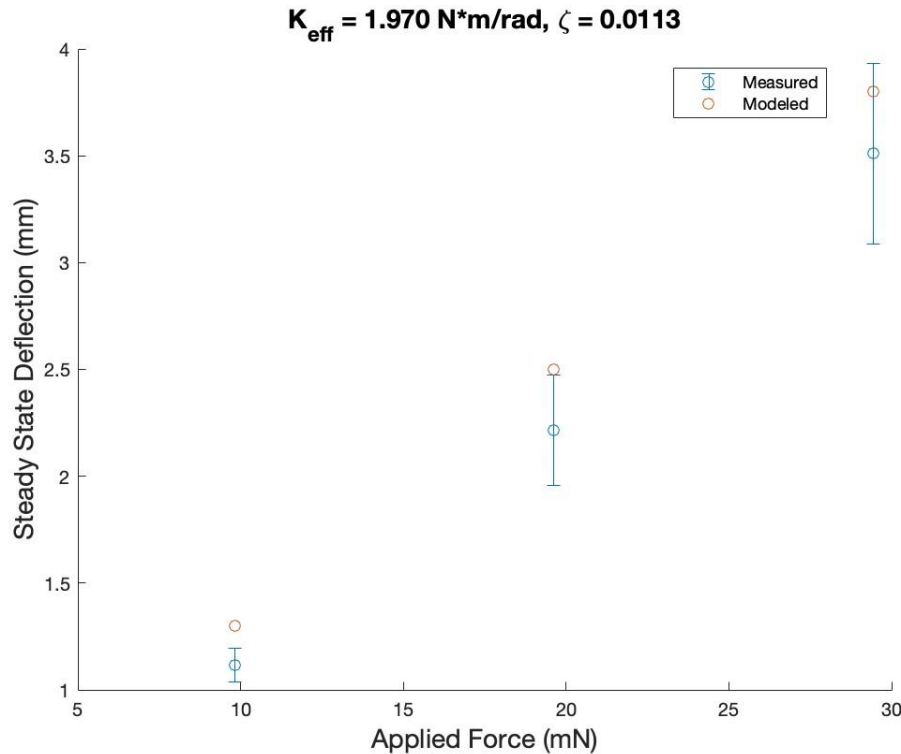


Fig. 8.3.2: Modeled vs. measured response of the pendulum due to a steady state force. Error bars derived from the standard deviation over ten trials.

Now that the model has shown a reasonably consistent difference compared to actual data, it can be used to make predictions for the steady state response of the pendulum under other conditions. It can also be used to make predictions about impulse response since the underlying mechanical system of the pendulum remains the same in either case.

The flexure buckling testing showed the 0.025" flexures do not buckle when loaded with 10 kg. Stability testing of these flexures showed that they become unstable when loaded with 1.375 kg (the design model predicts this will occur at 1.316 kg). This means that arbitrarily low effective spring constants for the pendulum may be achieved to satisfy the bottom test cases of system requirements 3 and 4. But this also means that at extremely low spring constants, the settling of the pendulum will rise exponentially. So a reasonable value of settling time must be chosen which will set a limit of the lowest acceptable value of the pendulum spring constant. This value will be determined at a fifteen second two-percent settling time, but this value may be different based on the needs of different experiments and operators. Since testing was completed with no damping device attached to the pendulum, settling time predictions were made assuming a damping coefficient of 0.3, which was the design goal for this pendulum. These values are shown in Fig. 8.3.3. The code used to generate this plot can be found in Appendix A.

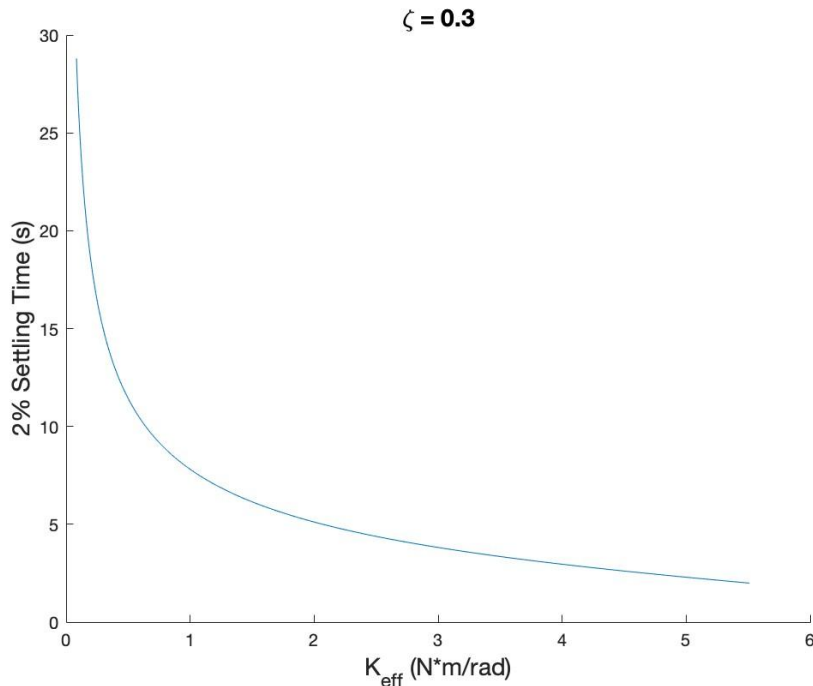


Fig. 8.3.3: Settling time compared to effective spring constant for a damping coefficient of 0.3.

The resolution of any inverted pendulum is limited by the lever arm length and the longest allowable settling time. This sets a bottom case of the minimum resolvable impulse regardless of the design choices set by the chamber diameter limiting the length of the lever arm. To achieve a fifteen second settling time, an effective spring constant of 0.300 N*m/rad is required given a damping coefficient of 0.3. Since the deflection measurement uncertainty given by the resolution of the rangefinder is 10 micron, and system requirements 3 and 4 define an uncertainty for the minimum resolvable value of one-half that value, then the pendulum must deflect at least 20 micron at the minimum resolvable value to satisfy that requirement.

Now by using the design model with a factor input to account for the difference between predicted and actual response, new predictions can be made for the ranges of impulse and steady state forces that the pendulum can resolve. Given an effective spring constant of 0.300 N*m/rad, an impulse of 45.5 $\mu\text{N*s}$ can be resolved with a peak deflection of 20 micron, giving an uncertainty of fifty percent. Although this value does not meet the requirements of system requirement 3, it is limited by the reasonable value of spring constant chosen to satisfy the operational settling time requirement. The minimum resolvable impulse to achieve the required uncertainty can be determined using Fig. 8.3.4. This figure shows the expected measurement uncertainty, which is directly tied to the expected deflection as described previously, for any given impulse. The code used to generate this plot can be found in Appendix A. It should be noted that for an effective spring constant of 0.009 N*m/rad, a 10 $\mu\text{N*s}$ impulse can be resolved with 25 micron of deflection, but this results in a two percent settling time of 87 seconds. Therefore, given the limitations on the lever arm and the settling time, it is not possible to meet system requirement 3 no matter the design of the pendulum.

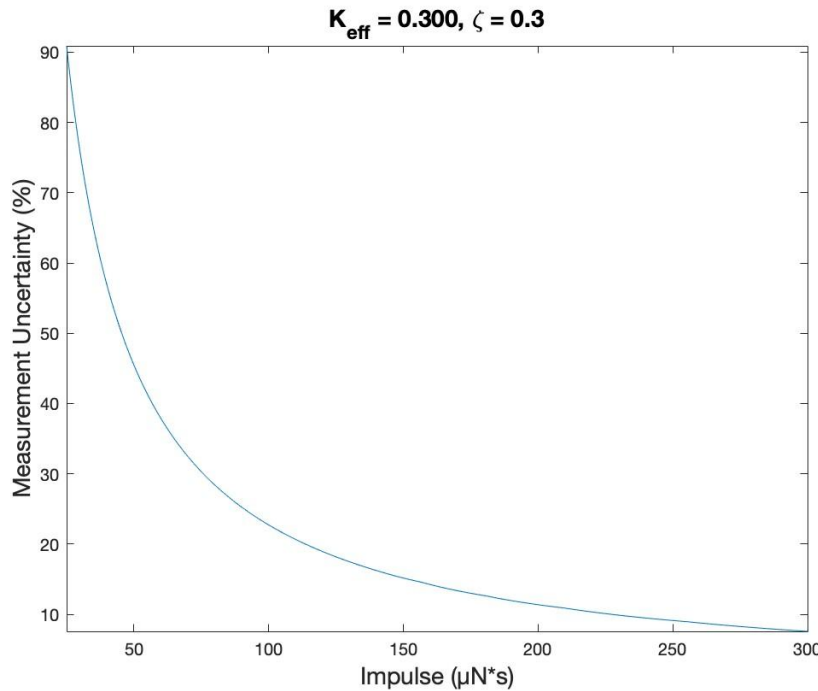


Fig. 8.3.4: Measurement uncertainty for a given impulse.

Predictions can also be made for steady state forces. Given an effective spring constant of 0.300 N*m/rad and a damping coefficient of 0.3, a 0.1 mN steady state force is predicted to result in 134 micron of deflection, which will have a thirteen percent measurement uncertainty on the 0.025" flexures. The values for measurement uncertainty of low end steady state force requirements are shown in Fig. 8.3.5. Again, this plot shows the expected measurement uncertainty, related to the expected steady state deflection, for a given steady state force. The code used to generate this plot can be found in Appendix A. Assuming linear trend for flexure spring constant prediction, 100 mN steady force is predicted to be resolved with 1.6 mm deflection on 0.040" thick flexures. This will result in a flexure total spring constant of 88.4 N/m and an effective spring constant of 25.656 N*m/rad. Therefore, system requirement 4 is met and has been verified through analysis.

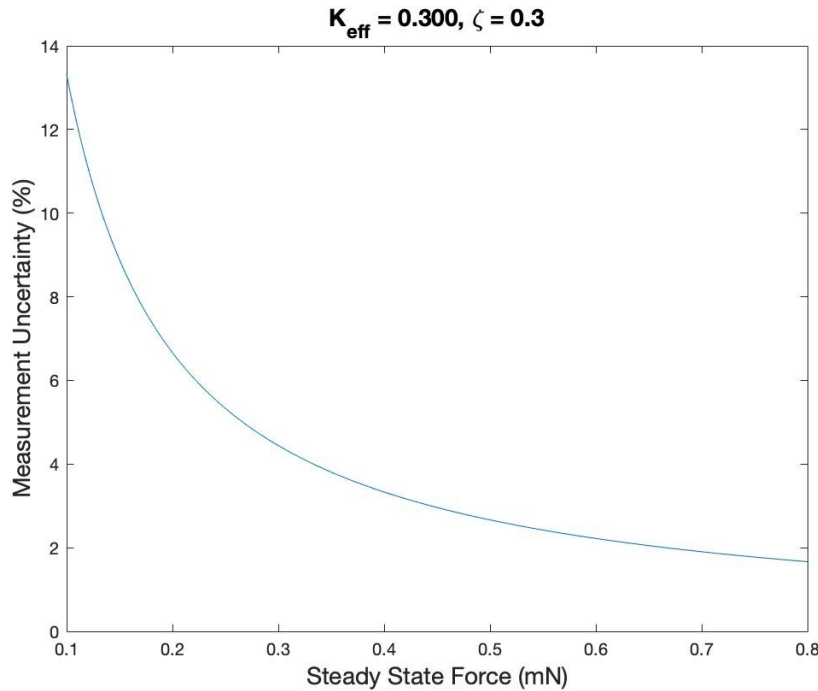


Fig. 8.3.5: Measurement uncertainty for a given steady state force.

System requirement 5 states that the structure must be able to support thrusters up to 8 kg and was verified through testing. This testing was the same testing that verified requirement Pm.1 was verified. To recount that process, the test procedure for buckling can be found [here](#), the test plan can be found [here](#). Verification of Sys.5 was done on the 0.025" flexure set with the larger PPT mounting shelf used for the crystal vacuum chamber installed. The results of the buckling test for the 0.025" flexure set can be seen below.

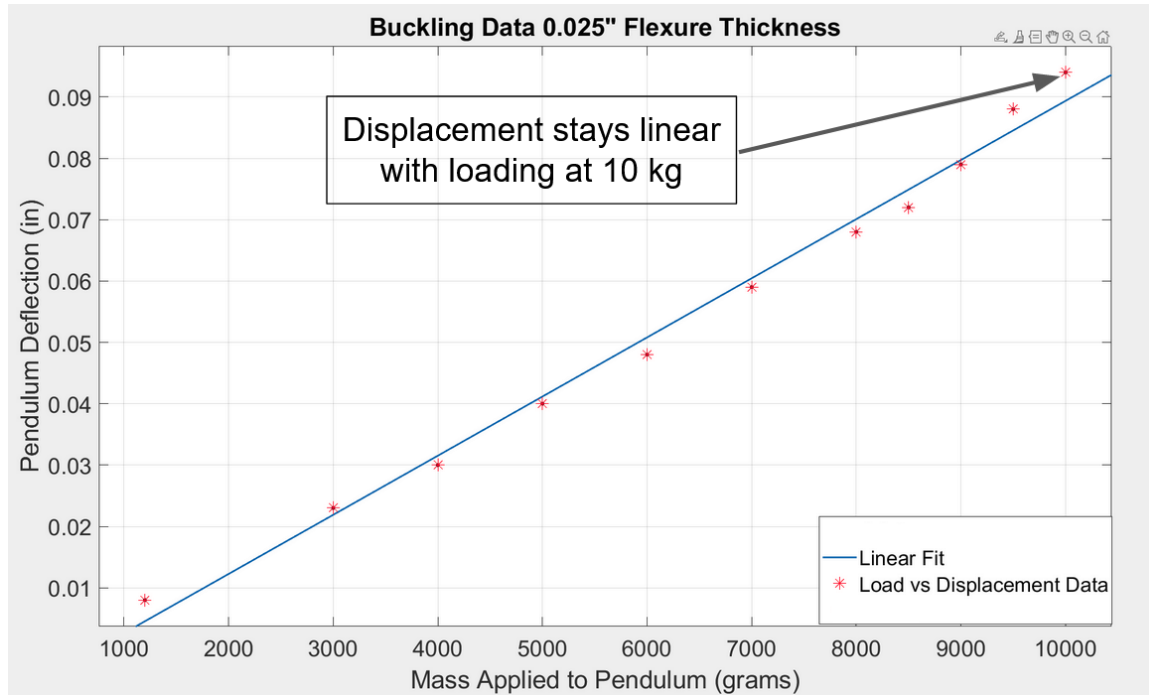


Fig. 8.3.6: Buckling data for 0.025" flexures

Buckling is indicated when the change in vertical displacement becomes non-linear relative to the change in applied loading. This test never reached the point where the change in vertical displacement never became non-linear because the overall displacement was large and potential plastic deformation of the flexures due to buckling needed to be avoided because there was only one set of 0.025" flexures that was successfully made. The results of this test showed that the flexures could support 8 kg of loading in addition to the thruster mounting shelf with a minimum factor of safety of at least 1.25. It was not noticed until system testing that the stand becomes unstable when loaded above 1.27 kg. This means that while the flexures didn't buckle with a 10 kg load, the test stand becomes unusable above 1.27 kg. While the requirement Sys.5 was verified as written, the mission objective related to supporting a variety of masses was not validated due to the stand not being operational at that loading.

System requirement 6 states that the test stand must accommodate thruster diameters up to 10.0 in, and thruster lengths up to 9.1 in, this requirement was verified through inspection. This inspection was the same inspection that verified requirement Pm.2. To recount that process, in accordance with the expectations of SPACE Lab, the PPT mounting shelf designed by this capstone group did not have to accommodate a 10 inch wide thruster, but the design of the pendulum itself had to allow for future development of a shelf that could accommodate such thrusters. The pendulum was designed in SolidWorks to have a gap of 10.52 inches between pendulum legs, which would allow for the design of future mounting systems for thrusters up to 10 inches wide. Consideration must be given to the center of gravity in these future thruster mounts. A thruster who's center of gravity is not below the pendulum top will cause the test stand to become unstable. Measurements of the constructed pendulum found that the distance between pendulum legs is 10.5 inches. This means that requirement Sys.6 has been verified through inspection.

System requirement 7 states that the test stand shall be able to be horizontally leveled to within ± 0.05 degrees. Due to time constraints the scope of this project got narrowed to only focus on the test stand pendulum and pendulum frame. The descoping of the project included the elimination of the leveling system. This system was designed and some parts were

manufactured, but the integration of this subsystem into the test stand will be a part of work done in the future. Due to this descoping, system requirement 7 was not verified.

System requirement 8 states that the test stand must return the thruster to 0.002 ± 0.001 degrees of zero-point between tests. This requirement was also part of the leveling subsystem, which was descoped. Due to this descoping, system requirement 8 was not verified.

System requirement 9 states that the stand must be installed, securely operated, and safely removed from the vacuum chamber without causing any structural or cosmetic damage to the chamber wall. The chamber interface system was also part of the project that was descoped. As it stands, there is no safe way to install the pendulum into the vacuum chamber. The chamber interface was designed, and some part were manufactured, but integration of this subsystem into the test stand will be a part of work done in the future. Due to this descoping, system requirement 9 was not verified.

To design and build an **operational, minimally conductive, inverted pendulum test stand** for the University of Washington's SPACE Lab with the ability to accurately **resolve impulses from pulsed plasma thrusters from $10 \mu\text{N}^*\text{s}$ to $100 \text{ mN}^*\text{s}$** and with the capacity to **accommodate a variety of thruster dimensions and masses**

*Validated

*Not Validated

Fig. 8.3.7: Validation of mission objective

Based on the verification of our system requirements, the validation of our mission objective was done. In the figure above, the green text represents parts of the mission objective that were validated, and red text represents parts of the mission objective that were not validated. The test stand we built is operational, impulses and thrust forces can be applied to the stand and a displacement will be measured from it. As outlined in the verification process for requirement Sys.2, the stand is minimally conductive. As outlined in the verification process for requirement Sys.1, the stand is an inverted pendulum style test stand. As outlined in the verification of requirement Sys.3, the test stand as constructed now cannot measure impulses as low as $10 \mu\text{N}^*\text{s}$ or as high as $100 \text{ mN}^*\text{s}$, so that part of the mission objective cannot be validated. As outlined in the verification process for requirement Sys.6, the test stand is capable of accommodating a variety of thruster dimensions. As outlined in the verification process for requirement Sys.5, while the stand can support thrusters up to a mass of 8kg, the test stand becomes unstable when supporting that much mass. This means that the part of the mission objective about supporting a variety of masses cannot be validated. Because of this, the mission objective as a whole was not validated for this project.

8.4 Lessons Learned & Future Work

Several challenges contributed to the limitations of this project, though they can largely be grouped into three categories: design flaws, manufacturing tolerances, and communication breakdown. In future iterations of this project, several recommendations can be made based on these shortcomings.

First, the static and dynamic models used to characterize the stand's rigidity and deflection need to be reconsidered. Despite calculations indicating otherwise, under one of the stand's nominal configurations with the VC1 arms and shelf, buckling occurred with all but flexure set FS1. Even with the largest flexure configuration, significantly larger impulses than anticipated, on the order of mN*s, were required to produce an output trace. More time was required to perfect this analysis, and had the project had a longer timeline, these issues could have been avoided. Some parts were also not designed with manufacturability in mind, like those with interior features or geometries incompatible with Garolite machining. This led to significant bottlenecks as redesigns and descopes occurred in response.

The waterfall was a significant risk factor, having an effective spring constant that doubled the effective spring constant of the flexures, which can introduce large amounts of noise and unforeseen perturbations in the pendulum motion. As previously mentioned, extensive waterfall calibration and iteration is recommended for future projects. In the future, teams should expect the waterfall to make a sizable contribution to their stands overall effective oscillation behavior, and should make allowances within the design to account for varying waterfall effective spring constants. It is currently known that the wire gauge, coating type and thickness, and even wire manufacturing brand can have a large effect on the waterfall's spring constant and subsequently all of these factors should be taken into consideration when designing the waterfall. One additional note is that the waterfall clamp attachment through holes were never drilled into the thruster shelf, and still needs to be added to this day.

In terms of manufacturing, having access to higher quality equipment would have improved the production quality of the parts. Due to limitations imposed on the use of the AA shop's single 3D printer, a team member's printer was used instead, which broke as it attempted to print parts out of carbon-fiber reinforced PETG filament. Additionally, because the AA department no longer has a laser cutter, the team had to work around using HFS's laser cutters in the 8 makerspace for some parts, while metal parts required using Vashon Aircraft's laser cutter. It was a slow process to find a waterjet that could accommodate the dimensions of our Garolite sheet. Even after we began to use the MSE shop's waterjet, there were significant issues with delamination that led to more delays in manufacturing as other alternatives were assessed. In the AA shop, the mill was often reserved and in use by other teams and labs, and few team members had the necessary training and experience to use it. The accumulation of tolerancing errors between water jetting parts, laser cutting their templates, affixing the templates, and drilling part holes meant that the degree of precision to which the parts should have been manufactured was not achieved. Many of these issues could have been solved by using a more readily machinable, non-fiberglass material with sufficient structural rigidity, vacuum-compatibility, and insulating properties.

On a less technical note, there were issues across the project caused by communication breakdown. Due to file management issues, some redundant or out of date parts saved in the Google Drive were mislabeled, which led to confusion and redundant work along the way. In future projects, clearly defining a nomenclature and archival system for parts as designs progress would go a long way in ensuring a smooth transition to manufacturing and testing. Project work assignments were also fluid, as the initial subsystem breakdown did not apply to the project. This led to a poor partition of work between team members. More clearly defining project roles from the announcement of the project would have helped to better define team members' roles and responsibilities to give them meaningful work throughout the project.

Team Contributors, Assignments

TABLE 1:

Section	Work done by	Section	Work done by	Section	Work done by
Exec Sum	AD	3.5	KLV	4.5.3	WW
1	LL, AD	3.5.1	KLV	4.5.4	WW
1.1	AD, WW, LL, KLV, NC, BF, FC	3.5.2	KLV	4.5.5	WW, LL
1.2	AD, WW, LL, KLV, NC, BF, FC	3.5.3	KLV	4.5.6	WW
1.3	AD NC	3.5.4	KLV, LL	4.6	LL
1.4	AD	3.5.5	KLV	5	AD
2	AD NC	3.5.6	KLV	5.1	AD
2.1	AD NC, LL	3.6	BF, KLV	5.2	AD, KLV
2.2	NC	4	LL	5.3	NC
2.3	NC	4.1	AD	5.4	AD
3	AD	4.2	LL	5.4.1	AD
3.1	BF, KLV	4.3	NC	5.4.2	AD
3.2	LL, KLV	4.4	AD	5.4.3	AD
3.3	NC	4.4.1	AD	5.4.4	WW
3.4	AD	4.4.2	AD	5.4.5	AD, LL
3.4.1	BF	4.4.3	BF, LL	5.4.6	AD
3.4.2	BF	4.4.4	LL	5.5	KLV
3.4.3	BF, LL	4.4.5	BF	5.5.1	KLV
3.4.4	BF, LL	4.4.6	BF	5.5.2	KLV

3.4.5	BF, LL	4.5	BF	5.5.3	KLV
3.4.6	BF	4.5.1	WW	5.5.4	KLV
3.4.7	BF, NC	4.5.2	WW	5.5.5	KLV

TABLE 2:

Section	Work done by	Section	Work done by	Section	Work done by
5.5.6	KLV	6.4.3	AD	7.4	FC
5.6	WW	6.4.4	BF, LL	7.4.1	FC
5.6.1	WW	6.4.5	LL	7.4.2	FC
5.6.2	WW	6.4.6	AD	7.4.3	FC
5.6.3	WW	6.5	NC	7.4.4	FC
5.6.4	WW	6.5.1	NC, LL	7.4.5	FC
5.6.5	WW, LL	6.5.2	NC, LL	7.4.6	FC, LL, NC
5.6.6	WW	6.5.3	NC	7.5	FC
5.7	LL	6.5.4	NC	7.5.1	FC
5.7.1	LL	6.5.5	NC, LL	7.5.2	FC
5.7.2	LL	6.5.6	NC, LL	7.5.3	FC
5.7.3	LL	6.6	LL, KLV	7.5.4	FC
5.7.4	FC	6.6.1	KLV	7.5.5	FC
5.7.5	FC	6.6.2	KLV	7.5.6	FC, NC
5.7.6	NC	6.6.3	KLV	7.6	FC
5.8	FC	6.6.4	KLV	8	LL
6	AD	6.6.5	LL, KLV	8.1	
6.1	AD	6.6.6	KLV	8.2	LL
6.2	AD, KLV, LL	6.7	BF	8.3	WW, AD, LL
6.3	NC	7	FC	8.4	
6.4	AD	7.1	FC	8.5	LL, KLV

6.4.1	AD	7.2	FC	APP A	WW
6.4.2	AD	7.3	NC	APP B	LL

List of References

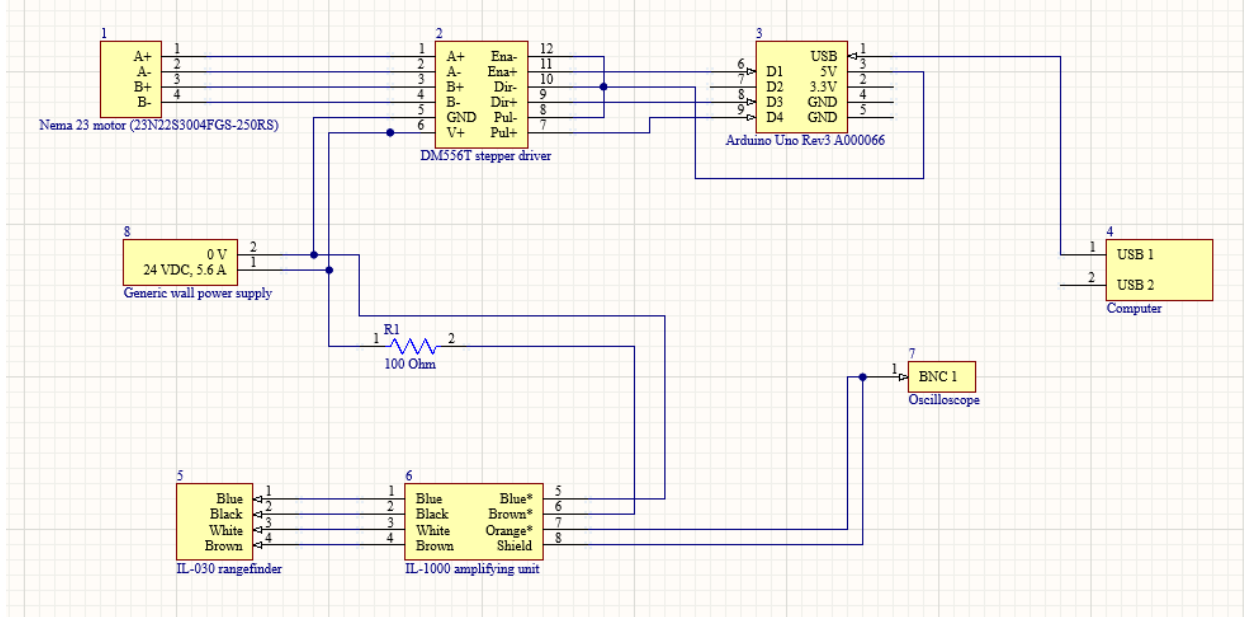
Manufacturing Plan - Attached to Submission
 Test Stand Drawing Package - Attached to Submission
 - CAD to be emailed as .zip to alvarso@uw.edu
 Assembly Plan - Late Submission by 06/07/2024
 Buckling Test Plan - Attached to Submission
 Buckling Test Procedure - Attached to Submission
 Leveling System Test Procedure - Attached to Submission
 Systems Test Plan - Attached to Submission
 Systems Test Procedure - Attached to Submission

Version Log

Ver	Date	By	E-mail	Notes
1.0	2024-06-04	Nathan Cheng Felicity Cundiff Adam Delbow Ben Fetter Lillie LaPlace Kai Laslett-Vigil Winston Wilhere	nkcheng@uw.edu fcundiff@uw.edu adelbow@uw.edu bfetters@uw.edu llapla@uw.edu klaslett@uw.edu wilhere@uw.edu	Initial Release

Appendix A - Wiring diagram and Code

Full system wiring diagram:



Initial flexure design code:

```

clear all
close all
g0=9.81; %m/s^2
m_arm=0.045; %mass of arms in kg
arm_number=4;
m_thruster=0.3;
impulse=25e-6; % Impulse magnitude (N*s)
m_shelf=0.3; %(kg)
m_pend=0.253+m_shelf; % mass of the pendulum no shelf (kg)
m_top=m_thruster+m_pend; %total mass of pendulum and thruster (kg)
m_total=m_top+m_arm*arm_number; %total mass of stand (kg)
lever_arm=19.8*0.0254; % length of lever arm (m), ref: 19.8
zeta=0.3; %damping ratio,
Ip=((1/3)*m_arm*arm_number*lever_arm^2)+(m_top*lever_arm^2); %account for
center of gravity of arms
thruster_offset=0.00; %Thruster location offset horizontally in meters
%Flexure dimensions
% w=0.75*0.0254; % width of flexures (m)
% h=0.01*0.0254; % thickness of flexures (m)
% l=1.64*0.0254; % length of flexures (m)
% Material properties
E_steele=205e9; % Elastic modulus of steel (Pa)
G=80e9; %Shear modulus of steel (Pa), both E and G are for 1095 spring steel

```

```

rho_steel=7850; %kg/m^3
list=[];
for w1 = 0.2:0.005:0.75
w1
for h1= 0.005:0.005:0.02
for l1=2.5:0.05:5
w=w1*0.0254;
h=h1*0.0254;
l=l1*0.0254;

Iflex=w*h^3/12;
gammaflex=((w*h^3)/16)*((16/3)-3.36*(h/w)*(1-((h^4)/(12*w^4)))); %from
wikipedia for a rectangle with 4% error
Jflex=w*h*(w^2+h^2)/12;
c=sqrt(G*gammaflex/(rho_steel*Jflex));
ebs=l/(2*E_steel*Iflex); %specific strain bending energy, energy stored per
(N*m)^2 applied to the system
ets=l/(2*G*Jflex); %specific strain torsion energy
Eratio=ebs/ets; %energy ratio, want to be much greater than 1
w1flex=pi*c/(2*l)/(2*pi); %in Hz
w2flex=3*pi*c/(2*l)/(2*pi); %in Hz
w3flex=5*pi*c/(2*l)/(2*pi); %in Hz
k=(3*E_steel*Iflex)/(l^3); %one flexure
keff=((2/k)^-1)*arm_number); %eight flexures. 4 sets of 2 series flexure, all
with the same properties
xrad=0.4519; %distance required for 1 rad deflection through an arc length
krad=(keff*xrad*lever_arm)-(m_top*g0*lever_arm)-(m_arm*arm_number*g0*0.5*lever_
arm); %N*m/rad
P=g0*m_total/arm_number;
k1=1.2; %buckling effective length factor
alpha=1/lever_arm;
lambda_cr=(1/(3.4*(alpha-0.015)))^(2/3); %valid assumption for a range of alpha
from ~ 0.05 to 0.25
Pcr=lambda_cr*pi^2*E_steel*Iflex/(l^2);
Pcr=Pcr/1.8; %realism factor from testing
omega_n=sqrt(krad/Ip); % natural frequency (rad/s)
omega_nHz=omega_n/(2*pi);
omega_d=omega_n*sqrt(1-zeta^2);
c=2*zeta*sqrt(Ip*krad); %N*m*s/rad
%omega_n=sqrt((krad*0.5^2-m*g0*0.5-0.136*g0*0.5*0.5)/((m+0.136/3)*0.5^2)); %
natural frequency (rad/s)
%c=2*zeta*omega_n*m; % damping coefficient (N*s/m)
t_peak=(1/omega_d)*atan(omega_d/(zeta*omega_n));
angle_peak=impulse*lever_arm/(Ip*omega_n)*(1/sqrt(1-zeta^2))*exp(-zeta*omega_n*
t_peak)*sin(omega_d*t_peak);
deflection_peak=angle_peak*lever_arm;
%theta=torque*L/(G*Iflex)
if krad > 0 && 1.2 < Pcr/P
% Impulse force
duration=0.0000003; % duration of impulse (s)
F_impulse=impulse/duration; % impulse force (N)
% Motion
tspan=[0 duration]; % simulation time span (s)
[t1, x1]=ode89(@(t,x) system_eqns(t,x,krad,c,F_impulse,lever_arm,Ip), tspan,
[0; 0]);
r0=x1(end,1);
w0=x1(end,2);

```

```

tspan=[duration 50];
[t2, x2]=ode89(@(t,x) system_eqns(t,x,krad,c,0,lever_arm,Ip), tspan, [r0; w0]);
%odeset('AbsTol', 1e-10)
max1=max(x2(:,1))*lever_arm;
if max1>=30E-6
%list=vertcat(list,[max1*1E6, deflection_peak*1E6,
2*abs(deflection_peak-max1)/(deflection_peak+max1), w/0.0254, h/0.0254,
1/0.0254, krad, c, omega_n, t_peak, Pcr/P, zeta, Ip]);
list=vertcat(list,[max1*1E6, w/0.0254, h/0.0254, 1/0.0254, krad, omega_nHz,
Pcr/P, Eratio, wlflex, w2flex, w3flex, alpha]);
% figure()
% hold on
% plot(t2, x2(:,1)*lever_arm, 'k');
% plot(t_peak, deflection_peak, 'o');
% hold off
end
end
end
end
flexure_table=array2table(list,'VariableNames',{'Defl', 'w', 't', 'l', 'k',
'omega_n (Hz)', 'FoS', 'Eratio', 'wl (Hz)', 'w2', 'w3', 'alpha'});
% System_eqns function
function dxdt = system_eqns(t, x, k, c, F_impulse, lever_arm, Ip)
% State variables
r=x(1); % Displacement angular, small angle approx.
w=x(2); % Velocity angular
% Derivatives
drdt=w; %dxdt angular
dwdt=(1/Ip)*((F_impulse*lever_arm)-(k*r)-(c*w)); %dvdt angular
% Output derivatives
dxdt=[drdt; dwdt];
end

```

Flexure spring constant analysis code:

```

close all
clear all
% Enter Values used in experiment:
h1=0.025; %thickness of flexure in inches
%Input mass added to pendulum for each test in order:
masses=[0.97 0.97 0.97 1.07 1.07 1.070 1.170 1.170 1.170 1.270 1.270 1.270];
%kg
%constants calculated from pendulum characteristics:
g0=9.81; %m/s^2
zeta=0; %damping ratio
m_arm=0.045; %mass of arms in kg
arm_number=4;
m_pend=0.253; % mass of the pendulum (kg) no shelf
lever_arm=19.8; % length of lever arm (in)
in_to_m = 0.0254; %convert inches to meters
E_steeel=205e9; % Elastic modulus of steel (Pa)
G=80e9; %Shear modulus of steel (Pa), both E and G are for 1095 spring steel
rho_steeel=7850; %kg/m^3
w=0.6*in_to_m; %convert dimensions of inches to m
l=3.6*in_to_m;
h=h1*in_to_m;

```

```

lever_arm=lever_arm*in_to_m;
xrad=lever_arm; %distance required for 1 rad deflection through an arc length
units of m/rad
%set range of files to view
start=29;
last=40;
data_values=[];
for i = start:last
A=readmatrix("/Users/winstonwilhere/Desktop/capstone
testing/TEK00"+num2str(i)+".CSV");
A(1:15, :)=[];
t=A(:,4);
defl=A(:,5);
zero_point=mean(defl); %average all data to find where it oscillates about
defl=defl-zero_point; %zero point data
max_defl=max(defl); %find first peak
peak_min_ind=find(defl==min(defl)); %find first minimum
peak_min_ind=peak_min_ind(1); %find indice of first min to split data into two
sections
t_min=t(peak_min_ind); %find what time the first min occurs
peak1=max(defl(1:peak_min_ind)); %find the peak before that min time
peak2=max(defl(peak_min_ind:end)); %find the peak after that min time
%now determine damping during this test with the two peak values
sigma=log(peak1/peak2);
zeta=1/sqrt(1+(2*pi/sigma)^2);
t_peak10=t(find(defl(1:peak_min_ind)==peak1)); %find the indices of time for
which the first peak occurs
t_peak1=mean(t_peak10); %average those times
t_peak20=t(find(defl(peak_min_ind:end)==peak2)+peak_min_ind);
t_peak2=mean(t_peak20);
omega_d=1/(t_peak2-t_peak1); %solve for natural frequency in Hz
omega_n=omega_d/sqrt(1-zeta^2);
data_values=vertcat(data_values, [max_defl, omega_n, zeta]); %add max
deflection and natural frequency to a vector
if i == last
    data_values;
end
%figure()
% plot(t, defl)
% xlim([-1 max(t)])
% ylabel('mm')
% xlabel('seconds')
%title('tek00'+num2str(i));
end
kflex_vals=[];
max_defl_vals=[];
for i = 1:length(masses)
tm=masses(i); %mass applied to pendulum
m_top=m_pend+tm; %total mass of pendulum and thruster (kg)
m_total=m_top+(m_arm*arm_number); %total mass of stand (kg)
lever_arm=19.8*0.0254; %length of lever arm (m), ref: 19.8
Ip=((1/3)*m_arm*arm_number*lever_arm^2)+(m_top*lever_arm^2); %account for
center of gravity of arms
omega_n=data_values(i, 2)*2*pi; %pull nat frequency for this test from
previous, convert to rad/s
keff=Ip*omega_n^2; %units of N*m

```

```

kpend=(m_top*g0*lever_arm)+(m_arm*arm_number*g0*0.5*lever_arm); % Torque per
radian of tilt for pendulum body
% keff=(keff*xrad*lever_arm)-kpend %old code to solve for keff, now rearranged
below to solve for kflext
kflext=(keff+kpend)/(xrad*lever_arm); %rearranged math
kflext_vals(i)=kflext;
end
kflext_vals(6)=[];
masses(6)=[];
kflext=mean(kflext_vals)
kflextstd=std(kflext_vals)
scatter(masses, kflext_vals)
xlabel('Mass applied to pendulum (kg)', 'FontSize', 14)
ylabel('Derived Flexure Spring Constant (N/m)', 'FontSize', 14)
title('0.025" Flexures', 'FontSize', 14)
% System_eqns function
function dxdt = system_eqns(t, x, k, c, F_impulse, lever_arm, Ip)
% State variables
r=x(1); % Displacement angular, small angle approx. units of rad
w=x(2); % Velocity angular, units of rad/s
% Derivatives
drdt=w; %dxdt angular
dwdt=(1/Ip)*(F_impulse*lever_arm)-(k*r)-(c*w)); %dvdt angular
% Output derivatives
dxdt=[drdt; dwdt];
end

```

Steady state testing analysis code:

```

close all
clear all
% Enter Values used in experiment:
h1=0.025; %thickness of flexure in inches
%Input vector of ss force imparted to pendulum for each test in order:
ss=[0.001*9.81, 0.002*9.81, 0.003*9.81]; %N
measured_deflections=[1.116E-3, 2.214E-3 3.51E-3]; %ss deflection in m
%Input mass added to pendulum for each test in order:
applied_mass=0.97; %in kg
%constants calculated from pendulum characteristics:
g0=9.81; %m/s^2
zeta=0; %damping ratio
m_arm=0.045; %mass of arms in kg
arm_number=4;
m_pend=0.253; % mass of the pendulum (kg) no shelf
lever_arm=19.8; % length of lever arm (in)
in_to_m = 0.0254; %convert inches to meters
E_steeel=205e9; % Elastic modulus of steel (Pa)
G=80e9; %Shear modulus of steel (Pa), both E and G are for 1095 spring steel
rho_steeel=7850; %kg/m^3
w=0.6*in_to_m; %convert dimensions of inches to m
l=3.6*in_to_m;
h=h1*in_to_m;
lever_arm=lever_arm*in_to_m;
xrad=lever_arm; %distance required for 1 rad deflection through an arc length
units of m/rad
Iflex=w*h^3/12;

```

```

k=(3*E_steele*Iflex)/(l^3); %one flexure
kflex_model=((2/k)^-1)*arm_number; %eight flexures. 4 sets of 2 series
flexure, all with the same properties
zeta=0.0113;
tm=applied_mass; %mass applied to pendulum
m_top=m_pend+tm; %total mass of pendulum and thruster (kg)
m_total=m_top+(m_arm*arm_number); %total mass of stand (kg)
lever_arm=19.8*0.0254; % length of lever arm (m), ref: 19.8
Ip=((1/3)*m_arm*arm_number*lever_arm^2)+(m_top*lever_arm^2); %account for
center of gravity of arms
kpend=(m_top*g0*lever_arm)+(m_arm*arm_number*g0*0.5*lever_arm); % Torque per
radian of tilt for pendulum body
kflex=33.4; %N/m determined from other testing is 33.4
keff=(kflex*xrad*lever_arm)-kpend; %N*m/rad
%kflex_offset=kflex_model/kflex;
for i = 1:length(ss)
% now model response based on data
duration=10000; % duration of impulse (s)
F_ss=ss(i);
c=2*zeta*Ip*1;
% Motion
tspan=[0 duration]; % simulation time span (s)
[t1, x1]=ode89(@(t,x) system_eqns(t,x,keff,c,F_ss,lever_arm,Ip), tspan, [0;
0]);
max1=x1(end, 1)*lever_arm;
modeled_defl_vals(i)=max1;
%meas_uncert=10/(max1*1E6)*100; %uncertainty of the measurement in percent
end
predicted_diffs=modeled_defl_vals./measured_deflections; %determine ratio of
actual deflection to the predicted value
model_offset=mean(predicted_diffs)
model_offset_std=std(predicted_diffs)
% System_eqns function
function dxdt = system_eqns(t, x, k, c, F_impulse, lever_arm, Ip)
% State variables
r=x(1); % Displacement angular, small angle approx. units of rad
w=x(2); % Velocity angular, units of rad/s
% Derivatives
drdt=w; %dxdt angular
dwdt=(1/Ip)*((F_impulse*lever_arm)-(k*r)-(c*w)); %dvdt angular
% Output derivatives
dxdt=[drdt; dwdt];
end

```

Impulse response prediction code:

```

close all
clear all
% Enter Values used in experiment:
h1=0.025; %thickness of flexure in inches
offset=1.114;
for i = 1:0.01:12
%Input impulse valued that will be tested:
impulse=i*25E-6; %N*s
%Input mass added to pendulum for each test in order:
applied_mass=0.97+0.2855; %in kg, 0.2855 for Keff = 0.300

```

```
%constants calculated from pendulum characteristics:
g0=9.81; %m/s^2
zeta=0; %damping ratio
m_arm=0.045; %mass of arms in kg
arm_number=4;
m_pend=0.253; % mass of the pendulum (kg) no shelf
lever_arm=19.8; % length of lever arm (in)
in_to_m = 0.0254; %convert inches to meters
E_steele=205e9; % Elastic modulus of steel (Pa)
G=80e9; %Shear modulus of steel (Pa), both E and G are for 1095 spring steel
rho_steele=7850; %kg/m^3
w=0.6*in_to_m; %convert dimensions of inches to m
l=3.6*in_to_m;
h=h1*in_to_m;
lever_arm=lever_arm*in_to_m;
xrad=lever_arm; %distance required for 1 rad deflection through an arc length
units of m/rad
Iflex=w*h^3/12;
k=(3*E_steele*Iflex)/(l^3); %one flexure
kflex_model=((2/k)^-1)*arm_number); %eight flexures. 4 sets of 2 series
flexure, all with the same properties
zeta=0.3;
tm=applied_mass; %mass applied to pendulum
m_top=m_pend+tm; %total mass of pendulum and thruster (kg)
m_total=m_top+(m_arm*arm_number); %total mass of stand (kg)
lever_arm=19.8*0.0254; % length of lever arm (m), ref: 19.8
Ip=((1/3)*m_arm*arm_number*lever_arm^2)+(m_top*lever_arm^2); %account for
center of gravity of arms
kpend=(m_top*g0*lever_arm)+(m_arm*arm_number*g0*0.5*lever_arm); % Torque per
radian of tilt for pendulum body
kflex=kflex_model/16.158; %N/m determined from other testing is 32...
keff=(kflex*xrad*lever_arm)-kpend; %N*m/rad
omega_n=sqrt(keff/Ip);
% now model response based on data
duration=0.00003; % duration of impulse (s)
F_impulse=impulse/duration;
c=2*zeta*Ip*omega_n;
% Motion
tspan=[0 duration]; % simulation time span (s)
[t1, x1]=ode89(@(t,x) system_eqns(t,x,keff,c,F_impulse,lever_arm,Ip), tspan,
[0; 0]);
r0=x1(end,1);
w0=x1(end,2);
tspan=[duration 20];
[t2, x2]=ode89(@(t,x) system_eqns(t,x,keff,c,0,lever_arm,Ip), tspan, [r0; w0]);
%odeset('AbsTol', 1e-10)
max1=max(x2(:, 1))*lever_arm/offset;
index=int32(i*100-99);
meas_uncert=10/(max1*1E6)*100; %uncertainty of the measurement in percent
uncert_list(index)=meas_uncert;
impulse_list(index)=impulse*1E6;
max_list(index)=max1;
end
plot(impulse_list,uncert_list)
xlabel('Impulse (\mu N*s)', 'FontSize', 14)
ylabel('Measurement Uncertainty (%)', 'FontSize', 14)
title('K_{eff} = 0.300, \zeta = 0.3', 'FontSize', 14)
```

```

xlim([min(impulse_list) max(impulse_list)])
ylim([min(uncert_list) max(uncert_list)])
% figure()
% hold on
% plot(t1, x1(:,1)*lever_arm, 'k');
% plot(t2, x2(:,1)*lever_arm, 'k');
% xlabel('t (s)')
% ylabel('Defl (m)')
% hold off
% System_eqns function
function dxdt = system_eqns(t, x, k, c, F_impulse, lever_arm, Ip)
    % State variables
    r=x(1); % Displacement angular, small angle approx. units of rad
    w=x(2); % Velocity angular, units of rad/s
    % Derivatives
    drdt=w; %dxdt angular
    dwdt=(1/Ip)*(F_impulse*lever_arm)-(k*r)-(c*w)); %dvdt angular
    % Output derivatives
    dxdt=[drdt; dwdt];
end

```

Steady state step response prediction code:

```

close all
clear all
% Enter Values used in experiment:
h1=0.025; %thickness of flexure in inches
offset=1.114;
for i = 1:0.01:8
%Input impulse valued that will be tested:
ss=i*1E-4; %N*s
%Input mass added to pendulum for each test in order:
applied_mass=0.97+0.2855; %in kg
%constants calculated from pendulum characteristics:
g0=9.81; %m/s^2
zeta=0; %damping ratio
m_arm=0.045; %mass of arms in kg
arm_number=4;
m_pend=0.253; % mass of the pendulum (kg) no shelf
lever_arm=19.8; % length of lever arm (in)
in_to_m = 0.0254; %convert inches to meters
E_steeel=205e9; % Elastic modulus of steel (Pa)
G=80e9; %Shear modulus of steel (Pa), both E and G are for 1095 spring steel
rho_steeel=7850; %kg/m^3
w=0.6*in_to_m; %convert dimensions of inches to m
l=3.6*in_to_m;
h=h1*in_to_m;
lever_arm=lever_arm*in_to_m;
xrad=lever_arm; %distance required for 1 rad deflection through an arc length
units of m/rad
Iflex=w*h^3/12;
k=(3*E_steeel*Iflex)/(l^3); %one flexure
kflex_model=((2/k)^-1)*arm_number); %eight flexures. 4 sets of 2 series
flexure, all with the same properties
zeta=0.3;
tm=applied_mass; %mass applied to pendulum
m_top=m_pend+tm; %total mass of pendulum and thruster (kg)

```

```

m_total=m_top+(m_arm*arm_number); %total mass of stand (kg)
lever_arm=19.8*0.0254; % length of lever arm (m), ref: 19.8
Ip=((1/3)*m_arm*arm_number*lever_arm^2)+(m_top*lever_arm^2); %account for
center of gravity of arms
kpend=(m_top*g0*lever_arm)+(m_arm*arm_number*g0*0.5*lever_arm); % Torque per
radian of tilt for pendulum body
kflex=kflex_model/16.158; %N/m determined from other testing is 32...
keff=(kflex*xrad*lever_arm)-kpend; %N*m/rad
omega_n=sqrt(keff/Ip);
% now model response based on data
c=2*zeta*Ip*omega_n;
% Motion
tspan=[0 100]; % simulation time span (s)
[t1, x1]=ode89(@(t,x) system_eqns(t,x,keff,c,ss,lever_arm,Ip), tspan, [0; 0]);
max1=x1(end, 1)*lever_arm/offset;
index=int32(i*100-99);
meas_uncert=10/(max1*1E6)*100; %uncertainty of the measurement in percent
max_list(index)=max1;
uncert_list(index)=meas_uncert;
ss_list(index)=ss;
end
plot(ss_list*1E3,uncert_list)
xlabel('Steady State Force (mN)', 'FontSize', 14)
ylabel('Measurement Uncertainty (%)', 'FontSize', 14)
title('K_{eff} = 0.300, \zeta = 0.3', 'FontSize', 14)
% figure()
% hold on
% plot(t1, x1(:,1)*lever_arm/offset, 'k');
% xlabel('t (s)')
% ylabel('Defl (m)')
% hold off
% System_eqns function
function dxdt = system_eqns(t, x, k, c, F_impulse, lever_arm, Ip)
% State variables
r=x(1); % Displacement angular, small angle approx. units of rad
w=x(2); % Velocity angular, units of rad/s
% Derivatives
drdt=w; %dxdt angular
dwdt=(1/Ip)*((F_impulse*lever_arm)-(k*r)-(c*w)); %dvdt angular
% Output derivatives
dxdt=[drdt; dwdt];
end

```

Data analysis - Leveling System Arduino code:

```

#include <AccelStepper.h>
const int stepPin = 2; // Step pin connected to Arduino digital pin 2
const int dirPin = 3; // Direction pin connected to Arduino digital pin 3
AccelStepper stepper(AccelStepper::DRIVER, stepPin, dirPin); // Stepper motor
object
void setup() {
    stepper.setMaxSpeed(1000); // Set maximum speed
    stepper.setAcceleration(500); // Set acceleration
    Serial.begin(9600); // Initialize serial communication
}
void loop() {
    stepper.run(); // Continuously run the stepper motor
}

```

```

if (Serial.available() > 0) { // Check if there's serial data available
    char command = Serial.read(); // Read the command sent from Python

    // Check the command received
    switch (command) {
        case 'A': // Forward 100 steps
            moveForward(100);
            break;
        case 'B': // Backward 100 steps
            moveBackward(100);
            break;
    }
}

void moveForward(int steps) {
    stepper.moveTo(steps); // Move forward by the specified number of steps
}

void moveBackward(int steps) {
    stepper.moveTo(-steps); // Move backward by the specified number of steps
}

```

Data analysis - Leveling System Python code:

```

import serial
import serial.tools.list_ports
import tkinter as tk
import math

def move_custom(direction, degrees):
    global current_steps, step_counter_label, current_degrees      # Declare
variables as global
    steps_per_revolution = 200 #confirm this empirically
    mm_per_revolution = 1.37 #confirm this empirically
    lever_arm = 20 #inches
    inch_to_mm = 25.4
    degress_to_rad = math.pi/180
steps=math.sin(degrees*degress_to_rad)*lever_arm/(mm_per_revolution/inch_to_mm)
*steps_per_revolution
    if direction == 'Up': # Check if the direction is forward
        current_steps += steps # Increment the current position by the number
of steps
        current_degrees +=degrees
        command = 'A' + str(steps) + '\n' # Command for forward movement
    elif direction == 'Down':
        current_steps -= steps # Decrement the current position by the number
of steps
        current_degrees -=degrees
        command = 'B' + str(steps) + '\n' # Command for backward movement
    #print(f"Sending command: {command}") # Debug print
    ser.write(command.encode()) # Send the command to Arduino
    step_counter_label.config(text=f"Angular position: {current_degrees}") # Update the step counter
# Function to stop everything immediately
def stop_all():
    ser.write(b'S\n') # Send the stop command to Arduino
    ser.flush() # Flush the serial buffer to ensure the command is sent
immediately

```

```

# Function to move motor to zero position
def move_to_zero():
    global current_steps, current_degrees # variable global
    if current_steps >=0: # Check if there are steps needed to move to zero
        command= 'B' + str(abs(current_steps)) + '\n' # Command to move
backward to zero position
        ser.write(command.encode())
    elif current_steps <0:
        command= 'A' + str(abs(current_steps)) + '\n' # Command to move
backward to zero position
        ser.write(command.encode())
    current_steps = 0 # Reset current position
    current_degrees = 0
    step_counter_label.config(text="Angular position: 0")
# Function to quit
def quit_app():
    move_to_zero()
    ser.close()
    root.quit()
# GUI setup
def create_gui():
    global root, current_steps, step_counter_label, current_degrees # Declare
root as a global variable
    root = tk.Tk()
    root.title("Stepper Motor Control")
    current_steps = 0
    current_degrees=0
        custom_button = tk.Button(root, text="Move (degrees)", command=custom_steps)
    custom_button.grid(row=0, columnspan=2, padx=10, pady=10)
    quit_button = tk.Button(root, text="Quit", command=quit_app)
    quit_button.grid(row=1, columnspan=2, padx=10, pady=10)
    step_counter_label = tk.Label(root, text="Angular position: 0")
    step_counter_label.grid(row=2, columnspan=2, padx=10, pady=10)
    root.mainloop()
# Function for custom steps input
def custom_steps():
    custom_window = tk.Toplevel(root)
    custom_window.title("Move (degrees)")
    direction_label = tk.Label(custom_window, text="Direction:")
    direction_label.grid(row=0, column=0, padx=10, pady=10)
    direction_var = tk.StringVar(value="Up")
    direction_menu = tk.OptionMenu(custom_window, direction_var, "Up", "Down")
    direction_menu.grid(row=0, column=1, padx=10, pady=10)
    steps_label = tk.Label(custom_window, text="Degrees:")
    steps_label.grid(row=1, column=0, padx=10, pady=10)
    steps_entry = tk.Entry(custom_window)
    steps_entry.grid(row=1, column=1, padx=10, pady=10)
    confirm_button = tk.Button(custom_window, text="Move", command=lambda:
move_custom(direction_var.get(), int(steps_entry.get())))
    confirm_button.grid(row=2, columnspan=2, padx=10, pady=10)
# Arduino port
def get_arduino_port():
    ports = serial.tools.list_ports.comports()
    for port in ports:
        if 'COM3' in port.device:
            return port.device

```

```

        return None
# Main
arduino_port = get_arduino_port()
if arduino_port:
    ser = serial.Serial(arduino_port, baudrate=9600, timeout=1)
    create_gui()
else:
    print('Arduino not found on any port!')

```

Deflection Data Analysis code:

```

import tkinter as tk # Importing the tkinter library for GUI DAQ_Python.py
from tkinter import ttk # Importing themed widgets from tkinter for a modern
look and feel
import nidaqmx # Importing nidaqmx for interacting with National Instruments
Data Acquisition hardware
import numpy as np # Importing numpy for numerical computing
import matplotlib.pyplot as plt # Importing matplotlib.pyplot for plotting and
visualization
from matplotlib.backends.backend_tkagg import FigureCanvasTkAgg # Importing
FigureCanvasTkAgg from matplotlib.backends.backend_tkagg for embedding
matplotlib figures in Tkinter GUIs
import serial # Importing serial for serial communication
import pandas as pd # Importing pandas for data manipulation and analysis
from scipy.signal import butter, lfilter # pass filter

# Global variables for raw deflection data and uncertainties
deflection_data = []
uncertainties = []
# Define known impulses and their corresponding V_max values
known_impulses = [1, 2, 3] # Insert known impulses
v_max_values = [] # Store the V_max values obtained from find_peak()
# 1) Function to record raw deflection data from the rangefinder
def record_deflection():
    global deflection_data # Declaring a global variable to store the
deflection data
    try:
        # Create a task for data acquisition
        with nidaqmx.Task() as task: # Establishing a task for NI-DAQmx
operations
            task.ai_channels.add_ai_voltage_chan("COM3") # Configuring an
analog input channel for voltage readings
            # Configure the timing for data acquisition
            task.timing.cfg_samp_clk_timing(rate=1000,
sample_mode=nidaqmx.constants.AcquisitionType.CONTINUOUS) # Configuring the
sampling clock timing
            # Read raw deflection data from the DAQ device
            deflection_data = task.read(number_of_samples_per_channel=1000) #
Reading raw data from the DAQ device
            # Handle any DAQ errors that may occur
    except nidaqmx.DaqError as e:
        print(f"DAQ Error: {e}")
        print(f"Error Code: {e.error_code}")
        print(f"Error Details: {e.__cause__}")

# 2) have code identify the v_0 cause voltage won't automatically start at 0
# 3) Function to find the peak value

```

```

        # This function aims to determine the peak value of the given
deflection_data array.

        # The peak value is crucial for calibrating a linear impulse plot to find
'c'.def find_peak():

def find_peak():
    global deflection_data
    if deflection_data:
        try:
            data_array = np.array(deflection_data)
            if data_array.size > 0:
                peak_value = np.max(data_array)
                return peak_value
            else:
                print("Empty array. No peak value found.")
                return None
        except Exception as e:
            print(f"An error occurred: {e}")
            return None
    else:
        print("No deflection data available. Please record deflection data
first.")
        return None
def plot_peak():
    global deflection_data
    peak_value = find_peak()
    if peak_value is not None:
        plt.plot(deflection_data, label='Deflection Data')
        plt.plot(np.argmax(deflection_data), peak_value, 'ro', label=f'Peak
Value: {peak_value}')
        plt.xlabel('Time')
        plt.ylabel('Deflection')
        plt.title('Deflection Data with Peak Value')
        plt.legend()
        plt.grid(True)
        plt.show()
    else:
        print("Unable to plot. No peak value found.")

# 4) Function to calculate the calibration constant c using linear regression
# The calibration constant c is calculated as the ratio of V_max to the number
of impulses (c = V/N)

def calculate_c():
    global known_impulses, v_max_values
    # Checking if the number of recorded known impulses matches the number of
recorded V_max values
    if len(known_impulses) != len(v_max_values):
        print("Please ensure you have recorded all V_max values for known
impulses.")
        return
    # Plotting V_max vs known impulses
    plt.figure(figsize=(8, 6))
    plt.scatter(known_impulses, v_max_values, color='blue', label='Data
Points')
    plt.xlabel('Known Impulses')
    plt.ylabel('V_max')
    plt.title('V_max vs Known Impulses')
    plt.grid(True)
    # Performing linear regression to find the slope (c)

```

```

slope, intercept = np.polyfit(known_impulses, v_max_values, 1)
# Plotting the linear regression line
x_values = np.array(known_impulses)
y_values = slope * x_values + intercept
plt.plot(x_values, y_values, color='red', label='Linear Regression')
# Printing the slope (c), which represents the calibration constant
print("Slope (c):", slope)
# Adding legend
plt.legend()
# Displaying the plot
plt.show()

# 5) Function to apply low-pass filter
def apply_lowpass_filter(data):
    # Define filter parameters
    fs = 1000 # Sampling frequency
    cutoff_frequency = 50 # Cutoff frequency in Hz
    # Normalize the cutoff frequency
    nyquist_frequency = 0.5 * fs
    normal_cutoff = cutoff_frequency / nyquist_frequency
    # Define filter order and get filter coefficients
    order = 5
    b, a = butter(order, normal_cutoff, btype='low', analog=False)
    # Apply filter to data
    filtered_data = lfilter(b, a, data)
    return filtered_data

# 6) Uncertainty
def c_and_I_uncertainty(force, time):
    try:
        # Constants
        constant_uncertainty = 0.1 # Adjust this value based on your specific
case
        # Calculate uncertainty for force and time
        force_uncertainty = constant_uncertainty * force
        time_uncertainty = constant_uncertainty * time
        # Propagation of uncertainty for impulse
        impulse = force * time
        impulse_uncertainty = math.sqrt((force_uncertainty * time)**2 +
(time_uncertainty * force)**2)
    except Exception as e:
        print(f"An error occurred during Uncertainty: {e}")

# 7) Function to display graph
def display_graph():
    global deflection_data, c_and_I_uncertainty
    try:
        # Apply low-pass filter to smoothen noise
        deflection_data_filtered = apply_lowpass_filter(deflection_data)
        # Plot filtered data
        fig = plt.figure(figsize=(8, 6))
        plt.plot(deflection_data_filtered)
        plt.xlabel('Time')
        plt.ylabel('Voltage')
        plt.title('Thruster Impulse')
        plt.grid(True)
        # Display the plot
        plt.show()
    except Exception as e:
        print(f"An error occurred during graph display: {e}")

```

```

# Function to export figures and raw data
def export_data():
    global deflection_data, uncertainties
    try:
        # Save raw data to a CSV file
        df = pd.DataFrame({'Deflection': deflection_data})
        df.to_csv('raw_data.csv', index=False)
        print("Raw data exported successfully.")
    except Exception as e:
        print(f"An error occurred during data export: {e}")

def plot_v_max():
    global known_impulses, v_max_values
    if len(known_impulses) != len(v_max_values):
        print("Please ensure you have recorded all V_max values for known
impulses.")
    return
    # Plot V_max vs known impulses
    plt.figure(figsize=(8, 6))
        plt.scatter(known_impulses, v_max_values, color='blue', label='Data
Points')
    plt.xlabel('Known Impulses')
    plt.ylabel('V_max')
    plt.title('V_max vs Known Impulses')
    plt.grid(True)
    # Perform linear regression
    slope, intercept = np.polyfit(known_impulses, v_max_values, 1)
    # Plot the linear regression line
    x_values = np.array(known_impulses)
    y_values = slope * x_values + intercept
    plt.plot(x_values, y_values, color='red', label='Linear Regression')
    # Print the slope (c)
    print("Slope (c):", slope)
    # Add legend
    plt.legend()
    # Show plot
    plt.show()

# Create main window
root = tk.Tk()
root.title("Deflection Data Analysis")
# Create frame for buttons
button_frame = ttk.Frame(root)
button_frame.pack(pady=5)
# Test Section Header
test_header_label = ttk.Label(button_frame, text="Calibration ", font=('Arial',
12, 'bold'))
test_header_label.grid(row=0, columnspan=2, pady=5)
# Create buttons for recording, converting, and displaying data
record_button = ttk.Button(button_frame, text="Record Raw Deflection",
command=record_deflection)
record_button.grid(row=1, column=0, padx=5)
peak_button = ttk.Button(button_frame, text="Calculate Constant C",
command=find_peak)
peak_button.grid(row=1, column=1, padx=5)
calculate_button = ttk.Button(button_frame, text="Plot: Vmax Peak",
command=calculate_c)
calculate_button.grid(row=2, column=0, padx=5)

```

```
# Plot V_max vs Known Impulses button
plot_v_max_button = ttk.Button(button_frame, text="Plot: Linear Impulse",
command=plot_v_max)
plot_v_max_button.grid(row=2, column=1, padx=5)
# Add separator line
separator = ttk.Separator(button_frame, orient='horizontal')
separator.grid(row=3, columnspan=2, sticky='ew', pady=5)
# Calibration Section Header
calibration_header_label = ttk.Label(button_frame, text="Testing",
font=('Arial', 12, 'bold'))
calibration_header_label.grid(row=4, columnspan=2, pady=5)
# Display Graph button
display_graph_button = ttk.Button(button_frame, text="Test",
command=display_graph)
display_graph_button.grid(row=5, column=0, padx=5)
# Display Graph button
display_graph_button = ttk.Button(button_frame, text="Plot: Thruster Impulse",
command=display_graph)
display_graph_button.grid(row=5, column=1, padx=5)
# Export Data button
export_button = ttk.Button(button_frame, text="Export Data and Plots",
command=export_data)
export_button.grid(row=6, column=1, padx=5)
# Create quit button
quit_button = ttk.Button(root, text="Quit", command=root.quit)
quit_button.pack(pady=5)
root.mainloop()
```

Appendix B - Manufacturing Plan



Test Stand Manufacturing Plan

Version 1.0
2024-06-01

SPACE Lab Thrust Stand

Team Members: Nathan Cheng
Felicity Cundiff
Adam Delbow adelbow@uw.edu
Ben Fetter bfetters@uw.edu
Lillie LaPlace llapla@uw.edu
Kai Laslett-Vigil
Winston Wilhere

Faculty Advisor: Dr. Justin Little

TA: Harry Furey-Soper

Table of Contents

- 1 - Introduction
- 2 - Technical Description
 - 2.1 - Overview
 - 2.2.1 - Chamber Interface
 - 2.1.2 - Leveling System
 - 2.1.3 - Pendulum
 - 2.1.4 - PPT Mount
 - 2.1.5 - Housing
 - 2.1.6 - Magnetic Damper
 - 2.1.7 - Wire Waterfall
- 3 - Detailed Drawings
- 4 - Bill of Materials
- 5 - Assembly Plans
- 6 - Check-Out
- 7 - Schedule

1 Introduction

This plan outlines the procedures required to manufacture and assemble every structural component that makes up the Test Stand. Each subsystem's components' manufacturing is detailed, followed by an instruction manual for both the assembly and disassembly of the Test Stand's structure. Following this assembly, the stand will be capable of leveling the pendulum through the GUI-controlled stepper motor and leave the stand ready for test operation with the pendulum returning to its zero point after every firing.

2 Technical Description

2.1 Overview

2.1.1 Chamber Interface:

The chamber interface consists of 29 manufactured parts. Two materials are used: G10 Garolite for structural components and Buna-N rubber for vibration damping. Additionally, two sleeve bearings and a stepper motor were purchased and used in their off-the-shelf form.

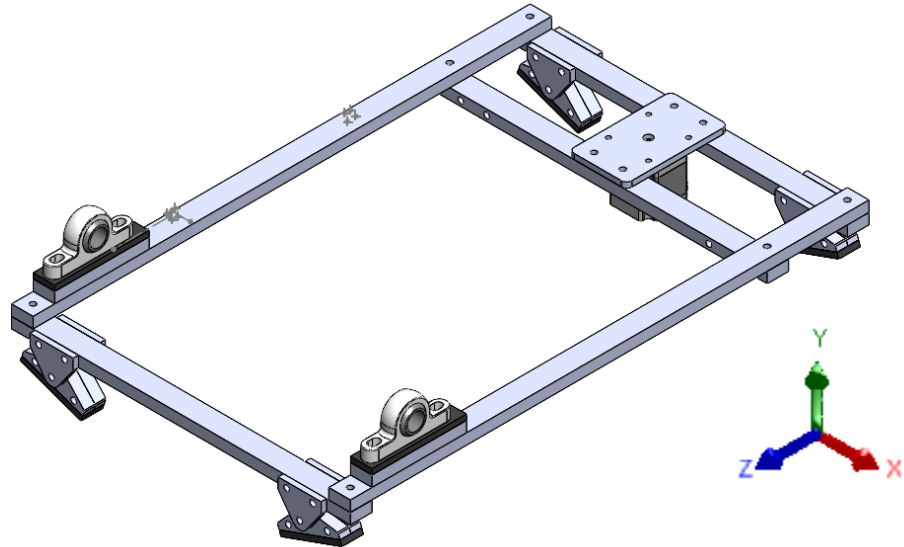


Figure 2.1.1.1. Chamber Interface System Overview

2.1.2 Leveling System:

The leveling system consists of 8 manufactured parts. The stepper motor is mounted between the chamber interface and leveling system, and is a key, COTS component of both systems' structures. The longitudinal and radial struts are all made from 0.5" G10 Garolite sheet, while the doublers are made of 0.125" G10 Garolite sheet doubled together to produce 0.25" assemblies.

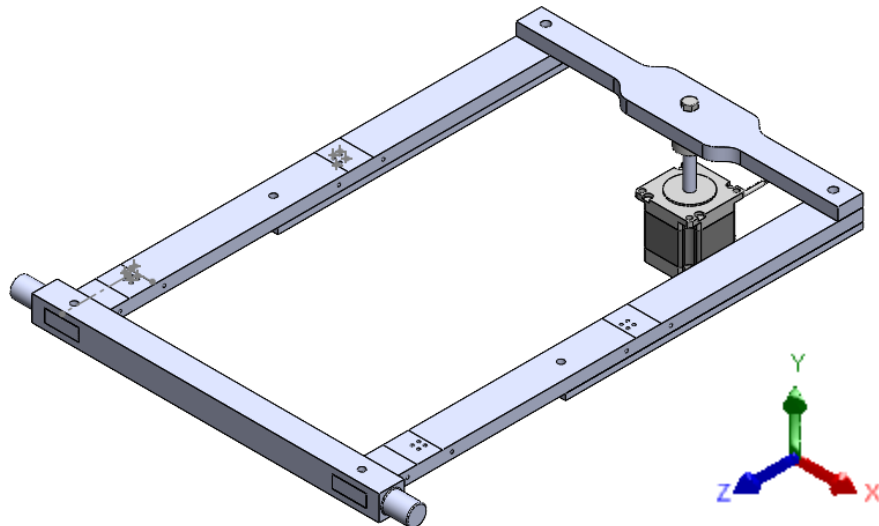


Figure 2.1.2.1. Leveling System Overview

2.1.3 Pendulum:

The pendulum consists of 55 total manufactured components, with 27 parts included in any flexure configuration. All parts are made of G10 Garolite, with brackets consisting of 0.125" thickness 1x1" angle stock, the top being cut from 0.125" thickness G10 Garolite sheet stock, two sets of 8.125" thickness arms, 16 bracket connectors, and 4 sets of 8 flexures made of spring steel in thicknesses of 0.01", 0.015", 0.020", and 0.025".

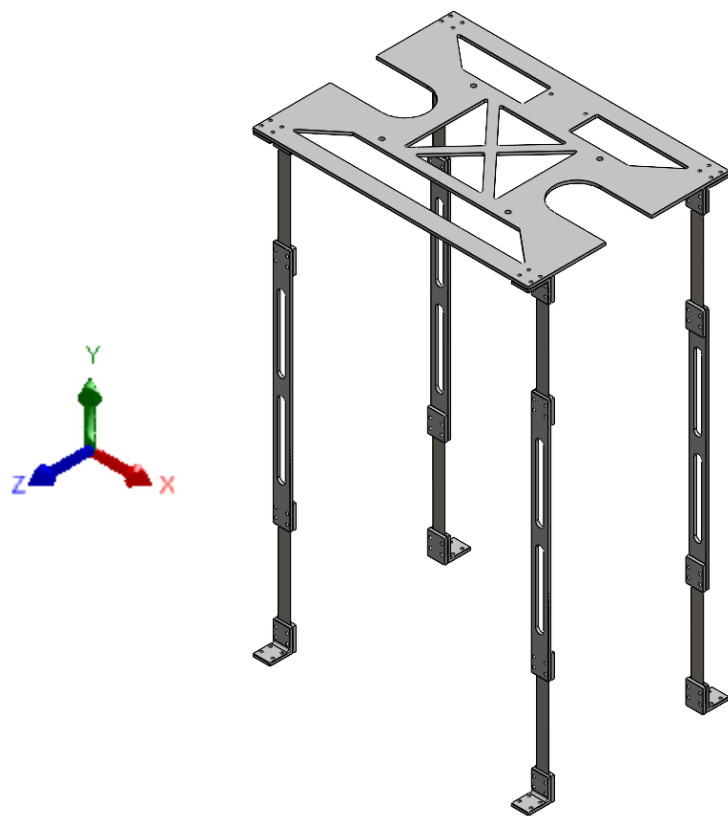


Figure 2.1.3.1. Pendulum

2.1.4 PPT Mount:

The PPT Mount consists of 6 manufactured parts, with 4 used in a given configuration. All components are made of 0.5" Delrin sheet stock. The mount consists of a base upon which thrusters are placed, 2 sets of 2 side panels to accommodate VC1 and VC2's dimensions, and a strap to ensure structural rigidity of the mount.

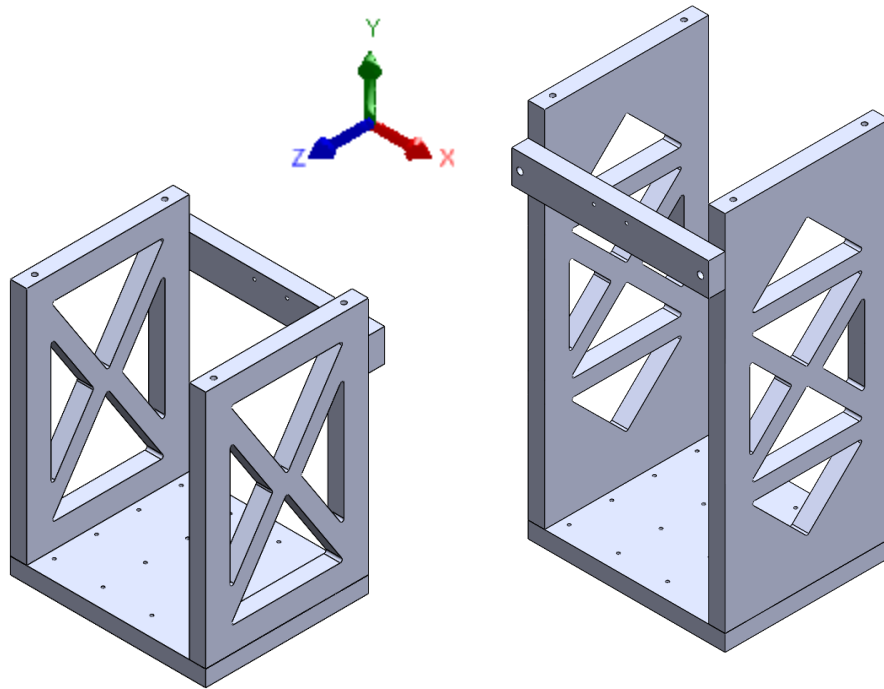


Figure 2.1.4.1. PPT Mount VC1 (Left) and VC2 (Right) Configurations

2.1.5 Pendulum Housing:

The pendulum housing consists of 15 manufactured parts. The four arms are made of 1/8" 1x1" G10 Garolite angle stock and the four leveling brackets, three top panels, and four side panels are made of 1/8" G10 Garolite sheet stock.

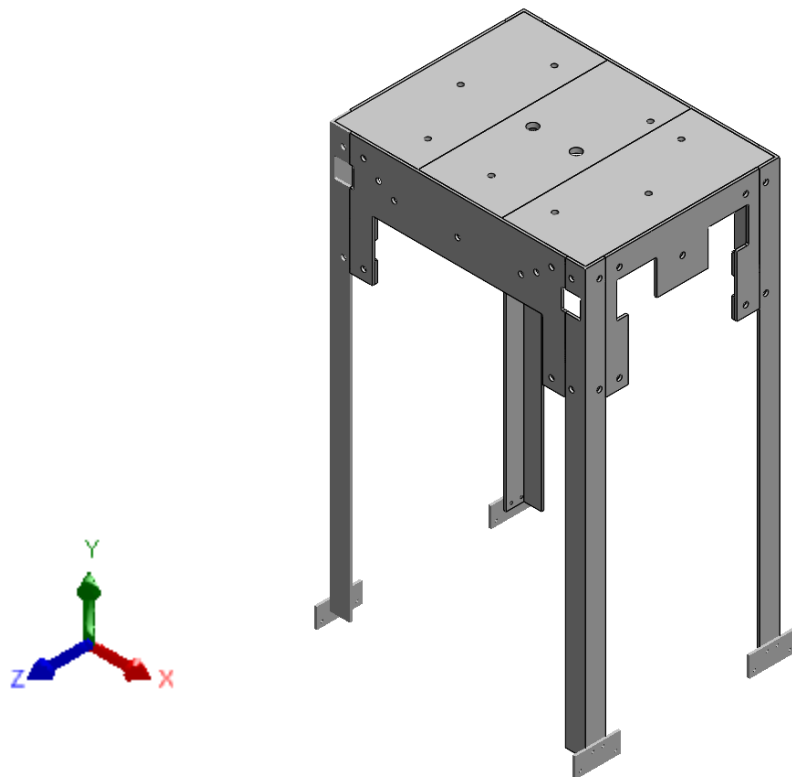


Figure 2.1.5.1. Pendulum Housing

2.1.6 Magnetic Damping System:

The magnetic damping system consists of 2 manufactured parts: a magnet housing and aluminum plate. The magnet housing was 3D printed out of PLA, while the 0.1" thick aluminum plate was cut out of larger sheet stock using shears.

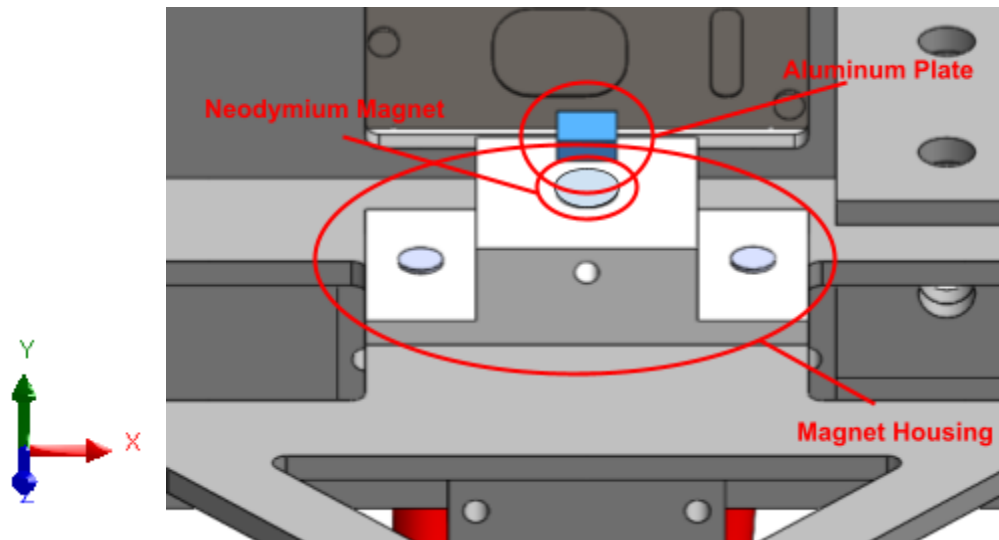


Figure 2.1.6.1. Magnetic Damping System

2.1.7 Wire Waterfall System:

The wire waterfall system's structure consists of four manufactured clamp parts from a single design. The clamp part is symmetrical, and is printed from carbon-fiber reinforced PETG.

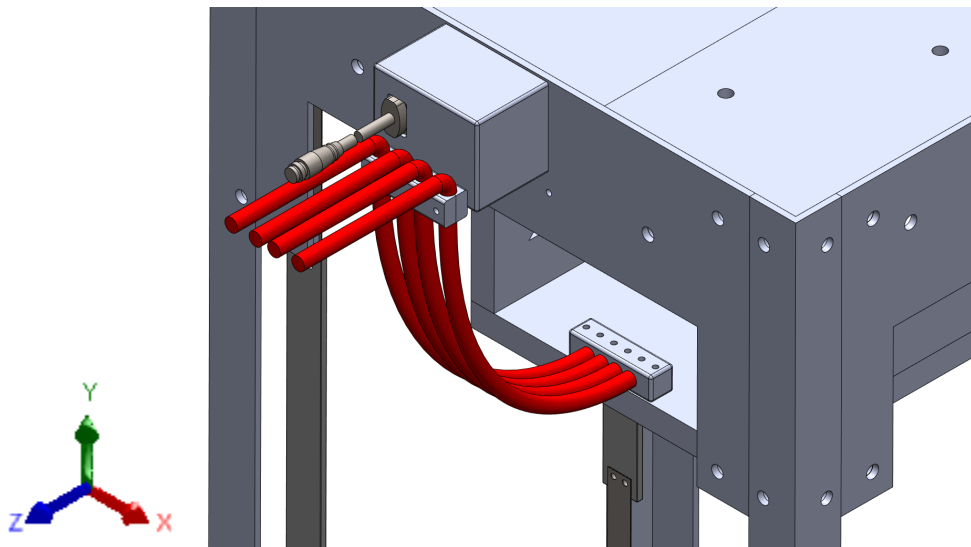


Figure 2.1.7.1. Wire Waterfall System

3 Detailed Drawings

All parts manufactured were produced using the following equipment and any further references to these tools are made with respect to their shortened titles below:

- Laser cutter: The 8 Makerspace Universal Laser System ILS12.75
- Drill press: C. Bossart Machine Shop Atlas 863 drill press
- Waterjet: Material Science & Engineering Shop Omax 2652 30 HP 60,000 PSI waterjet
- Dremel: C. Bossart Machine Shop Dremel 332-5 rotary cutting tool
- Bandsaw: C. Bossart Machine Shop bandsaw

Several manufacturing procedures are detailed below, for which standard procedures were defined: waterjetting, laser cutting, and drilling Garolite holes. For any work involving cutting Garolite outside of a waterjet, PPE including an N95 mask, safety glasses, and nitrile gloves were required.

All Garolite sheet stock parts were waterjetted to size without any internal features to avoid delamination using the following procedure:

1. Export .dxf from SolidWorks for relevant parts' feature faces to QCAD
 - a. Export all parts for the same thickness Garolite sheet stock into the same QCAD workspace
 - b. Delete all internal feature (lightening or screw holes) lines
2. Arrange all .dxf files for the same thickness Garolite sheet to fit within 26"x52" Omax waterjet area
3. Save file as single .dxf for all parts to be cut

4. Send .dxf file to MSE shop with one part's reference dimension for approval
5. Bring appropriate Garolite sheet stock to MSE shop
6. Return cut parts to AERB 139 lab space when notified of part completion

Paper templates were then laser cut for each part with all internal features included using the following procedure:

1. Export .dxf from SolidWorks for relevant parts' feature faces to QCAD
2. Arrange all .dxf files to fit within the ILS12.75 laser cutter's 24"x48" area (create several pages to accommodate all parts) for a 22"x34" sheet

For templates only:

- a. Use masking tape to tape together 8 sheets of copier paper in two rows of four arranged into a 22"x34" sheet
- b. Tape the 22"x34" sheet to the laser cutter bed to prevent any shifting during cutting

For all other parts:

- a. Place part material into upper lefthand corner ensuring square alignment with cutter bed
3. Email the .dxf generated in QCAD to one of the 8 Makerspace's computers and open in Adobe Illustrator
4. Select all drawing features and set line thickness to 0.01 pt and color to RGB: 255,0,0
5. Select Adobe Illustrator's print command to export the file to the laser cutter using the 8 Makerspace's presets, ensuring the print position on the laser cutter bed is set to the upper left corner
6. Open the file in the ILS application and ensure proper cut location in upper left corner
7. Turn on air compressor underneath computer by opening valve and flipping power switch
8. Turn on fume hood by pushing green button
9. Turn on laser cutter by flipping power switch
10. When laser cutter has powered on, re-zero the Z-height and X,Y position using the ILS application commands
11. Under ILS application material tab, set material to "printer paper" and do not change any other settings
12. Click the play button on the ILS application
13. When cutting has finished, remove the part templates and remaining paper from the cutter bed and discard excess material
14. Turn off laser cutter, fume hood, and air compressor using reverse steps from 9-11

All internal hole features were added using the following procedure:

1. Put on safety glasses, nitrile gloves, and an N95 mask
2. Tape paper template to part using masking tape, ensuring square alignment with all corners
3. Clamp part to drill press base

4. Use a second clamp to attach a shop vacuum nozzle to the drill press base and position to remove drilled debris
5. Select and install appropriate drill bit, for holes larger than 17/128", use a 17/128" pilot hole and step through larger drill bits until target size is reached
6. Align clamp-part assembly below drill bit and center bit on template hole center (check front and side for visible alignment)
7. Turn on vacuum
8. Turn on drill press
 - a. If speed is not set to 1000 RPM, change while turned on
9. Drill hole
10. Turn off drill press
11. Realign clamp-part assembly and bit to drill next hole
12. Repeat Steps 8-11 until all holes are drilled

Any additional interior or external features in a part not cut using a drill press were added using a Dremel as specified in their relevant drawings. Internal features for the Garolite angle stock were added prior to any bandsaw cuts to produce individual brackets and arms. For all Dremel and bandsaw cuts, proper PPE including gloves, safety glasses, N95 respirators were used in addition to continuously operating a shop vacuum chamber.

3D Printed Parts

1. Load filament into Prusa i3
 - a. If any filament is previously loaded, unload
 - b. If filament settings are not set to PETG, change accordingly
2. Export SolidWorks file as .stl
3. Open .stl file in PrusaSlicer
4. Set filament to PETG
5. Set print settings to 0.10 mm DETAIL
6. Set supports to "Support on build plate only"
7. Level part and place largest flat side on print bed in print editor
8. Export .gcode to SD card
9. Insert SD card into Prusa i3 and load file
10. Start print
11. When print is complete, remove from print bed
12. Remove excess support material (sanding as needed)

Technical drawings are attached as a separate document named "Test Stand Technical Drawings" and specify all dimensions and materials. Manufacturing instructions above detail how to produce each feature called out in each drawing.

4 Bill of Materials

Purchased Parts			
Fasteners			
Part	Quantity	Specification	
94613A537 (McMaster)	40	1/4"-20 x 3/8" hex bolt (nylon)	Frame bolts
94613A537 (McMaster)	40	1/4"-20 nut (nylon)	Frame nuts
94613A108 (McMaster)	18	#4-40 x 3/8" hex bolt (nylon)	Bolts for pendulum arms to top, and magnet housing to top
94812A700 (McMaster)	20	#4-40 nut (nylon)	Nuts for pendulum top and laser mount
B0C3QLVR 6J (Amazon)	40	#40-40 x 3/8" (stainless steel)	Bolts for flexures and frame to radial struts
92314A108 (McMaster)	32	#40-40 x 3/8" (stainless steel)	Bolts for flexures and frame to leveling brackets
B0C3QLVR 6J (Amazon)	96	#4-40 nut (stainless steel)	Nuts for pendulum top and laser mount
94613A831 (McMaster)	16	#10-32 x 3/4" hex bolt (nylon)	Bolts for thruster shelf, no nuts needed, tapped holes
95649A229 (McMaster)	16	#10 ID-0.203" OD-0.438" Washer (UHMW Plastic)	Washers for thruster shelf bolts
B0C3QLVR 6J (Amazon)	16	#4-40 x 1" hex bolt (stainless steel)	Pendulum to radial strut bolts
95868A266 (McMaster)	4	#4-40 x 1 1/8" hex bolts (nylon)	Laser mount to frame and laser to laser mount bolts
92196A215 (McMaster)	8	#40-4 x 1 5/8" hex bolts (stainless steel)	Leveling bracket to radial strut bolts

Part	Quantity	Material	Manufacturing Technique	Complete?	Re-Manufacture?
VS1	4	1/8" G10 Sheet	waterjet, drill press holes, dremel lightening slots	Y	Y
CILS1	2	1/2" G10 Sheet	waterjet, drill press holes	Y	N
CIRS1	3	1/2" G10 Sheet	waterjet, drill press holes	Y	N
CILS1	2	1/2" G10 Sheet	waterjet, drill press holes	Y	N
LSL1	2	1/2" G10 Sheet	waterjet, drill press holes	Y	N

LSR1	1	1/2" G10 Sheet	waterjet, drill press holes	Y	N
LSP1	1	2" G10 Bar Stock	N/A, planned lathe and drill press	N	Y
CISMM1	1	1/2" G10 Sheet	N/A, planned waterjet and mill	N	Y
LSD1	4	1/8" G10 Sheet	waterjet, drill press holes (double to reach 1/4" thickness)	Y	N
CIFU1	8	1/2" G10 Sheet	waterjet, drill press holes	Y	Y
CIFL1	4	Buna-N Rubber Sheet	N/A, planned to cut out	Y	N
CIFM1	8	1/8" G10 Sheet	waterjet, drill press holes	Y	N
CIBED1	2	1/2" G10 Sheet	waterjet, drill press holes	Y	N
CIBD1	2	Buna-N Rubber Sheet	N/A, planned to cut out	Y	N
FB2	4	1/8" G10 Sheet	waterjet, drill press holes	Y	N
BC1	16	1/8" G10 Sheet	waterjet, drill press holes	Y	Y
CB4	8	1/8" Thick 1x1" G10 Angle Stock	drill press holes, bandsaw individual brackets	Y	Y
FX1	8	0.010" Spring Steel Sheet	laser cut	Y	N
FX2	8	0.0150" Spring Steel Sheet	laser cut	Y	N
FX3	8	0.020" Spring Steel Sheet	laser cut	Y	N
FX4	8	0.0250" Spring Steel Sheet	laser cut, dremel to release flexures not fully cut	Y	N
LG1	2	1/8" Thick 1x1" G10 Angle Stock	bandsaw to length, drill press holes, dremel access tabs	Y	N
LG2	2	1/8" Thick 1x1" G10 Angle Stock	bandsaw to length, drill press holes, dremel access tabs	Y	N
FT1	2	1/8" G10 Sheet	waterjet, drill press holes	Y	N
FT2	1	1/8" G10 Sheet	waterjet, drill press holes	Y	N
FS2	1	1/8" G10 Sheet	waterjet, drill press holes	Y	N

FS3	1	1/8" G10 Sheet	waterjet, drill press holes	Y	N
FS1	2	1/8" G10 Sheet	waterjet, drill press holes	Y	N
FB1	12	1/8" Thick 2x2" G10 Angle Stock	drill press holes, bandsaw individual brackets	Y	Y
PT1	1	1/8" G10 Sheet	waterjet, drill press holes, dremel lightening slots	Y	Y
SS1	2	1/2" Delrin Sheet	laser cut, drill press holes, tap holes	Y	N
SS2	2	1/2" Delrin Sheet	laser cut, drill press holes, tap holes	Y	N
SB1	1	1/2" Delrin Sheet	laser cut, drill press holes, tap holes	Y	N
FB3	1	1/2" Delrin Sheet	laser cut, drill press holes, tap holes	Y	N
MH1	1	PLA Filament	3D print	Y	N
MA1	1	0.1" Aluminum-6061 Sheet	cut with shears	Y	N
WF1	4	Carbon Fiber-Reinforced PETG Filament	3D print, drill press holes, tap holes	Y	Y
PSP1	2	Carbon Fiber-Reinforced PETG Filament	3D print	Y	N

Borrowed Parts

Name	Quantity	Specification	Owner	Location
printer paper	50 sheets	8.5"x11"	DBF	The 8 Makerspace
masking tape roll	1	1" wide	Capstone Lab	AERB 139

5 Assembly Plans

See "Assembly Plans" file attached with submission for full system assembly steps.

6 Check-Out

See “System Test Procedure” file attached with submission for details on full system functionality check-out..